On Transients, Lyapunov Functions and Turing Instabilities

Submitted by

Aiman Saleh Elragig

to the University of Exeter as a thesis for the degree of Doctor of Philosophy in Mathematics, June 2013

I certify that all material in this thesis which is not my own work has been identified and that no material is included for which a degree has previously been conferred upon me.

.....

Aiman Saleh Elragig

Abstract

Motivated by the papers [84, 85], this thesis considers the concepts of reactivity, Lyapunov stability and Turing patterns. We introduce the notion of P-reactivity, a new measure for transient dynamics. We extend a result by Shorten and Narendra [108] regarding joint dissipativity for second order systems. We derive an easy verifiable formula that determines systems P-reactivity with respect to a norm induced by the positive definite matrix P. An optimization problem aiming to determine the positive definite P with respect to which a stable system is most reactive is posed and solved numerically for second order systems. The stability radius is adopted as a measure of robustness of joint disspaptivity. We characterise the stability radius of joint dissipativity when the underlying systems are subject to certain specific perturbation structures. A detailed robustness analysis of the Shorten and Narendra conditions is also presented.

Using the notion of common Lyapunov function we show that the necessary condition in [85] is a special case of a more powerful (i.e tighter) necessary condition. Specifically, we show that if the linearised reaction matrix and the diffusion matrix share a common Lyapunov function, then Turing instability is not possible. The existence of common Lyapunov functions is readily checked using semi-definite programming. We also further extend this to include more

complicated movement mechanisms such as chemotaxis. Unlike the traditional techniques, this new necessary condition can be used to check Turing instability for systems with any dimension and any number of parameters. We apply our new conditions to various models in literature.

I dedicate this work to my mother ***Sharaf Elkilanee Abdulgader*** *and my father* ***Saleh Abdullah Elragig****.*

Also to

my beloved wife : ***Hanan****,*

my sisters : ***Entesar, Asia, Fatima, Basma, and Fareha****,*

my brothers : ***Rajab, Abdullah and Elkilanee****.*

Acknowledgements

First of all I would like to thank Allah "God" who gives me the support and energy to finish this work. Thanks for my supervisor Stuart Townley for his patient and extraordinary guidance and support during my study. Also I would like to thank Dr. Chris Guiver for his valuable comments. My deep thanks to Professor Idriss Ehfida Elmabrok for his extraordinary support during my earlier stages in mathematics. Also thanks to Dr. Mohamed Saidi for his constant support. Many thanks to Liz Roberts for her continuous assistance. Also I would like to express my thanks to the Libyan people for covering all the expenses needed to complete this work.

Contents

List of Figures

List of Tables

Chapter 1

Introduction

Biological systems exhibit a wide variety of intriguing phenomena which range across different scales and different levels of observation. For example, an ecosystem can be organised to smaller patches as a response to environmental changes [80]. Certain kinds of white blood cells, called Leukocytes, can migrate through the blood stream as a response to chemical changes resulting from the invasion of foreign micro-organisms such as bacteria [16, 17]. Metastasis, the migration of cancer to nearby healthy cells, has attracted the attention of a large number of pathologists in recent years [116]. Morphogenesis is one of these fascinating aspects of life. Flowers organizations, sand's shells, patterned animals skins and importantly the shape and form of human embryo are all, sometimes puzzling, interesting phenomena. Turing theory of Morphogenesis [115, 80] is a huge step for understanding how some patterns and shapes are formed. It suggests the mechanism by which some patterns are progressed. This includes the developing form and shape of the human embryo. It stresses the effect of movement (diffusion), which is believed to have a stabilizing effect on breaking the spatial symmetry of systems that include a stable reaction.

However, it is important to understand and predict circumstances when a biological systems will exhibit patterns in Turing mechanism called Diffusion Driven Instability.

The thesis is motivated and inspired by the following quote from Mike Neubert, Hal Caswell and Jim Murray:

"Reactivity is necessary for Turing instability".

This quote is taken from the paper [85] where a link is made between seemingly disparate topics, namely reactivity and Turing instability. Reactivity is a measure of transient dynamics whilst Turing instability is a mechanism triggering pattern formation in spatially distributed reaction-diffusion (RD) systems. The link, described in detail in Chapter 5, comes from an analysis of the matrix

$$A - ||\mathbf{k}||^2 D,$$

where A is the linearisation of the reaction part of the RD system, the matrix D quantifies system diffusitivity and $\mathbf{k}$ is a vector of wave numbers or spatial frequencies. A detailed account of this is given in Chapter 5.

The simple, yet powerful, observation captured by the quote above leads us on a journey where numerous features are intertwined. The destination of this journey is a proper understanding of the result in [85], but along the way we are led to study connections between transients and asymptotic stability (Chapter 2) and ideas of common Lyapunov function (CLF), determine maximal reactivity and related issues (Chapter 3), find robustness measures for existence of CLFs and finally apply our generalisation of the result in [85] to reaction systems with various forms of taxis - diffusion, chemoattractants and chemotaxis.

1.1 Thesis structure

Each chapter in the thesis is self contained with its own introduction. Here we summarise their contents. Chapter 2 includes preliminary material needed in the thesis. It also introduces the notion of P-reactivity as a generalization of reactivity in the sense of Neubert and Cawell [84]. The chapter also includes an extension of a result by Shorten and Narendra [108] regarding joint dissipativity in second order systems. The final section of this chapter shows, through examples, the importance of norm choice in determining system characteristics. Chapter 3 studies the notion of P-reactivity in detail. We derive a formula that determines system reactivity with respect to a norm induced by a positive definite matrix P. The chapter also includes a determination of the norm with respect to which a given system has maximum reactivity. We solve the maximum reactivity problem numerically for 2×2 systems. Chapter 4 addresses the robustness of joint-dissipativity. We define and then characterise a stability radius for joint-dissipativity when the underlying matrices are subject to certain specific perturbation structures. The chapter also explores the robustness of the Shorten and Narendra necessary and sufficient conditions for joint disspativity of second order systems [108]. In Chapter 5, we derive a new necessary condition for Turing instability based on joint dissipativity of the underlying linearised reaction matrix and diffusion matrix. We also further extend this result to include more complicated movement mechanisms such as chemotaxis. In Chapter 6, we apply the results in Chapter 5 to various examples found in literature. We show how the approach we develop can, with the aid of semi-definite programming code such as cvx, locate regions in parameter space where Turing patterns is not possible.

1.2 Publications

- A. S. Elragig, S. Townley. A new necessary conditions for Turing instabilities. *Mathematical Biosciences*, 239 (2012) 131-138

1.3 Submitted Manuscripts

- A. S. Elragig, S. Townley. Turing pattern in the Oregonator revisited. *Applied Mathematics Letters*, submitted.

1.4 Manuscripts in Preparation

- A. S. Elragig, S. Townley. On a negative relation between bacterial taxis and Turing pattern formation.

1.5 Notation and preliminaries

In this thesis $\mathbb{C}$, $\mathbb{C}_-$, $\mathbb{C}_+$ and $\mathbb{R}$ will denote the set of complex numbers, the left half-plane, the right half-plane and the real numbers, respectively. The set of $m \times n$ matrices with entries in $\mathbb{K}$ is denoted by $\mathbb{K}^{m\times n}$ where $\mathbb{K} = \mathbb{R}$ or $\mathbb{C}$. A square matrix A is Hurwitz if $\sigma(A) \subset \mathbb{C}_-$. For the $n \times n$ symmetric matrix X, we will denote its maximum eigenvalue by $\lambda_1(X)$ whereas the minimum eigenvalue is denoted by $\lambda_n(X)$. Also for a matrix $M \in \mathbb{K}^{m\times n}$ with rank r the singular values, in non-increasing order, are denoted by $\sigma_i(M), i = 1, 2, \ldots, r$.

Chapter 2

Interplay Between Transients and Stability

2.1 Introduction

Physical systems are prone to disturbances. Even for strongly robust systems, the response to those disturbances are often rich in behaviours and in many settings tracking the whole regime becomes a challenge. A system can exhibit oscillations, damping, growth or even a chaotic regime throughout different stages of its time course [93]. The problem becomes more challenging if the dynamics involve independent sub-dynamics, as in the case of switching (hybrid) systems [34]. In this chapter, we explore the interplay between a systems stability and its, possible, unstable transient behaviour. Our focus is on linear time-invariant systems. In Section 2.2 we discuss the notion of stability. In particular, for linear systems stability is typically the study of system dissipativity (i.e. convergence to steady state) with respect to certain, suitably defined, quadratic norms. We further this by studying joint dissipativity in

Section 2.3. In Section 2.4 we consider the transient behaviour of stable linear systems and review some recent literature that emphasizes the importance of such dynamics. Our focus is mainly on reactivity, introduced by Neubert and Caswell in [84], as one measure for transient dynamics. We stress the importance of norm (energy function) choice for capturing both the transient and the long term behaviours. Consequently, we introduce what we call P-reactivity as a generalization of reactivity in the sense of Neubert and Caswell [84]. In Section 2.5, using some specific examples, we demonstrate the utility of norm choice and its implications.

2.2 Lyapunov stability

Stability is often the most desirable characteristic of dynamical systems. There are many senses in which to look at stability. We will consider stability in the Lyapunov sense. Consider the non-linear, autonomous system

$$\dot{x}(t) = f(x), \quad x(0) = x_0. \tag{2.1}$$

Here $f : D \subset \mathbb{R}^n \to \mathbb{R}^n$ is a locally Lipschitz map,$x = x(t) \in \mathbb{R}^{n\times 1}$ is the state of the system at time t and x_0 is an initial state. For convenience we always drop t and simply write x. The state x_e is an equilibrium of the system (2.1) if

$$x_0 = x_e \Longrightarrow x(t) = x_e \quad \text{for all} \quad t \geq 0.$$

Equivalently, x_e is an equilibrium if

$$f(x_e) = 0.$$

For autonomous systems of the form (2.1), the equilibrium can, without loss of generality, always be assumed to be the origin since we can always shift coordinates using the transformation $z = x - x_e$. The origin 0 is then an equilibrium of the system in the new variable z. We replace z by x for convenience. In the sense of Lyapunov, stability refers to the situation when all solutions $x(t)$ remain near the origin 0 when the system is subjected to sufficiently small disturbances; otherwise, we will have instability. Asymptotic stability is where additionally $x(t)$ returns to the origin 0, as $t \to \infty$. These are defined precisely, see [56, 47], as follows:

Definition 1. *The steady state* 0 *of the system* (2.1) *is*

- *stable if, for each* $\varepsilon > 0$*, there exists* $\delta(\varepsilon) > 0$ *such that* $||x(0)|| < \delta$ *implies* $||x(t)|| < \varepsilon$*, for all* $t \geq 0$*;*
- *asymptotically stable if it is stable and there exists* $\eta > 0$ *such that if* $||x(0)|| < \eta$*, then* $lim_{t\to\infty}(x(t)) = 0$*.*

One of the drawbacks of checking stability using the $\varepsilon - \delta$ definition is that it requires finding a solution of the systems which may be difficult or sometimes impossible. Moreover, the functional form of the solution can be complicated so that it makes linking ε to the desired δ not obvious [56]. A Lyapunov function approach is an alternative method to check stability.

Lyapunov's direct method

Lyapunov's direct method is an elegant way for understanding the state of the system without looking at the system's details. It is based on defining a decreasing scalar function on the state space of the system. For the system (2.1), a Lyapunov function, see [56, 47], is a continuous real valued function V defined on some neighbourhood D of x_e with the properties

- x_e is a unique minimum of V in D;
- $V(\psi(t))$ decreases monotonically along any solution of $\psi(t)$ (2.1) which starts in D.

Lyapunov's direct method is a generalization of the concept of energy in mechanical systems. Accordingly, any initial condition starting in the domain D will remain trapped within the region defined by the level curves of V. If V is instead strictly decreasing, then the state of the system will eventually converge to x_e, see Figure 2.1. One of the challenges of using Lyapunov's direct method is that there is no general rule that can be used to determine Lyapunov functions.

Example 2.2.1. *Consider the autonomous system [91]*

$$\begin{aligned} \dot{x_1} &= x_2 - x_1(x_1^2 + x_2^2), \\ \dot{x_2} &= -x_1 - x_2(x_1^2 + x_2^2). \end{aligned} \tag{2.2}$$

To study the stability of the equilibrium $(0, 0)$ *we use the function*

$$V(x) = x_1^2 + x_2^2.$$

The time derivative of V *along the orbits of the system is given as*

$$\dot{V}(x) = 2x_1\dot{x_1} + 2x_2\dot{x_2} = -2(x_1 + x_2)^2 < 0.$$

In this case, V *is strictly decreasing along solutions for all* $x \neq 0$. *Hence the equilibrium is asymptotically stable. Figure 2.1 shows the behaviour of the trajectories over the level curves of* V.

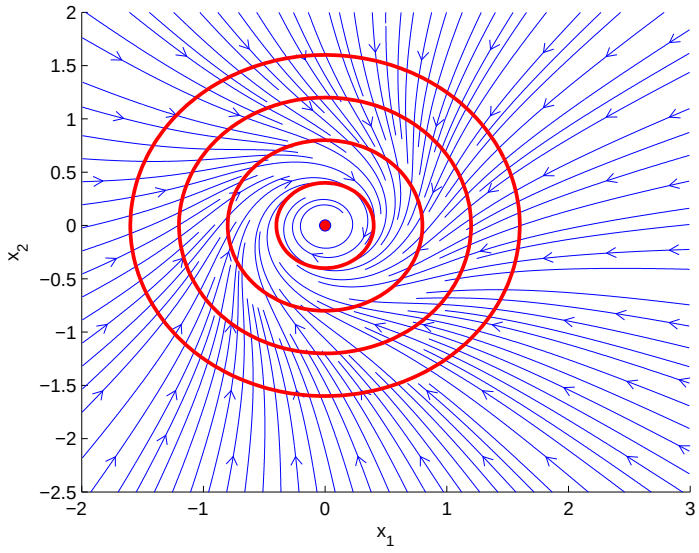

Figure 2.1: The phase portrait of the system (2.2) with the energy levels (in red) determined by the function V. All disturbed trajectories move to strictly lower energy levels of V.

Lyapunov stability of linear time-invariant systems

Consider the linear time-invariant system

$$\dot{x}(t) = Ax(t), \quad x(0) = x_0. \tag{2.3}$$

Whether system (2.3) is intrinsically linear or resulting from linearising a non-linear system, stability is determined by examining the eigenvalues of the matrix A. Let $\{\lambda_i\}$ be the set eigenvalues of A. If $\max(\text{real}(\lambda_i)) < 0$ (≤ 0) for all i then the origin 0 is asymptotically stable (stable). Stability of system (2.3) can also be checked by using Lyapunov function techniques. A natural candidate for a Lyapunov function is

$$V(x) = x^T P x = \langle x, x \rangle_P = ||x||_P^2.$$

Here P is a positive definite matrix and $||x||_P$ is the quadratic norm induced by P. The time derivative of V along solutions of system (2.3) is given as

$$\frac{d}{dt}(V(x)) = x^T(A^TP + PA)x.$$

The origin 0 is stable if $x^T(A^TP + PA)x$ is non increasing with time. In other words, if

$$A^TP + PA \leqslant 0,$$

then V is a Lyapunov function for system (2.3) and we say that A is P-dissipative. As we shall see in Chapter 3, the system is called P-nondissipative or P-reactive when $A^TP + PA \not\leqslant 0$.

Example 2.2.2. *Consider the linear system*

$$\dot{x}(t) = \begin{pmatrix} -2 & 20 \\ 0 & -15 \end{pmatrix} x(t).$$

The matrix

$$P_1 = \begin{pmatrix} 1 & 0 \\ 0 & 1 \end{pmatrix}$$

is not a Lyapunov function for this system since

$$A^TP_1 + P_1A = A^T + A = \begin{pmatrix} -2 & 0 \\ 20 & -15 \end{pmatrix} + \begin{pmatrix} -2 & 20 \\ 0 & -15 \end{pmatrix} = \begin{pmatrix} -4 & 20 \\ 20 & -30 \end{pmatrix} \not\leqslant 0.$$

Indeed $A + A^T$ *has the set of eigenvalues* -40.8537, 6.8537. *The matrix*

$$P_2 = \begin{pmatrix} 2 & 3 \\ 3 & 5 \end{pmatrix}$$

is a Lyapunov function since

$$A^T P_2 + P_2 A = \begin{pmatrix} -2 & 0 \\ 20 & -15 \end{pmatrix} \begin{pmatrix} 2 & 3 \\ 3 & 5 \end{pmatrix} + \begin{pmatrix} 2 & 3 \\ 3 & 5 \end{pmatrix} \begin{pmatrix} -2 & 20 \\ 0 & -15 \end{pmatrix}$$

$$= \begin{pmatrix} -8 & -11 \\ -11 & -30 \end{pmatrix} < 0.$$

The matrix P_1 is not a Lyapunov function since for some initial state the system moves to an outer level surface of P_1 and this means that over the energy levels defined by P_1 the system's energy can increase. In the case of P_2, the system state moves from high energy levels to lower levels and hence P_2 is a Lyapunov function. Analysing the system with various Lyapunov/non-Lyapunov functions sets up a frame work for understanding systems energy variations. These norm-dependent transient instability behaviours are as important as the stable asymptotic ones and in many natural settings they are the typical behaviour [84, 120, 40].

Keypoint I

Lyapunov's direct method is essentially concerned with finding a norm in which all solutions do not increase in norm.

2.3 Switching systems

Switching systems are an important class of hybride systems. Recently, switching systems have become quite prominent [34]. They arise in many practical situations such as biological networks, automotive engineering control, aircraft manufacturing and chemical process control [5, 72]. A switching dynamical system constitutes a finite set of subsystems and a switching rule that organises switching between these subsystems [66]. These sub-dynamics can be linear, non-linear or even can involve stochastic elements. A continuous-time switching systems can be described as a family of differential equations

$$\dot{x}(t) = f_\sigma(t, x), \quad t \geqslant 0,$$

where $\{f_\sigma(.,.) : \sigma \in \Sigma\}$ is a family of locally Lipschitz functions parametrised by some set Σ, typically a finite set, and $\sigma(t)$ is the time-varying switching rule (or signal) [41]. In this perspective, linear continuous-time switching systems, which will focus on, can be defined as follows. For the set of matrices $\{A_1, A_2, \cdots, A_n\}$, the dynamical system

$$\dot{x} = A_{\sigma(t)}x, \tag{2.4}$$

where $\sigma(t) \in \{1, \ldots, n\}$ is the switching rule, is called linear continuous-time switching system. Stability requires the dissipativity of all sub-dynamics. The function with respect to which all subdynamics dissipate is called a common Lyapunov function (CLF) or simultaneous Lyapunov function. It is worth adding here that for the linear switching system studying the stability involves examining the stability of all sub-dynamics it constitutes. Guaranteeing the

stability of all the subsystems does not imply the stability of the whole switching system [66] except for particular cases such as when A_i is normal [130] or the A_i are all pairwise commutative [129]. A typical way to check the stability of switching systems is to find one common Lyapunov function for all possible A_i. This is made more precise in the following.

Joint-disspativity in switching systems:

Definition 2. *For the switching system* (2.4)*, if there exists* $P > 0$ *so that*

$$A_i^T P + P A_i \leq 0 \quad \text{for all } i \in \{1, 2, ...n\},$$

then the quadratic function $V(x) = x^T P x$ *is a Common Lyapunov function (CLF) for the switching system* (2.4) *and the family of matrices* $A_i, i \in \{1, .., n\}$ *are called jointly* P*-dissipative.*

Recent research efforts have been devoted to finding necessary and sufficient conditions for the existence of CLFs for switching systems [66, 65]. Shorten and Narendra [108] derived necessary and sufficient conditions for the existence of a CLF for a finite number of stable second order systems. Their result is summarised in the following theorem.

Theorem 2.3.1. *(Shorten and Narendra 2002)*
Suppose A_1 *and* A_2 *are two Hurwitz matrices in* $\mathbb{R}^{2\times 2}$*. A necessary and sufficient condition for the dynamic governed by* A_1 *and* A_2 *to have a CLF is that the matrices* $A_1 A_2$ *and* $A_1 A_2^{-1}$ *do not have negative real eigenvalues.*

Example 2.3.3. *Consider*

$$A_1 = \begin{pmatrix} b-1 & a \\ -b & -a \end{pmatrix} \quad \text{and} \quad A_2 = \begin{pmatrix} -1 & 0 \\ 0 & -5 \end{pmatrix}.$$

Then

$$A_1A_2 = \begin{pmatrix} b-1 & a \\ -b & -a \end{pmatrix} \begin{pmatrix} -1 & 0 \\ 0 & -5 \end{pmatrix} = \begin{pmatrix} 1-b & -5a \\ b & 5a \end{pmatrix}$$

and

$$A_1A_2^{-1} = \begin{pmatrix} b-1 & a \\ -b & -a \end{pmatrix} \begin{pmatrix} -1 & 0 \\ 0 & -.2 \end{pmatrix} = \begin{pmatrix} 1-b & -0.2a \\ b & 0.2a \end{pmatrix}$$

Using the necessary and sufficient conditions in the above theorem we obtain Figure 2.2 which shows the region in the parameter space (a, b) *where* A_1 *and* A_2 *share a CLF.*

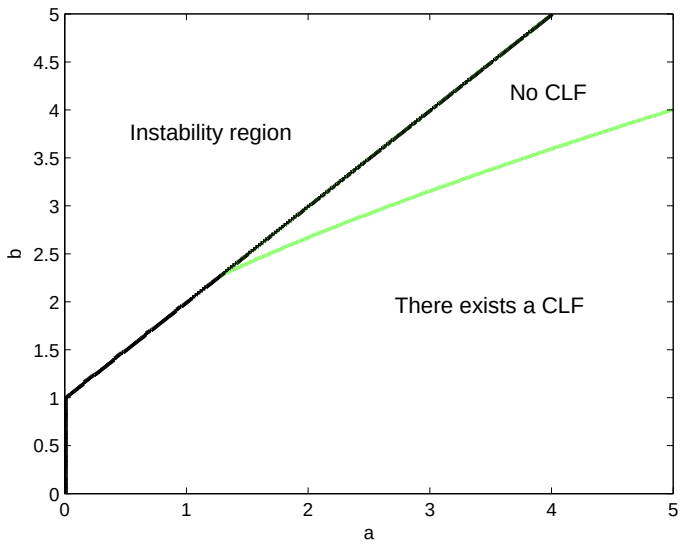

Figure 2.2: The stability region (below the black curve) is divided into two distinct regions. A region where A_1 and A_2 share a CLF (between the black and green curves) and another where they do not (above the green curve).

For the particular choice $a = 1$ and $b = 1.5$ we have

$$A_1 = \begin{pmatrix} 0.5 & 1 \\ -1.5 & -1 \end{pmatrix} \quad \text{and} \quad A_2 = \begin{pmatrix} -1 & 0 \\ 0 & -5 \end{pmatrix}.$$

Then $\sigma(A_1A_2) = \{2, 2.5\}$ and $\sigma(A_1A_2^{-1}) = \{-0.15 + 4231i, -0.15 - 4231i\}$. Therefore A_1 and A_2 share a CLF. A common Lyapunov function is given by

$$P = \begin{pmatrix} 11.1092 & 4.6035 \\ 4.6035 & 6.4635 \end{pmatrix}.$$

Remark 2.3.1. *The argument leading to the conclusion of Theorem 2.3.1 was based on defining Lyapunov functions with strict inequalities (i.e. strict Lyapunov function). For the purpose of later work we extend the Theorem 2.3.1 by allowing weaker inequalities, i.e. adopting the Definition 2. This leads to the following extension of Shorten and Narendra results.*

Proposition 2.3.1. *A_1 and A_2 share a CLF if, and only if, individually both matrices A_1A_2 and $A_1A_2^{-1}$ have no distinct negative real eigenvalues.*

Proof: We adapt the techniques used by Shorten and Narendra. See Subsection A.1.2 Appendix A for details.

Finding a necessary and sufficient conditions for the existence of a CLF for a general $n \times n$ switching system is an open question [66]. However, the problem is computationally tractable using some numerical algorithms such as the LMI toolbox [32]. Moreover, since finding a CLF for A_1 and A_2 is a Semidefinite

Programming (SDP) problem [118] i.e. optimization of a linear function under linear matrix inequality constraints. This can be solved very efficiently and with less programming efforts using a widely used Matlab based tool box called `cvx` introduced in [15]. See Appendix B.

Example 2.3.4. *Consider the two matrices,*

$$A_1 = \begin{pmatrix} -55 & 0 & 0 & 37 & -16 & 0 & 44 & -49 & 17 & 0 \\ 0 & -40 & 0 & 0 & 0 & 2 & -2 & 0 & -8 & 0 \\ 0 & 0 & -6 & -5 & 0 & 0 & -8 & 8 & -32 & 0 \\ 1 & 0 & 0 & -24 & -11 & 0 & 19 & -46 & 0 & 0 \\ 6 & 6 & -5 & -52 & -12 & 44 & -49 & 76 & -38 & -22 \\ 44 & 107 & -191 & -176 & 197 & 164 & -276 & 111 & -58 & 26 \\ -18 & 96 & -278 & -188 & 283 & 292 & -440 & 0 & 0 & 0 \\ -58 & -134 & 82 & 173 & -77 & -89 & 181 & -135 & 0 & 0 \\ 39 & 133 & -438 & -215 & 273 & 422 & -376 & 165 & 0 & 0 \\ 133 & -113 & 217 & 89 & -80 & -221 & 0 & -108 & 17 & -36. \end{pmatrix},$$

$$A_2 = \begin{pmatrix} -75 & 0 & 0 & 0 & -26 & 0 & 23 & 0 & 22 & 0 \\ 10 & -72 & 5 & 0 & 2 & 0 & -7 & 0 & -6 & 0 \\ 8 & 2 & -8 & -10 & 3 & 0 & -22 & 10 & -30 & 1 \\ 4 & 22 & 2 & -53 & -17 & 10 & 35 & -56 & 4 & 2 \\ 25 & 33 & -25 & -63 & -15 & 50 & -52 & 55 & -40 & -18 \\ 20 & 100 & -175 & -186 & 200 & 164 & -300 & 155 & -74 & 26 \\ -10 & 50 & -300 & -157 & 283 & 285 & -398 & 1 & 5 & 3 \\ -60 & -130 & 77 & 177 & -80 & -100 & 200 & -99 & 10 & 6 \\ 63 & 164 & -400 & -315 & 263 & 421 & -295 & 74 & 12 & 3 \\ 85 & -62 & 200 & 100 & 0 & -231 & 10 & -100 & 0 & -9. \end{pmatrix}.$$

These two matrices are similar to ones used in [11]. Using `cvx` *we find they share the CLF*

$$P = \begin{pmatrix} 151.0176 & 10.5565 & -88.2754 & -17.6837 & 53.1405 & 65.4895 & -37.1206 & 14.8879 & 1.9136 & 15.9521 \\ 10.5565 & 227.9709 & -18.1301 & -123.4884 & -28.4105 & 30.8213 & -52.8777 & -19.1084 & 24.3595 & -22.9054 \\ -88.2754 & -18.1301 & 332.8650 & -32.5420 & -148.2640 & -192.8825 & 62.6395 & -152.8850 & 8.5921 & -38.1044 \\ -17.6837 & -123.4884 & -32.5420 & 228.6863 & 56.0248 & -54.9520 & 71.8439 & -21.5091 & -33.0890 & 28.6729 \\ 53.1405 & -28.4105 & -148.2640 & 56.0248 & 108.9268 & 75.5634 & -22.4961 & 63.1685 & -7.1833 & 34.3685 \\ 65.4895 & 30.8213 & -192.8825 & -54.9520 & 75.5634 & 156.7282 & -71.8685 & 118.4509 & 9.1336 & 16.7224 \\ -37.1206 & -52.8777 & 62.6395 & 71.8439 & -22.4961 & -71.8685 & 70.6533 & -22.1807 & -22.8085 & 3.7827 \\ 14.8879 & -19.1084 & -152.8850 & -21.5091 & 63.1685 & 118.4509 & -22.1807 & 198.1232 & -6.2446 & 31.7575 \\ 1.9136 & 24.3595 & 8.5921 & -33.0890 & -7.1833 & 9.1336 & -22.8085 & -6.2446 & 24.4480 & -1.7274 \\ 15.9521 & -22.9054 & -38.1044 & 28.6729 & 34.3685 & 16.7224 & 3.782 & 731.7575 & -1.7274 & 20.4458. \end{pmatrix}$$

It is easy to verify that $\lambda_1(A_1^T P + P A_1) = -8.0104 < 0$ *and* $\lambda_1(A_2^T P + P A_2) = -21.1799 < 0$.

Keypoint II

Stability of switching systems is based on finding the right norm in which all subdynamics are dissipative.

2.4 Transient Dynamics

By way of motivation we will start with the two matrices

$$A_1 = \begin{pmatrix} -2 & 5 & -1 \\ 0 & -2 & 2 \\ 1 & 2 & -9 \end{pmatrix}, \quad A_2 = \begin{pmatrix} -1 & -3 & -5 \\ 0 & -3 & -10 \\ 0 & 0.1 & -50 \end{pmatrix}.$$

Both A_1 and A_2 are stable. However, the corresponding trajectories are qualitatively different, see Figure 2.3.

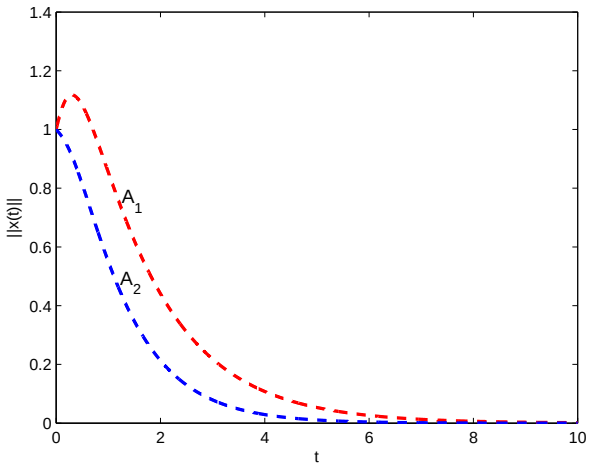

Figure 2.3: The transients and the asymptotic behaviours of A_1 (in red) and A_2 (in blue). A_1 shows a transient amplification of disturbances which is followed by a decay, whereas A_2 decays immediately.

.

The system governed by A_1 is unstable in the beginning of its evolution whereas the system A_2 decays, as expected, as time advances. These observations and others highlight the deficiency of eigenvalues in revealing the whole scenario of the dynamics under concern. This scenario is often exhibited by nonnormal operators and it is essentially ascribed to a lack of an orthogonal set of eigenvectors. The non-orthogonality (skewness) of eigenvectors drives the state of the system to move temporally away from the the equilibrium. A precise discussion can be found in [47, 109, 114]. This kind of behaviour is widely noticed in many physical systems. A comprehensive view on literature will be given in Chapter 3. To quantify and understand such observations a large amount of research works has ensued [84, 40, 39, 114]. In [84] a set of indices have been introduced. These are reactivity (v_0), the maximum amplification (ρ_{max}) and the time at which this amplification appears (t_{max}). Reactivity aims to measure how steep is the system response immediately after disturbances. It turns out that reactivity is given by the formula

$$v_0 = \lambda_1(\frac{A + A^T}{2}), \tag{2.5}$$

where λ_1 denotes to the maximum eigenvalue. For details of this derivation see Chapter 3. Reactivity is a measure based on using the quadratic norm $||x||_I = \sqrt{x^T x}$. However, a physical system can be treated with various norms which in turn can be used to seek further information about the system. In this regard we have introduced the notion of **P-reactivity** which measures the initial growth based on the norm $||x||_P = \sqrt{x^T P x}$. P-reactivity is measured by

$$v_0^P = \frac{1}{2}\lambda_1(P^{-\frac{1}{2}}(A^T P + PA)P^{-\frac{1}{2}}). \tag{2.6}$$

In the above example we have $\lambda_1(A_1^T + A_1) = 1.4287 > 0$, and hence the matrix A_1 is reactive. For the matrix A_2 we have $\lambda_1(A_2 + A_2^T) = -0.3936 < 0$ which means that it dissipates in the usual Euclidean norm. For the particular choice

$$P = \begin{pmatrix} -6.9574 & 47.1803 & -3.1428 \\ 0.5443 & -3.1428 & 8.0153 \\ 0 & 0.1 & -50 \end{pmatrix},$$

both matrices are P-reactive.

Keypoint III

The choice of norm influences reactivity of the system. Some systems are P-dissipative and some are P-reactive. A system can be P_1-dissipative but P_2-reactive.

2.5 Stability versus transients in biological systems

We have discussed the interplay between long term stability and short term transient and the role of choice of norm or Lyapunov function P in capturing these properties. In this section we explore this choice of norm and the corresponding consequences in a number of specific biological examples.

Predator prey system:

Consider the *Rosenzweing-MacArthur* predator prey model [101, 120]. The dynamics of the prey X and the predator Y are given as

$$\begin{aligned} \frac{dX}{dt} &= rX\left(1 - \frac{X}{K}\right) - \frac{aXY}{X+b} \\ \frac{dY}{dt} &= -dY + \frac{caXY}{X+b} \end{aligned} \tag{2.7}$$

The prey is assumed to increase logistically with intrinsic growth rate r within an environmental carrying capacity K. In the absence of prey the predator dies out with a rate d. The predator attacks the prey with a Holling Type II functional response. The parameter a represents the maximum killing rate whereas c stands for the conversion rate and b is the half saturation constant. The system has the positive equilibrium

$$X^* = \frac{bd}{ca - d} \quad \text{and} \quad Y^* = r\left(1 - \frac{X^*}{K}\right)\left(\frac{X^* + b}{a}\right).$$

Near (X^*, Y^*) the system behaves approximately like (2.3) with

$$A = \begin{pmatrix} r - \frac{2r}{K}X^* - \frac{abY^*}{(X^*+b)^2} & \frac{-aX^*}{X^*+b} \\ \frac{cabY^*}{(X^*+b)^2} & \frac{caX^*}{X^*+b} - d \end{pmatrix}.$$

Choosing $K = 1.25$, $a = 2.3$, $b = 1$, $r = 1$ and $c = 0.15$, Figure 2.4 shows the behaviour of stability ($\lambda_1(A)$), I-reactivity ($\lambda_1(A + A^T)$) and P-reactivity ($\lambda_1(P^{\frac{-1}{2}}(A^TP + PA)P^{-\frac{1}{2}})$) with $P = \begin{pmatrix} 2.2738 & 3.1588 \\ 3.1588 & 29.5485 \end{pmatrix}$, over a range of predator mortality rates d. As predator mortality increases, I-reactivity falls before it starts increasing. For the same range of parameters, first the system is P-reactive and then as we increase the parameter the system becomes P-dissipative. With a further increase in the parameter, the system returns to being P-reactive.

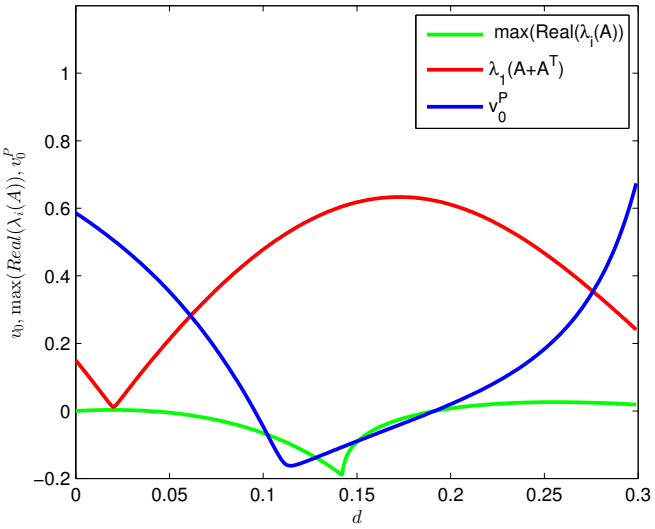

Figure 2.4: Stability (green), I-reactivity (blue) and P-reactivity (red) as functions of the predator death rate d. The rest of the parameters are chosen as : $K = 1.25$, $a = 2.3$, $b = 1$, $r = 1$ and $c = 0.15$. Note the contrasts between stability, I-reactivity and P-reactivity.

In [120], the dependence of I-reactivity on predation and conversion rate has been explored numerically. Figure 2.5 (left subplot) is a reconstruction of Figure 4 in [120] using a norm given by $P = I$, whereas Figure 2.5 (right subplot) is for the norm $||.||_{\widehat{P}}$ with

$$\widehat{P} = \begin{pmatrix} 2 & 3 \\ 3 & 5 \end{pmatrix}. \tag{2.8}$$

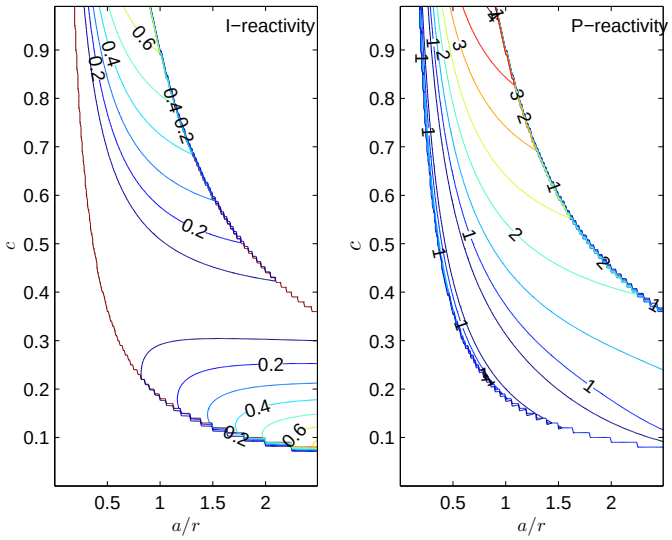

Figure 2.5: The values of I-reactivity and P-reactivity, labelled on the contour, over the $(\frac{a}{r}, c)$ parameter space. In the left subplot I-reactivity has two maxima. In the right subplot P-reactivity increases from bottom left to the top right. Here $P = \widehat{P}$ defined in (2.8).

Remark 2.5.2. *Since the per capita growth rate of the predator d is independent of its density then according to the result in [87] this food web must be reactive. However, this will not be the case if we consider all possible P-norms. This can be inferred from Figure 2.5 (left subplot) for $P = \widehat{P}$ from* (2.8)*. For instance, for the parameter choice* $(0.3, 0.8)$ *the resulting Jacobian becomes*

$$A = \begin{pmatrix} -0.3929 & -0.1250 \\ 0.2000 & 0 \end{pmatrix},$$

and the system is not $\widehat{P}$-reactive since

$$v_0^{\widehat{P}} = \frac{1}{2}\lambda_1(\widehat{P}^{-\frac{1}{2}}(A^T\widehat{P} + \widehat{P}A)\widehat{P}^{-\frac{1}{2}}) = -0.0745 < 0.$$

Reaction diffusion systems

Many biological phenomena are driven by two processes, so called reaction and diffusion. The reaction part affects the evolution in density. The diffusion part affects movement through space. We will study these in detail in Chapters 5, 6. Here we consider the Gray and Scott model [89, 37]. It is a reaction of two chemical compounds with concentrations u and v which are reacting and diffusing through space x. The equations of the model are

$$\begin{aligned} \frac{\partial u}{\partial t} &= d_u \nabla^2 u - uv^2 + F(1-u) \\ \tfrac{\partial v}{\partial t} &= d_v \nabla^2 v + uv^2 - (F+k)v \end{aligned} \tag{2.9}$$

We will focus only on the positive steady state

$$u = \frac{1-\sqrt{d}}{2}, \quad v = \frac{\alpha(1+\sqrt{d})}{2},$$

where $d = 1 - \frac{4(F+k)^2}{F} > 0$ (assumed) and $\alpha = \frac{F}{F+k}$, see Appendix A. Linearising (2.9) around this equilibrium yields the matrix pencil

$$A - \boldsymbol{k}^2 D,$$

where A is the Jacobian of the reaction part around the equilibrium,

$$D = \begin{pmatrix} d_u & 0 \\ 0 & d_v \end{pmatrix}$$

and $\boldsymbol{k}$ is the wave number. Details of this sort of analysis will be considered in Chapter 5. The stability of this matrix pencil is an indicator for pattern generation (Chapters 5, 6). More precisely, if for some wave number $\boldsymbol{k}$ this

matrix pencil has at least one eigenvalue with a positive real part then we will expect a heterogeneity in the distribution of u and v through the space. Let

$$P = \begin{pmatrix} 2.0680 & 0.8763 \\ 0.8763 & 1.4365 \end{pmatrix}.$$

The matrix $-D$ (with $d_u = 0.00006$ and $d_v = 0.00001$) is both I and P-dissipative. We investigate how A switches from being I and/or P reactive as we vary the parameter k. When A is P-dissipative then P is a Lyapunov function for A and $-D$. Then $A - \boldsymbol{k}^2 D$ is stable for all $\boldsymbol{k}$.

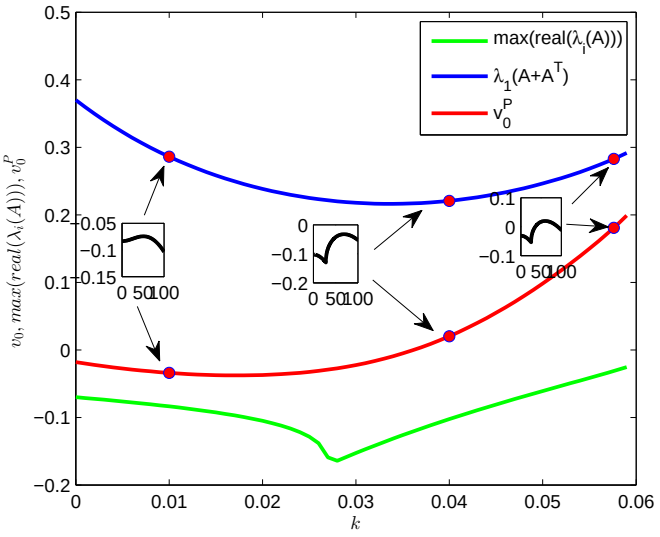

Figure 2.6: Stability, I-reactivity and P-reactivity as a function of parameter k: Green-solid depicts $\lambda(A)$, blue depicts I reactivity and red depicts P-reactivity. Note the contrasting values of these indicators as we vary k. In these plots, F=0.07.

For $k = 0.01$, A is stable and I-reactive but not P-reactive. In this case $A - \boldsymbol{k}^2 D$ is stable for all $\boldsymbol{k}$. For $k = .04$ A is both I and P-reactive but still $A - \boldsymbol{k}^2 D$ is stable for all $\boldsymbol{k}$. For $k = 0.05761$, A is stable and both I and P are reactive. In this case $A - \boldsymbol{k}^2 D$ is not stable for all $\boldsymbol{k}$ and pattern formation is

possible. The issue is that the choice of P is inconclusive for some parameter ranges. More thorough investigation of this is the focus of Chapters 5 and 6.

2.6 Concluding remarks

Finding a norm in which system energy dissipates is in fact the essence of Lyapunov's direct method contribution. In this chapter we stressed the importance of norm-choice (energy reference choice) for detecting stability and transients of LTI systems. We add a slight extension to Theorem 2.3.1 introduced in [108] which gives necessary and sufficient conditions for existence of CLF. Namely, we relax the hypothesis to include just distinct negative eigenvalues instead of all negative eigenvalues. Also we highlight the potential of the Matlab package `cvx` in finding common Lyapunov function for stable matrices of any order, Example 2.3.4. Furthermore, we pointed out that the traditional measure of initial amplification, reactivity, is based on using a very specific norm, namely $||x|| = \sqrt{x^T x}$. We extend this to what we called P-reactivity which, as we have mentioned, refers to the transient amplifications of disturbances with respect to the norm defined by P. The notion of P-reactivity is known in the literature as the initial growth. However, its use is new in the context of biological community. Indeed, as far as we are aware, it has never been used explicitly in a context of ecological studies . With the aid of a predator prey example in Section 2.7, we showed that the result proved in [87] which link reactivity with the density dependence of species is generally not valid for any norm, Remark 2.5.2.

Chapter 3

P-Reactivity

In this chapter we further stress the importance of transient dynamics via exploring related literatures, Section 3.1. We also introduce a formal definition for the notion of P-reactivity. We give a detailed derivation of the formula (2.6). In Section 3.2, we formulate an optimization problem aiming to determine the P-norm which yields maximum reactivity. We solve the problem in the particular case of 2×2 matrices numerically and through simulations.

3.1 Introduction

The scenario shown in Figure 2.3, Chapter 2, is widely noticed in many physical systems. In fluid mechanics, for instance, [114], flows in a moving fluid can have unstable appearance, although the underlying eigendata suggest that the fluid will eventually settle to a laminar state [114].

Theoretical ecology has traditionally relied on the analysis of long-term asymptotic behaviour as an approach to understanding ecological dynamics [39, 40]. However, often experiments are conducted in shorter time scales and the rel-

evant time scale can be too short. This can lead to a mismatch between observed experiments and the information gained from the theoretical models examined [39] since many systems can behave very differently in the first time steps of their time courses [39, 40, 84]. Ignoring such characteristics can result in useless information or even completely misleading predictions. The importance of such time scale related regimes has been recognised since the appearance of the epidemic models studied by Kermack and MacKendrick [55]. The emphasis was on the time evolution of the epidemic instead of its eventual picture. Recently, a growing recognition amongst the scientific community of the relevance of these non-asymptotic scenarios has been reported [114, 47, 39]. In [39] the role of a system transients on understanding its long-time state has been stressed. The argument has been supported by various examples. In [84], the significance of resilience and asymptotic stability of stable linear systems has been argued. The authors showed that a stable system can show temporal instability that is inconsistent with the underlying eigendata which suggest stable behaviour. In applications, for instance ecosystems restoration [84, 86], managers are interested in both the long-term and the short-term consequences of their actions. This can have major economical impacts. The effects of short-time dynamics on biological pest control has also been explored [57]. It is worth adding here that these transients dynamics can be indicators for the appearance of some systems characteristics. A recent example, see Chapter 5, is the necessity of reactivity for Turing pattern formation [85]. Our main result in Chapter 5 goes in the same direction. It seems that this approach of linking transients with other systems characteristics warrants deeper exploration. Henceforth, quantifying and understanding these transients is significant. For this, a large amount of research has ensued [84, 47, 109, 114]. One prevailing

measure of transient behaviour is its *transient bound* [47]. It gives the extent of deviation of a system state after perturbation. In [114] the idea of Pseudospectrum is introduced as a qualitative approach which can be used to understand the extent of transients. [114] is an excellent source which provides a comprehensive thorough on systems transients. Reactivity (v_0), as we have mentioned in Chapter 2, is aiming to measure how steep is the system response immediately after disturbances. The following section provides a detailed analysis of reactivity.

3.1.1 Reactivity or Initial Growth

Reactivity has been documented in many ecological systems such as predator prey models, food web models, stage structured models and ecosystem compartment models [120]. Although the underlying idea is not new [19, 47], reactivity has recently captured the attention of ecological researches. According to Neubert and Caswell [84], the system (2.3) is reactive if for some x_0 the trajectory $x(t)$ temporarily moves away from the origin before approaching it as $t \to \infty$. In numerical linear algebra, reactivity is called initial growth [19, 47].

Definition 3.1.1. *Reactivity v_0 of the system* (2.3) *is the maximum, over all initial perturbations x_0, of the rate at which trajectories depart from the origin. Following [84], mathematically this can be written as*

$$v_0 = \max_{||x_0|| \neq 0} \left[\left(\frac{1}{||x(t)||} \frac{d||x(t)||}{dt} \right)_{t=0} \right]. \tag{3.1}$$

A simple formula for calculating reactivity has been derived in [84] as follows

First with $||x|| = \sqrt{x^T x}$ we have for $x \neq 0$

$$\frac{d||x(t)||}{dt} = \frac{x(t)^T(dx(t)/dt) + (dx(t)/dt)^T x}{2||x(t)||} = \frac{x(t)^T(A + A^T)x(t)}{2||x(t)||}.$$

Hence

$$\frac{1}{||x(t)||}\frac{d||x(t)||}{dt} = \frac{x(t)^T(A + A^T)x(t)}{||x(t)||^2} = \frac{x(t)^T(A + A^T)x(t)}{2x(t)^T x(t)}.$$

Evaluating this at an arbitrary disturbance $x(0) = x_0$ we get

$$\left(\frac{1}{||x(t)||}\frac{d||x(t)||}{dt}\right)_{t=0} = \frac{x_0^T(A + A^T)x_0}{2x_0^T x_0}$$

and hence over all normalised disturbances (i.e. $||x_0|| = 1$), we have

$$v_0 = \max_{x_0^T x_0 = 1} \frac{x_0^T(A + A^T)x_0}{2x_0^T x_0}.$$

Using the *Rayleigh principle* [50] we get

$$v_0 = \lambda_1(\frac{A + A^T}{2}), \tag{3.2}$$

where λ_1 refers to the maximum eigenvalue. This maximum value is attained when the system is perturbed in the direction of the eigenvector corresponding to the maximum eigenvalue of $A+A^T$. If $\lambda_1(A+A^T) > 0$, then the equilibrium is said to be reactive, otherwise it is not reactive.

Remark 3.1.3. *Note that non reactivity of* (2.3) *is equivalent to*

$$A^T + A \leq 0.$$

This means that the identity matrix I is a Lyapunov function for the system (2.3) *and consequently the systems state with respect to the underlying quadratic norm ($x^T x$) will converge to, or at least remains near to, the origin* 0.

It is worth emphasizing here that reactivity essentially refers to the instantaneous growth rate of a system state with respect to a very particular quadratic norm ($||.||_P$, with $P = I$). As we have mentioned earlier, a system can be non-dissipative with respect to, a rather different, P-norm. This observation motivates us to extend reactivity in the Neubert and Caswell sense to what we call P-reactivity. In this sense, reactivity in Neubert et. al [84] corresponds to $P = I$.

3.1.2 P-Reactivity

The system (2.3) is P-reactive if for some initial state $x(0)$ the trajectory $x(t)$ temporarily moves from an inner level surface of $V = x^T P x$ to an outer one before returning to the origin as $t \to \infty$. Following the same argument carried out above, P-reactivity can be defined as follows.

Definition 3.1.2. *P-reactivity of the system* (2.3) *with respect to the quadratic norm defined by the positive definite matrix P is*

$$v_0^P := \max_{||x_0||_P \neq 0} \left[\left(\frac{1}{||x(t)||_P} \frac{d||x(t)||_P}{dt} \right)_{t=0} \right].$$

Proposition 3.1.2. *The system* (2.3) *is P-reactive if, and only if,*

$$\lambda_1(P^{-\frac{1}{2}}(A^T P + PA)P^{-\frac{1}{2}}) > 0.$$

Proof

With $||x|| = \sqrt{x(t)^T P x(t)}$, we have for $x \neq 0$ that

$$\frac{d||x(t)||_P}{dt} = \frac{d\sqrt{x(t)^T P x(t)}}{dt} = \frac{x(t)^T P\dot{x}(t) + \dot{x}(t)^T P x(t)}{2\sqrt{x(t)^T P x(t)}}$$
$$= \frac{x(t)^T (A^T P + PA) x(t)}{2||x(t)||_P}.$$

Then

$$\left(\frac{1}{||x(t)||_P}\frac{d||x(t)||_P}{dt}\right)_{t=0} = \frac{x_0^T (A^T P + PA) x_0}{2x_0^T P x_0}.$$

Taking the maximum over all the x_0 we obtain

$$\max_{x_0^T P x_0 = 1} \left(\frac{x_0^T (A^T P + PA) x_0}{2x_0^T P x_0}\right). \tag{3.3}$$

Now we can write

$$x_0^T P x_0 = x_0^T P^{\frac{1}{2}} P^{\frac{1}{2}} x_0 = (P^{\frac{1}{2}} x_0)^T P^{\frac{1}{2}} x_0 = z^T z,$$

where $z = P^{\frac{1}{2}} x_0$ and $x_0 = P^{-\frac{1}{2}} z$. Substituting in (3.3) we obtain

$$\max_{x_0^T P x_0 = 1} \left(\frac{x_0^T (A^T P + PA) x_0}{2x_0^T P x_0}\right) = \max_{z^T z = 1} \left(\frac{(P^{\frac{-1}{2}} z)^T (A^T P + PA) P^{\frac{-1}{2}} z}{2z^T z}\right)$$

$$= \max_{z^T z = 1} \left(\frac{(z^T P^{\frac{-1}{2}} (A^T P + PA) P^{\frac{-1}{2}} z}{2z^T z}\right) = \frac{1}{2}\lambda_1 (P^{\frac{-1}{2}} (A^T P + PA) P^{\frac{-1}{2}}).$$

Hence we obtain

$$v_0^P = \frac{1}{2}\lambda_1 (P^{\frac{-1}{2}} (A^T P + PA) P^{\frac{-1}{2}}), \tag{3.4}$$

and this value is attained at the eigenvector corresponding to the maximum eigenvalue of $P^{\frac{-1}{2}}(A^TP + PA)P^{\frac{-1}{2}}$.

Corollary 3.1.1. *For the stable matrix A and the positive definite matrix $P > 0$ the following hold*

- $\lambda_1(P^{\frac{-1}{2}}(A^TP + PA)P^{\frac{-1}{2}}) > 0$ *is equivalent to* $\lambda_1(A^TP + PA) > 0$.
- *A is P-reactive if, and only if, P is not a Lyapunov function for A.*

Example 3.1.5. *Consider the matrix*

$$A = \begin{pmatrix} -5 & 5 \\ 0 & -2 \end{pmatrix}.$$

Here

$$A + A^T = \begin{pmatrix} -5 & 5 \\ 0 & -2 \end{pmatrix} + \begin{pmatrix} -5 & 0 \\ 5 & -2 \end{pmatrix} = \begin{pmatrix} -10 & 5 \\ 5 & -4 \end{pmatrix} < 0.$$

Hence A is not I-reactive (i.e I is a Lyapunov function), but A is P-reactive with

$$P = \begin{pmatrix} 2 & 3 \\ 3 & 5 \end{pmatrix},$$

since,

$$A^TP + PA = \begin{pmatrix} -10 & -15 \\ 4 & 5 \end{pmatrix} + \begin{pmatrix} -10 & 4 \\ -15 & 5 \end{pmatrix} = \begin{pmatrix} -20 & -11 \\ -11 & 10 \end{pmatrix},$$

which gives $\lambda_1(P^{\frac{-1}{2}}(A^TP + PA)P^{\frac{-1}{2}}) = 12.2354 > 0$. Figure 3.1 shows the behaviour of the perturbed origin. Perturbations are amplified with respect to

the norm defined by P (blue curve) whereas with respect to the norm defined by I perturbations die out (red curve).

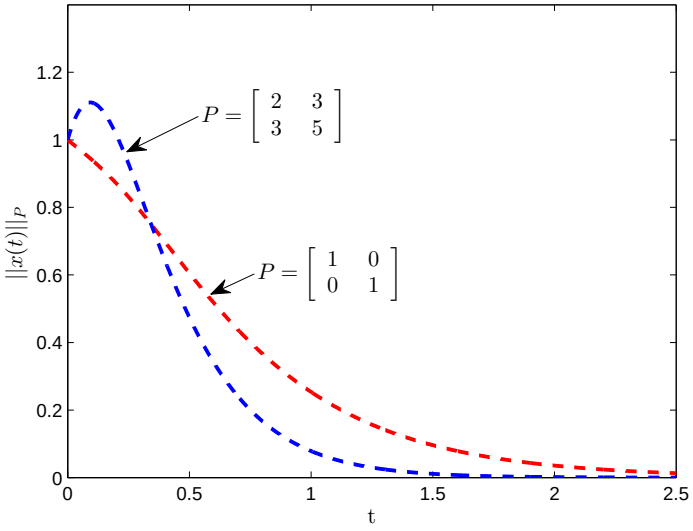

Figure 3.1: The transient response for the matrix A traced by two different P-norms. The system is not I-reactive (red curve) but it is P-reactive (blue curve).

3.2 P-Reactivity Optimization

Finding the quadratic norm $\sqrt{x^T P x}$ with respect to which a stable system is maximally amplified is in its own right mathematically interesting. Maximum P-reactivity represents the worst case scenarios over all the possible quadratic norms $||.||_P$ induced by $P > 0$. The bigger the P-reactivity the greater the sensitivity to perturbations to the state. In this section we pose an optimization problem seeking the norm which yields maximum P-reactivity.

3.2.1 Main problem

For a given stable matrix A, we are seeking the positive definite matrix P which yields maximum P-reactivity. Mathematically this can be written as

$$\begin{aligned} &\text{maximize} \quad \lambda_1(P^{-\frac{1}{2}}(A^TP + PA)P^{-\frac{1}{2}}) \\ &\text{subject to} \quad P > 0. \end{aligned} \tag{3.5}$$

For convenience we drop the $\frac{1}{2}$ in (3.4). In this optimization problem the decision variable is a positive definite matrix $P > 0$ and the objective function is a nonlinear, convex function in the variable P. The problem itself is not a convex optimization problem because it involves maximization instead of minimization [9]. This problem often has multiple maxima, and hence finding an analytic solution of this problem is, in most cases, extremely hard particularly in high dimensional cases. One possible way to tackle this problem is to replace the objective function with a concave relaxation and use `cvx`. This approach demands finding the best relaxation which we couldn't find yet. Moreover this approach always remains an approximation. In this chapter we will develop a numerical based scheme to find an approximate solution to the problem in the case when the dimension is 2. We specifically combine simulations with using a global optimization algorithm, namely the genetic algorithm (GA). We utilize the genetic algorithm to numerically compute the maxima.

3.2.2 Second Order Matrices

Set

$$X = P^{-\frac{1}{2}}(A^TP + PA)P^{-\frac{1}{2}},$$

where

$$A = \begin{pmatrix} a & b \\ c & d \end{pmatrix}.$$

We are interested in the maximum eigenvalue of X and how this depends on P. Now the maximum eigenvalue of X is given by

$$\lambda_1(X) = \frac{\text{trace}(X) + \sqrt{(\text{trace}(X))^2 - 4\text{det}(X)}}{2}$$

We have

$$\begin{aligned} \text{trace}(X) &= \text{trace}((P^{-\frac{1}{2}}(A^TP + PA)P^{-\frac{1}{2}})) \\ &= \text{trace}(P^{-\frac{1}{2}}A^TP^{\frac{1}{2}} + P^{\frac{1}{2}}AP^{-\frac{1}{2}}) = 2\text{trace}(A) < 0. \end{aligned}$$

Hence the trace of X is independent of the matrix P. Therefore the objective function in (3.5) becomes

$$\text{trace}(A) + \sqrt{(\text{trace}(A))^2 - \text{det}(X)}.$$

It follows that P-reactivity is maximised when $\text{det}(X)$ is minimised. In other words we can, instead, solve the optimization problem

$$\begin{aligned} &\text{minimize} \quad \text{det}(P^{-\frac{1}{2}}(A^TP + PA)P^{-\frac{1}{2}}). \\ &\text{subject to} \quad P > 0. \end{aligned} \tag{3.6}$$

For the positive definite matrix

$$P = \begin{pmatrix} p & q \\ q & r \end{pmatrix},$$

and using determinant properties, the problem (3.6) can be rewritten as

$$\begin{aligned} &\text{minimize} \quad \frac{\det(A^T P + PA)}{pr - q^2}, \\ &\text{subject to} \quad pr > q^2, p > 0, r > 0, \end{aligned} \tag{3.7}$$

It turns out that this objective function can be unbounded unless we pose some suitable restrictions on P. To see this we consider the following possible candidate

$$P = \begin{pmatrix} p & 1 \\ 1 & r \end{pmatrix}.$$

Accordingly, the objective function, $\det(X)$, of (3.7) becomes

$$\begin{aligned} \det(X) = \big(&- a^2 + 2abp - 2acr + 4adpr - 2ad - b^2p^2 - 2bcpr + 4bc \\ &- 2bdp - c^2r^2 + 2cdr - d^2\big)\big(pr - 1\big)^{-1}. \end{aligned}$$

Dividing both the numerator and the denominator by pr we get

$$\det(X) = \frac{C_1 - (\frac{p}{r})b^2 - (\frac{r}{p})c^2 + (\frac{1}{pr})C_2 + (\frac{1}{p})C_3 + (\frac{1}{r})C_4}{1 - \frac{1}{pr}}, \tag{3.8}$$

where

$$\begin{cases} C_1 = 4ad - 2bc = 4\det(A) + 2bc, \\ C_2 = -(a^2 + 2ad + d^2 - 4bc) = -(\text{trace}(A))^2 - 4bc, \\ C_3 = 2(cd - ac), \\ C_4 = 2(ab - bd). \end{cases}$$

Note:

It is clearly seen that expression (3.8) is finite for finite choices of p and r but possibly unbounded as $pr \to 1$. For large values of p and r it can be

unbounded and hence P-reactivity can be infinity. To make this point clear we will examine (3.8) based on the values of b and c as follows.

- **Assume $b = c = 0$:**

  The expression (3.8) is reduced to

  $$\det(X) = \frac{4ad + (\frac{1}{pr})\text{trace}(A)}{1 - \frac{1}{pr}}.$$

  If $4ad + a + d < 0$ then $\det(X) \to -\infty$ as $pr \to 1$.

- **Assume $b = 0$ and $c \neq 0$:**

  In this case (3.8) becomes

  $$\frac{4ad - (\frac{r}{p})c^2 - (\frac{1}{pr})(a-d)^2 + 2(\frac{1}{p})(cd - ac)}{1 - \frac{1}{pr}}.$$

  Now along any path with r faster than p (e.g. $p(s) = p_0$, $r(s) = s$, where s is a parameter) we have

  $$\det(X) \to -\infty \quad \text{as} \quad r \to \infty$$

- **Assume $b \neq 0$ and $c \neq 0$:**

  In this case $\det(X) \to -\infty$ for any path where either p is faster than r and $p \to \infty$ or r is faster than p and $r \to \infty$.

Corollary 3.2.2. *P-reactivity is unbounded on*

$$\boldsymbol{P} = \left\{ \begin{pmatrix} p & q \\ q & r \end{pmatrix} : p, r > 0, pr > q^2 \right\},$$

The problem is an ill-posed problem if we do not consider the limits of p and r, which essentially reflect the lengths of the major and minor axis of P. In other words we need to restrict the P-norm.

3.3 A new problem set up: A well-posed version

One obvious approach to tackle this problem is to bound the maximum eccentricity of the desired P. To make this point clear, first we know that we always can write

$$\begin{aligned} P = Q^T D Q = Q^T \begin{pmatrix} d_1 & 0 \\ 0 & d_2 \end{pmatrix} Q = d_1 Q^T \begin{pmatrix} 1 & 0 \\ 0 & \frac{d_2}{d_1} \end{pmatrix} Q \\ = d_1 Q^T D Q = d_1 Q^T \begin{pmatrix} 1 & 0 \\ 0 & e \end{pmatrix} Q, \end{aligned}$$

where

$$Q = \begin{pmatrix} \cos(\theta) & -\sin(\theta) \\ \sin(\theta) & \cos(\theta) \end{pmatrix}$$

is a rotation matrix. The parameters d_1 and d_2 are the singular values of P and they are exactly the lengths of the major and the minor axes of the ellipse $x^T P x = c$. Without loss of generality we can assume that $d_1 > d_2$.

Here, the parameter e is the maximum eccentricity of P. We will constrain the problem by letting our decision variables be confined between two ellipses with eccentricity e_c and 1. Now returning to the objective function in (3.6), substitution leads to

$$\det(X) = \frac{1}{e}\det\left(A^T Q^T \begin{pmatrix} 1 & 0 \\ 0 & e \end{pmatrix} Q + Q^T \begin{pmatrix} 1 & 0 \\ 0 & e \end{pmatrix} QA\right) \tag{3.9}$$

Equation (3.9) is a two variable function which can be maximised using an optimization routine such as genetic algorithm (GA).

Example 3.3.6. *Consider the predator prey model* (2.7) *in Chapter 2. For the sake of illustration we will restrict the eccentricity to be within* $[0.2, 1]$. *Implementing* (3.9) *in Matlab, Figure 3.2 shows all possible values of 3.9 in the* (θ, e) *parameter space.*

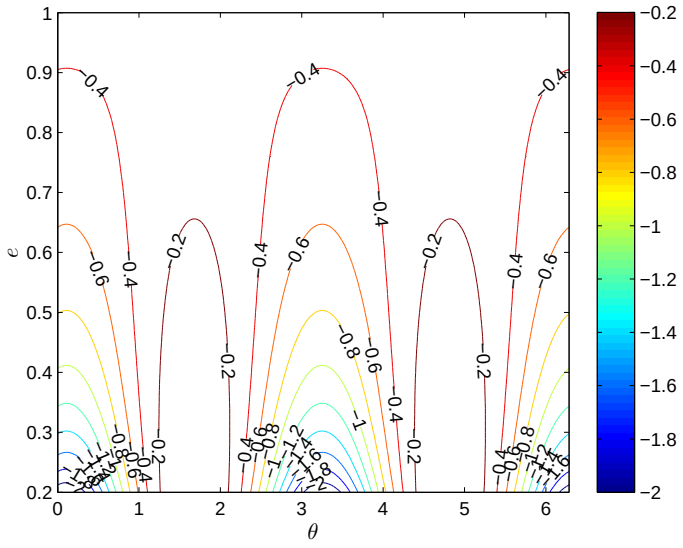

Figure 3.2: The values of (3.9) of the predator prey model (2.7). It is clear that maximum P-reactivity can be attained at many choices of θ and e. The parameters are chosen as : $K = 1.25$, $a = 2.3$,$b = 1$ $r = 1$ and $c = 0.15$.

It is evidently clear that 3.9 has many minima. Applying the genetic algorithm, with (3.9) *as a fitness function, the optimum value is* $det(X) \approx -2.168$ *and this value can be attained at* $(\theta, e) \approx (0.1086, 0.2000)$. *Hence maximum* P*-reactivity is approximately* 0.6733. *Accordingly the optimum* P *is given as*

$$P_1 = \begin{pmatrix} 0.9906 & -0.0862 \\ -0.0862 & 0.2094 \end{pmatrix}. \tag{3.10}$$

Figure 3.3 depicts the maximum amplification rate in the predator prey state space model with respect to the P*-norm defined by* (3.10).

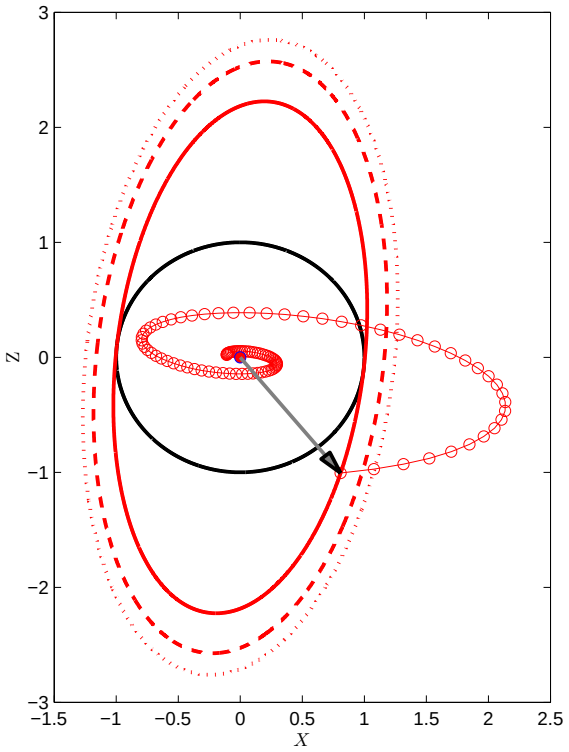

Figure 3.3: The maximum P-reactivity of the predator prey system. The parameters are chosen the same as in Figure 3.2

3.4 Notes and Concluding Remarks

This chapter focused on reactivity which is an important index of transient dynamics introduced in [84]. Reactivity, in Neubert and Caswell sense, has been extended to what we called P-reactivity which refer to the maximum possible departure rate, over all perturbations, of the system state from the origin with respect to the norm $\sqrt{x^T P x}$. A precise mathematical definition for P-reactivity has been given. We derived the formula (3.4) which determine systems P-reactivity. When $P = I$ the formula is equivalent to the one derived in [84]. We speculate that P-reactivity can be more significant than reactivity in Neubert and Caswell sense where energy variations of physical systems are often constrained. In other words, the energy variation needed to be maintained can be so specific so that can not captured by the norm defined by I. An optimization problem aiming to determine the norm with respect to which a system has maximum P-reactivity has been introduced. The problem has been solved numerically for second order systems.

Chapter 4

Robustness of Joint Dissipation

In this chapter we further explore joint-dissipativity (that is CLF existence). We specifically discuss the capability of jointly-dissipative systems to sustain this property when they are exposed to certain levels of disturbances. We use stability radii as a quantitative measure of this robustness. For analysis we adapt the approach used in [47, 46, 45]. Section 4.1 discusses the main aspects of the analysis of this approach. In Section 4.2.1, we investigate the robustness with respect to a specific CLF. For this we focus on perturbations with k parameters of the form $\Delta_1 = \Sigma_{i=1}^{k} \delta_i D_i E_i$, where D_i and E_i are, respectively, columns and rows. In Section 4.2.2, the robustness of the necessary and sufficient condition for the existence of a CLF is explored for perturbations of the form $\Delta_2 := D\Delta E$, where Δ is a possibly unstructured, arbitrary matrix.

4.1 Motivation

Even a very well controlled physical system is prone to system uncertainties. Model uncertainties can arise for several reasons: Parameter uncertainty, im-

perfect knowledge of the system dynamics and model simplifications [47, 123]. In biological systems model uncertainty can happen due to paucity of data. Examining the capability of a stable system to preserve some of its dynamic properties in the presence of uncertainty is a central issue in robustness analysis [47, 123, 44]. There are various tools for this purpose [47]. Spectral value sets, for example, visualise how the location of system eigenvalues respond to parameter changes for various level of uncertainties. They enable us to judge, in some sense, the fragility of the system under study. This approach, beside being a qualitative approach, can not be used for certain classes perturbation [123, 47].

Often systems' desired characteristic(s) are expressed by constraints on the spectrum. A system is said to be $\mathbb{C}_g$-stable if its eigenvalues lie in the set $\mathbb{C}_g$ (g for good). The complement of $\mathbb{C}_g$ is $\mathbb{C}_b$ (b for bad) is where the characteristic(s) are not of interest or often need to be avoided [44]. The goal of robustness analysis, in this context, is to look at the uncertainty levels which can be tolerated without losing the property that the system spectrum lies in $\mathbb{C}_g$ [47]. A very elegant, but sometimes intractable, approach to do this is to measure the stability radius, see [46], associated with the problem. The stability radius is a quantitative measure which provides the smallest uncertainty level needed to move the spectrum of the system to intersect with $\mathbb{C}_b$. The following section recalls the main aspects of the analysis performed in [47] to characterise stability radii. Subsection 4.1.1 considers arbitrary $\mathbb{C}_b$ whereas Subsection 4.1.2 is devoted to the specific case $\mathbb{C}_b = i\mathbb{R}$.

4.1.1 A stability radii: A general frame work

For illustration we restrict attention to a particular perturbation structure. We will assume that the system (2.3) is perturbed to

$$\dot{x}(t) = (A + D\Delta E)x(t). \tag{4.1}$$

Here $(A, D, E) \in \mathbb{K}^{n\times n} \times \mathbb{K}^{n\times m} \times \mathbb{K}^{p\times n}$, $\Delta \in \mathbb{K}^{m\times p}$ is an unknown perturbation matrix, $\mathbb{K} = \mathbb{C}$ or $\mathbb{R}$, and the matrices D and E determine the structure of the perturbation. This perturbation is referred to as a structured perturbation. If $D = E = I$ the perturbation is called unstructured. The stability radius of the matrix A under the perturbation $D\Delta E$, with respect to a given $\mathbb{C}_g$, can be defined as

$$r_{\mathbb{K}}(A; D, E; \mathbb{C}_g) = \inf\{||\Delta|| : \sigma(A + D\Delta E) \not\subset \mathbb{C}_g\}.$$

The norm $||.||$ refers to the spectral norm. Equivalently

$$r_{\mathbb{K}}(A; D, E; \mathbb{C}_g) = \inf\{||\Delta|| : \sigma(A + D\Delta E) \cap \mathbb{C}_b \neq \phi\}.$$

As we have mentioned the choice of $\mathbb{C}_g$ depends on the characteristics we are interested in. Often it is a subset of the left half of the complex plane. For illustration and making things more concrete we will discuss in detail the case when $\mathbb{C}_g = \mathbb{C}_-$, the open left half of the complex plane. This obviously means that we are interested in studying the robustness of A to preserve its asymptotic stability in the Hurwitz sense.

4.1.2 A special Case: The Destabilizing Δ

The aim of this section is to outline, through a particular case, the main aspects of the approach used in [47] for studying robustness through arability radii. This will make the analysis in the Subsections 4.2.1 and 4.2.2 easy to follow. The particular case we will address here is the robustness of the system (2.3) to preserve stability. In this case the stability radius is the smallest $||\Delta||$ which puts an eigenvalue of A on the boundary of the set $\mathbb{C}_g = \mathbb{C}_-$ (i.e. on $i\mathbb{R}$). In other words we need the smallest $||\Delta||$ which satisfies

$$(A + D\Delta E)v = i\omega v \quad \text{for some} \quad v \neq 0, \quad \omega \in \mathbb{R}. \tag{4.2}$$

Since A is Hurwitz it does not have an eigenvalue on the imaginary axis, so we have $Ev \neq 0$. Rearranging 4.2 gives

$$v = (i\omega I - A)^{-1} D\Delta E v \quad \Longrightarrow \quad Ev = E(i\omega I - A)^{-1} D\Delta E v.$$

Taking norms on both sides we get

$$||Ev|| \leq ||E(i\omega I - A)^{-1} D|| ||\Delta|| ||Ev||.$$

Since the aim is to find the smallest destabilizing perturbation then we can look for a value of ω which minimizes the right hand side. Hence destabilizing $||\Delta||$s must satisfy

$$||\Delta|| \geq \min_{\omega \in \mathbb{R}} \frac{1}{||E(i\omega I - A)^{-1} D||}. \tag{4.3}$$

Converting the inequality to an equality is elegantly done in [47]. The idea is to find at least one destabilizing Δ with

$$||\Delta|| = \min_{\omega\in\mathbb{R}} \frac{1}{||E(i\omega I - A)^{-1}D||}.$$

Assume that ω^* gives the minimum. That is, we have

$$\min_{\omega\in\mathbb{R}} \frac{1}{||E(i\omega I - A)^{-1}D||} = \frac{1}{||E(i\omega^* I - A)^{-1}D||} = r, \quad \text{for some } r.$$

We can write

$$||E(i\omega^* I - A)^{-1}D|| = ||E(i\omega^* I - A)^{-1}Du|| \quad \text{for some} \quad ||u|| = 1.$$

Let

$$v := E(i\omega^* I - A)^{-1}Du.$$

In [47], the candidate Δ^* to achieve the minimum is introduced as

$$\Delta^* = \frac{uv^*}{||v||^2}. \tag{4.4}$$

We need to show that this Δ^* is the minimum and that it destabilises. It is clear that

$$||\Delta^*|| = \frac{||uv^*||}{||v||^2} = \frac{||u||||v||}{||v||^2} = \frac{1}{||v||} = r.$$

Hence $||\Delta||$ is exactly the minimum. Moreover we have

$$\Delta^* v = \frac{uv^*}{||v||^2} v = u.$$

Now we define

$$x := (i\omega^* I - A)^{-1} Du \quad \text{then} \quad Ex = E(i\omega^* I - A)^{-1} Du = v.$$

Hence we have

$$(i\omega^* I - A)x = Du = D\Delta^* v = D\Delta^* Ex,$$

equivalently we have

$$(A + D\Delta^* E)x = i\omega x,$$

which indicates that Δ^* is destabilising. Since Δ^* is complex (since u and v are) we in fact have showed that

$$\begin{aligned} r_{\mathbb{C}}(A; D, E, \mathbb{C}_-) &= \min_{\omega \in \mathbb{R}} \frac{1}{||E(i\omega I - A)^{-1} D||} = \min_{\omega \in \mathbb{R}} \sigma_n(E(i\omega I - A)^{-1} D) \\ &= \min_{\omega \in \mathbb{R}} ||G(i\omega)||^{-1}. \end{aligned}$$

Here, $G(i\omega) = E(i\omega I - A)^{-1} D$ is referred to as the transfer function. The term is borrowed from control theory as the perturbation (4.1) can be viewed as a feedback control problem, see [47]. If Δ is real then the previous argument fails. In this case all we know is

$$r_{\mathbb{R}}(A; D, E, \mathbb{C}_-) \geq \min_{\omega \in \mathbb{R}} \frac{1}{||E(i\omega I - A)D)^{-1}||}.$$

For the complex stability radius (less natural in applications) there do exist computable formulae. One approach is to construct the Hamiltonian matrix associated with the problem see [47, p.602]. Unlike the complex stability ra-

dius, finding a computable formula for real stability radius is, in most cases, quite tricky. Large amounts of effort have been devoted to finding computable formulae for $r_{\mathbb{R}}$, see [44, 43, 100, 42]. There has been some success in this direction. However this is just for a few limited cases. In Qui et. al [100], for instance, a computable formulae has been developed. The computation involves finding of the μ-value of a matrix related to the problem. For the cases when D is a column or E is a row, easy computable formulae have been developed in [42].

As the computation of stability radii involves determination of the resolvent $(\lambda I - A)^{-1}$, a formula known as *Sherman-Morrison-Woodbury* formula, see [35, p.50], has been used in the characterisation of stability radii [48]. The formula is given as follows. For dimensionally compatible matrices U and V such that A and $A + UV$ are invertible, we always have

$$(A + UV)^{-1} = A^{-1} - (A^{-1}U(I + VA^{-1}U)^{-1}VA^{-1}).$$

A key consequence of this formula is the following: If λ is not an eigenvalue of A, then λ is an eigenvalue of $A + UV$ if, and only if,

$$1 \quad \text{is an eigenvalue of} \quad V(\lambda I - A)^{-1}U. \tag{4.5}$$

For proof see Appendix A. We will use (4.5) in the characterisation of the stability radii in Section 4.2.1. As we shall see a crucial step of the analysis is to write $\Sigma_{i=1}^{k} \delta_i D_i E_i = UV$. Now we state the main problem of the chapter.

4.2 The Main Problem

If the stable matrices A and B share a strict CLF $P > 0$ and one of them (say A) is perturbed as $A + \Delta$, then we seek the largest ρ such that if $||\Delta|| < \rho$, then P is still a strict CLF for $A + \Delta$ and B, meaning that

$$(A + \Delta)^T P + P(A + \Delta) < 0$$
$$B^T P + PB < 0.$$

The above problem can be equivalently written as: Find

$$\min ||\Delta|| \quad \text{so that}$$
$$(A + \Delta)^T P + P(A + \Delta) \not< 0.$$

We can rewrite the constraint as

$$A^T P + PA + (\Delta^T P + P\Delta) \not< 0.$$

Which is equivalent to $A^T P + PA + (\Delta^T P + P\Delta)$ having a nonnegative eigenvalue. This stability radius problem is significantly different from the one considered in the previous section. In here the good set is $\mathbb{C}_g = (-\infty, 0)$ whereas the bad set is $\mathbb{C}_b = \mathbb{C} \setminus (-\infty, 0)$. The smallest $||\Delta||$ which preserve this property is the stability radius of this problem. In other words the largest ρ so that, $||\Delta|| < \rho$ preserves joint dissipativity. In the context of P reactivity we are seeking the smallest uncertainty level that forces the subsystem A to be P-reactive.

To analyse this robustness problem we will use the approach developed in Section 4.1 which is essentially borrowed from [46] and [47].

4.2.1 Robustness with respect to a particular CLF

We consider general n by n matrices A and B which share a strict CLF P.

- **One-parameter perturbations:**

  We perturb A as

  $$A + \delta DE, \tag{4.6}$$

  where $D \in \mathbb{R}^{n\times 1}$, $E \in \mathbb{R}^{1\times n}$ and $0 \neq \delta \in \mathbb{R}$. We need to find the extent of δ so that P remains a CLF. So we need to study the matrix

  $$M_\Delta := (A + D\delta E)^T P + P(A + D\delta E) = M + \delta(E^T D^T P + PDE),$$

  where $M = A^T P + PA$.

  First notice that since M_Δ is symmetric, the eigenvalues of this matrix are all real and hence the change of sign of the eigenvalues occurs through the origin. Therefore we only need to look at the eigenvalue $\lambda = 0$ where the change in sign takes place. We are seeking the smallest $|\delta|$ which forces M_Δ to have 0 as an eigenvalue. Now M_Δ can be written as

  $$M_\Delta = M + \begin{pmatrix} PD & E^T \end{pmatrix} \delta \begin{pmatrix} E \\ D^T P \end{pmatrix}$$

  Using (4.5), we can say 0 (the desired eigenvalue) is an eigenvalue of M_Δ if, and only if,

  $$1 \quad \text{is an eigenvalue of} \quad \delta \begin{pmatrix} E \\ D^T P \end{pmatrix} (0I - M)^{-1} \begin{pmatrix} DP & E^T \end{pmatrix}.$$

Equivalently we can write

$$\frac{1}{\delta} \quad \text{is an eigenvalue of} \quad \begin{pmatrix} E(-M)^{-1}PD & E(-M)^{-1}E^T \\ D^TP(-M)^{-1}PD & D^TP(-M)^{-1}E^T \end{pmatrix}.$$

That is

$$\frac{1}{\delta} \quad \text{is an eigenvalue of} \quad \begin{pmatrix} \langle PD, E^T\rangle_{-M^{-1}} & \|E^T\|^2_{-M^{-1}} \\ \\ \|PD\|^2_{-M^{-1}} & \langle PD, E^T\rangle_{-M^{-1}} \end{pmatrix},$$

where $\langle ., . \rangle_{-M^{-1}}$ denotes the inner product weighted by the positive definite matrix $-M^{-1}$.

Proposition 4.2.3. *0 is an eigenvalue of $M + \delta(E^TD^TP + DEP)$ if, and only if, $\frac{1}{\delta}$ is an eigenvalue of*

$$G := \begin{pmatrix} \langle PD, E^T\rangle_{-M^{-1}} & \|E^T\|^2_{-M^{-1}} \\ \\ \|PD\|^2_{-M^{-1}} & \langle PD, E^T\rangle_{-M^{-1}} \end{pmatrix}.$$

As a consequence of Proposition 4.2.3 we have

Corollary 4.2.3. *For the two Hurwitz matrices A and B which share a CLF P. If A is perturbed as in (4.6), then $A + \delta DE$ and B still share P as a CLF as long as*

$$|\delta| \leq \min\left(\frac{1}{\lambda_+}, \frac{1}{|\lambda_-|}\right), \tag{4.7}$$

where

$$\lambda_{\pm} = \langle PD, E^T \rangle_{-M^{-1}} \pm \|E^T\|_{-M^{-1}} \|PD\|_{-M^{-1}}.$$

Proof:

The matrix G can be viewed as

$$\begin{pmatrix} G_{11} & G_{12} \\ G_{21} & G_{22} = G_{11} \end{pmatrix},$$

hence the eigenvalues value are

$$\lambda_{\pm} = \frac{2G_{11} \pm \sqrt{4G_{11}^2 - (4G_{11}^2 + G_{12}G_{21})}}{2} = G_{11} \pm \sqrt{G_{12}G_{21}},$$

in other words we have

$$\lambda_{\pm} = \langle PD, E^T \rangle_{-M^{-1}} \pm \|E^T\|_{-M^{-1}} \|PD\|_{-M^{-1}}.$$

Example 4.2.7. *Let*

$$A = \begin{pmatrix} -74 & -47 & -41 & -2 \\ 15 & -45 & 3 & -7.6 \\ 121 & 77.9 & 45 & 9 \\ -155 & 65 & -.54 & -4.7. \end{pmatrix}, \quad B = \begin{pmatrix} -70 & -37 & -31 & -3 \\ 15 & -55 & 3 & -7 \\ 111 & 79 & 40 & 9 \\ -118 & 65 & -0.4 & -9. \end{pmatrix}.$$

With the aid of `cvx` *the two matrices share the Lyapunov function*

$$P = \begin{pmatrix} 173.3370 & 49.0238 & 98.3600 & 2.3839 \\ 49.0238 & 52.7169 & 46.8478 & 7.6620 \\ 98.3600 & 46.8478 & 71.0770 & 3.5658 \\ 2.3839 & 7.6620 & 3.5658 & 4.4706. \end{pmatrix}.$$

If A is perturbed with

$$D = \begin{pmatrix} 1 \\ 1 \\ 0 \\ 0 \end{pmatrix}, \quad E^T = \begin{pmatrix} 1 \\ 1 \\ 1 \\ 0. \end{pmatrix},$$

then according to the above formula, P will remain a CLF for $A + \delta DE$ and B if $\delta < 1.9$.

- **Two-parameter perturbations**

  Here the perturbed matrix A will take the form

$$A + \delta_1 D_1 E_1 + \delta_2 D_2 E_2. \tag{4.8}$$

  In this case we are looking for the largest perturbation magnitude $||\Delta|| = \sqrt{\delta_1^2 + \delta_2^2}$ so that we still have

$$(A + \delta_1 D_1 E_1 + \delta_2 D_2 E_2)^T P + P(A + \delta_1 D_1 E_1 + \delta_2 D_2 E_2) < 0.$$

  This is a question of finding the minimum $||\Delta||$ so that zero is an eigen-

value of the matrix

$$(A + \delta_1 D_1 E_1 + \delta_2 D_2 E_2)^T P + P(A + \delta_1 D_1 E_1 + \delta_2 D_2 E_2). \tag{4.9}$$

Similar to the rank one parameter case (4.9) can be written as

$$M_\Delta := M + \delta_1(E_1^T D_1^T P + P D_1 E_1) + \delta_2(E_2^T D_2^T P + P D_2 E_2) \tag{4.10}$$

where $M = A^T P + PA$. Also 4.10 can be written as

$$M_\Delta = M + \overbrace{\begin{pmatrix} PD_1 & E_1^T & PD_2 & E_2^T \end{pmatrix}}^{U} \overbrace{\begin{pmatrix} \delta_1 & 0 & 0 & 0 \\ 0 & \delta_1 & 0 & 0 \\ 0 & 0 & \delta_2 & 0 \\ 0 & 0 & 0 & \delta_2. \end{pmatrix}}^{V} \begin{pmatrix} E_1 \\ D_1^T P \\ E_2 \\ D_2^T P \end{pmatrix}$$

Now applying (4.5) we see that 0 is an eigenvalue of M_Δ if, and only if,

$$1 \quad \text{is an eigenvalue of} \quad V(-M)^{-1}U$$

This means that there is a nonzero vector $\begin{pmatrix} y_1 & y_2 & y_3 & y_4 \end{pmatrix}^T$ such that

$$\begin{pmatrix} E_1 NPD_1 & E_1 NE_1^T & E_1 NPD_2 & E_1 NE_2^T \\ D_1^T PNPD_1 & D_1^T PNE_1^T & D_1^T PNPD_2 & D_1^T PNE_2^T \\ E_2 NPD_1 & E_2 NE_1^T & E_2 NPD_2 & E_2 NE_2^T \\ D_2^T PNPD_1 & D_2^T PNE_1^T & D_2^T PNPD_2 & D_2^T PNE_2^T \end{pmatrix} \begin{pmatrix} y_1 \\ y_2 \\ y_3 \\ y_4 \end{pmatrix} = \begin{pmatrix} \frac{1}{\delta_1} y_1 \\ \frac{1}{\delta_1} y_2 \\ \frac{1}{\delta_2} y_3 \\ \frac{1}{\delta_2} y_4 \end{pmatrix},$$

where $N = -M^{-1}$. In other words we can write

$$\begin{pmatrix} G_{11} & G_{12} & G_{13} & G_{14} \\ G_{21} & G_{22} & G_{23} & G_{24} \\ G_{31} & G_{32} & G_{33} & G_{34} \\ G_{41} & G_{42} & G_{43} & G_{44} \end{pmatrix} \begin{pmatrix} y_1 \\ y_2 \\ y_3 \\ y_4 \end{pmatrix} = \begin{pmatrix} \frac{1}{\delta_1} y_1 \\ \frac{1}{\delta_1} y_2 \\ \frac{}{\delta_2} y_3 \\ \frac{1}{\delta_2} y_4 \end{pmatrix}$$

Here G_{ij} is defined as follows. For $i, j \in \{1, 2\}$ we have

$$\begin{aligned} G_{2i-1,2j-1} &= E_i N P D_j, \\ G_{2i-1,2j} &= E_i N E_j^T, \\ G_{2i,2j-1} &= D_i^T P N P D_j, \\ G_{2i,2j} &= D_i^T P N E_j^T. \end{aligned} \tag{4.11}$$

In a more compact form this can be written as

$$\overline{G} := \begin{pmatrix} \overline{G}_{11} & \overline{G}_{12} \\ \overline{G}_{21} & \overline{G}_{22} \end{pmatrix} \begin{pmatrix} Z_1 \\ Z_2 \end{pmatrix} = \begin{pmatrix} \rho_1 Z_1 \\ \rho_2 Z_2 \end{pmatrix},$$

where each $\overline{G}_{ij}$ $(i, j \in \{1, 2\})$ is the (i, j) 2×2 block matrix in G, $Z_1 = \begin{pmatrix} y_1 \\ y_2 \end{pmatrix}$, $Z_2 = \begin{pmatrix} y_3 \\ y_4 \end{pmatrix}$ and $\rho_i = \frac{1}{\delta_i}$.

Proposition 4.2.4. 0 *is an eigenvalue of* M_Δ *if, and only if,*

$$\rho_2 \in \sigma(G_{22} + G_{21}(\rho_1 I - G_{11})^{-1} G_{12}). \tag{4.12}$$

It is worth adding that (4.12) hold if, and only if,

$$\det \begin{pmatrix} \rho_1 I_2 - \overline{G}_{11} & -\overline{G}_{12} \\ -\overline{G}_{21} & \rho_2 I_2 - \overline{G}_{22}. \end{pmatrix} = 0. \tag{4.13}$$

Then the stability radius is the minimum of $||\Delta|| = \sqrt{\delta_1^2 + \delta_2^2}$ over all δ_1 and δ_2 which force the above determinant to be zero. Geometrically and based on the usual Euclidean norm this means the shortest distance form the origin to the curve in the (δ_1, δ_2) plane where (4.13) holds. We can pose the optimization problem

$$\begin{aligned} &\text{minimize} \quad \sqrt{\delta_1^2 + \delta_2^2} \\ &\text{subject to} \quad \det \begin{pmatrix} \rho_1 I_2 - \overline{G}_{11} & -\overline{G}_{12} \\ -\overline{G}_{21} & \rho_2 I_2 - \overline{G}_{22}. \end{pmatrix} = 0. \end{aligned} \tag{4.14}$$

Example 4.2.8. *Consider the same pair of matrices as in Example 4.2.7 but with the perturbation* (4.8)*. We choose D_1, E_1, D_2 and E_2 as follows*

$$D_1 = \begin{pmatrix} 1 \\ 1 \\ 0 \\ 0 \end{pmatrix}, \quad E_1^T = \begin{pmatrix} 1 \\ 1 \\ 1 \\ 0 \end{pmatrix}, \quad D_2 = \begin{pmatrix} 1 \\ 1 \\ 1 \\ 0 \end{pmatrix}, \quad E_2^T = \begin{pmatrix} 1 \\ 1 \\ 1 \\ 0 \end{pmatrix}.$$

Using the parameter dependence in Proposition 4.2.4, Figure 4.1 exhibits regions in the parameter space (δ_1, δ_2) where A and B still share a CLF inside the red curve. On this curve zero is an eigenvalue of the matrix (4.9)*. The shortest distance from this red curve to the origin is essentially the stability radius of this problem.*

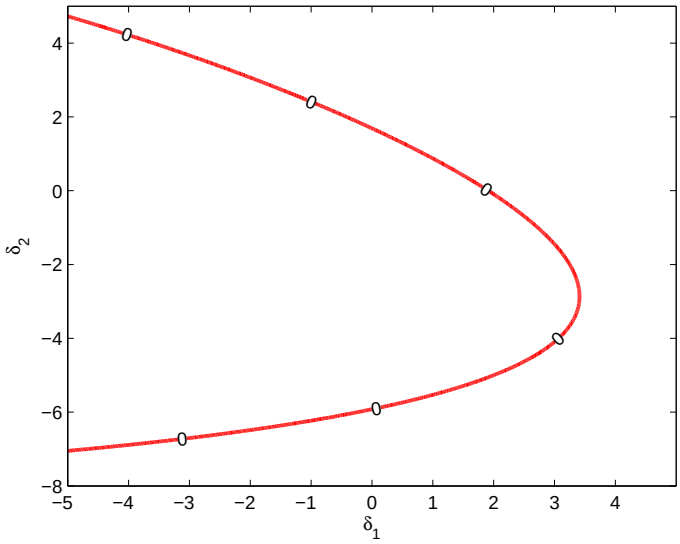

Figure 4.1: The red contour curve represents the set of parameters (δ_1, δ_2) where the determinant in (4.13) becomes zero. That is, it gives a zero eigenvalue of (4.9). Inside this curve M_Δ has all its eigenvalues negative whereas outside at least one of its eigenvalues is positive

- **k-parameter perturbations**

  In this case we have

  $$A + \Sigma_{i=1}^{k} \delta_i D_i E_i.$$

  As in the previous two cases we are interested in the smallest $||\Delta|| = \sqrt{\Sigma_{i=1}^{k} \delta_i^2}$ so that

  $$M_\Delta = M + \Sigma_{i=1}^{k} \delta_i E_i^T D_i^T P + \Sigma_{i=1}^{k} \delta_i P D_i E_i.$$

  has 0 as an eigenvalue. Applying (4.5) we get the following result.

  Proposition 4.2.5. *Suppose that* 0 *is not an eigenvalue of* A*. Then* 0 *is an eigenvalue of* M_Δ *if, and only if,* 1 *is an eigenvalue of the* $2k \times 2k$

matrix:

$$\begin{bmatrix} \mathbf{D_{11}} & \dots & 0 \\ \vdots & \ddots & \vdots \\ 0 & \cdots & \mathbf{D_{kk}} \end{bmatrix} \begin{bmatrix} G_{11} & \dots & G_{12k} \\ \vdots & \ddots & \vdots \\ G_{2k1} & \cdots & G_{2k2k} \end{bmatrix}.$$

where G_{ij} are defined as in (4.11)*. The block matrices $\mathbf{D_{ii}}$ are defined as*

$$\mathbf{D_{ii}} = \begin{pmatrix} \delta_i & 0 \\ 0 & \delta_i \end{pmatrix}_{\mathbf{2\times 2}}.$$

For details see Appendix A.

Remark 4.2.4.

- *(Special case $P = I$) This case is essentially a question of finding the level of uncertainty within which the stable system does not initially amplified after perturbation, in other words remains not I-reactive.*
- *As it can be seen from Propositions 4.2.3, 4.2.4 and 4.2.5 the stability radii obtained do not contain any information about the matrix B. The matrix B will ahve an effect if it is perturbed as well and in this case the stability radius will be the minimum of the ones resulting form A and B.*

4.2.2 Robustness with Respect to All Possible CLFs

This question is generally very hard to answer. The main challenge is that we do not have a general mathematical statement efficiently characterising the existence of CLFs for $n > 2$. For second order systems ($n = 2$), there do exist such characterisations as we have mentioned in Chapter 2. We assume that the two stable matrices A and B share a CLF. We also assume that one of them

is perturbed. In here we have $\mathbb{C}_b = (-\infty, 0]$. Here, as we have mentioned, we are interested in testing the robustness of this problem under the perturbation structure $D\Delta E$.

Perturbing A

The goal is to find the smallest $||\Delta||$ which takes at least one of the eigenvalues of $(A + D\Delta E)B$ or $(A + D\Delta E)B^{-1}$ to the negative real axis. Following the premises of Theorem 2.3.1 we will address this problem in cases.

- **The case** AB

  Here we want Δ so that

  $$(A + D\Delta E)Bv = \omega v \quad \text{for some} \quad v \neq 0 \quad \text{and} \quad \omega \in (-\infty, 0].$$

  This can be written as

  $$ABv + D\Delta EBv = \omega v.$$

  Hence we have

  $$(\omega I - AB)v = D\Delta EBv.$$

  Now we can write

  $$v = (\omega I - AB)^{-1} D\Delta EBv$$

  Multiplying both sides by EB and taking norms we get

  $$||EBv|| \leq ||EB(\omega I - AB)^{-1}D||||\Delta||||EBv||$$

  This implies

  $$||\Delta|| \geq \frac{1}{||EB(\omega I - AB)^{-1}D||},$$

and we have

$$r_{\mathbb{R}}(AB, D, EB; \mathbb{C}\setminus(-\infty, 0]) = \min_{\omega\in(-\infty,0)} \left(\frac{1}{||G_1(\omega)||}\right) = \min_{\omega\in(-\infty,0)} (\sigma_n(G_1(\omega))$$

where $G_1(\omega) = EB(\omega I - AB)^{-1}D$ is the transfer function and σ_n refers to the smallest singular value.

- **The case** AB^{-1}

  Similarly in this case we are after a Δ such that

$$(A + D\Delta E)B^{-1}v = \omega v \quad \text{for some} \quad v \neq 0 \quad \text{and} \quad \omega \in (-\infty, 0].$$

  This can be written as

$$(\omega I - AB^{-1})v = D\Delta EB^{-1}v,$$

  which implies

$$v = (\omega I - AB^{-1})^{-1}D\Delta EB^{-1}v.$$

  Multiplying by EB^{-1} each side and taking norms we get

$$||\Delta|| \geq \frac{1}{||EB^{-1}(\omega I - AB^{-1})^{-1}D||}.$$

  Therefore the stability radius is

$$r_{\mathbb{R}}(AB^{-1}, D, EB^{-1}; \mathbb{C}\setminus(-\infty, 0]) = \min_{\omega\in(-\infty,0)} \left(\frac{1}{||G_2(\omega)||}\right) = \min_{\omega\in(-\infty,0)} (\sigma_n(G_2(\omega)),$$

where $G_2(\omega) = EB^{-1}(\omega I - AB^{-1})^{-1}D$. Therefore the overall stability radius is given by

$$r_1 := \min\left(r_{\mathbb{R}}(AB, D, EB; \mathbb{C}\setminus(-\infty, 0]), r_{\mathbb{R}}(AB^{-1}, D, EB^{-1}; \mathbb{C}\setminus(-\infty, 0]\right).$$

Perturbing B:

Perturbing B Conceptually follows the same analysis as when we perturb A. In this case we need the smallest Δ which takes at lease one of the eigenvalues of $A(B + D\Delta E)$ or $A(B + D\Delta E)^{-1}$ to the negative real axis. Analysis leads to

- **The case AB:**

$$\begin{aligned} r_{\mathbb{R}}(AB; AD, E; \mathbb{C}\setminus(-\infty, 0]) &= \min_{\omega\in(-\infty,0)}\left(\frac{1}{||G_3(\omega)||}\right) \\ &= \min_{\omega\in(-\infty,0)}(\sigma_n(G_3(\omega)), \end{aligned}$$

  where $G_3(\omega) = E(\omega I - AB)^{-1}AD$.

- **The case AB^{-1}**

  In this case we need

$$A(B + D\Delta E)^{-1}v = \omega v \quad \text{for some} \quad v \neq 0 \quad \text{and} \quad \omega \in (-\infty, 0].$$

  Lets consider the case when $\omega \neq 0$. Multiplying both sides by A^{-1} and $(B + D\Delta E)$ we get

$$v = \omega BA^{-1}v + \omega D\Delta EA^{-1}v.$$

Multiplying both sides by AB^{-1} we get

$$AB^{-1}v = \omega v + \omega AB^{-1}D\Delta EA^{-1}v.$$

Hence we have

$$(\omega I - AB^{-1})v = -\omega AB^{-1}D\Delta EA^{-1}v,$$

therefore we have

$$v = -\omega(\omega I - AB^{-1})^{-1}AB^{-1}D\Delta EA^{-1}v.$$

Multiplying both sides by EA^{-1} we get

$$EA^{-1}v = -\omega EA^{-1}(\omega I - AB^{-1})^{-1}AB^{-1}D\Delta EA^{-1}v.$$

Now taking norms we get

$$1 \leq |\omega|||EA^{-1}(\omega I - AB^{-1})^{-1}AB^{-1}D||||\Delta||,$$

and hence we have

$$|||\Delta|| \geqslant \frac{1}{|\omega|||EA^{-1}(\omega I - AB^{-1})^{-1}AB^{-1}D||}$$

Its clear that small values of ω yields a not interesting case (i.e. very large perturbation). So We just restrict to the values when $\omega \neq 0$. Hence

we get

$$r_{\mathbb{R}}(BA^{-1}; D, EA^{-1}; \mathbb{C}\backslash(-\infty, 0]) = \min_{\omega\in(-\infty,0)} \left(\frac{1}{||G_4(\omega)||}\right)$$
$$= \min_{\omega\in(-\infty,0)} (\sigma_n(G_4(\omega))$$

where $G_4(\omega) = EA^{-1}(\frac{1}{\omega}I - BA^{-1})^{-1}D$.

Hence the overall stability radius is

$$r_2 := \min\left(r_{\mathbb{R}}(AB; AD, E; \mathbb{C}\backslash(-\infty, 0]), r_{\mathbb{R}}(AB^{-1}; D, EA^{-1}; \mathbb{C}\backslash(-\infty, 0])\right)$$

4.3 A special Case: Rank One Perturbation

We consider the perturbation (4.6). Here, for illustration, we will study the case when B is perturbed. Perturbing A needs almost the same mathematical steps apart from some appropriate changes. Since the functions G_3 and G_4 are both continuous, bounded and have zero limits as $|\omega| \to \infty$, their maxima are achieved at finite ωs. Also, in this case, G_3 and G_4 are scalar-valued function and hence we can use the first derivative test for critical points. From standard calculus a function f attains its minima when either $f' = 0$ or f' is undefined. To apply this on G_3 and G_4, first set

$$f_1 = \frac{1}{||G_3||} \quad \text{and} \quad f_2 = \frac{1}{||G_4||}.$$

It is clear that

$$||G_3||^2 = (E(\omega I - AB)^{-1}AD)^2 \quad \text{and} \quad ||G_4||^2 = (EA^{-1}(\frac{1}{\omega}I - BA^{-1})^{-1}D)^2.$$

For f_1 we need all ω that give

$$(f_1^2)' = \frac{-2||G_3||||G_3||'}{||G_3||^4} = \frac{-2||G_3||'}{||G_3||^3} = 0$$

Hence whether G_3 is negative or positive, the ω we seek always satisfies

$$G_3' = 0 \Longrightarrow E(\omega I - AB)^{-2}AD = 0.$$

Therefore

$$E(\omega I - AB)^{-2}A = \beta D^{\perp} \quad \text{for some} \quad \beta \in \mathbb{R}.$$

Here $D^{\perp}$ refers to a perpendicular vector of D. Multiplying both side by A^{-1}, $(\omega I - AB)^2$ and then by $E^{\perp}$ we eventually get

$$(D^{\perp}A^{-1}E^{\perp})\omega^2 - (2D^{\perp}BE^{\perp})\omega + D^{\perp}A^{-1}(AB)^2E^{\perp} = 0 \tag{4.15}$$

A similar argument can be carried out for f_4. We eventually get

$$(D^{\perp}(BA^{-1})^2AE^{\perp})\omega^2 - (2D^{\perp}BE^{\perp})\omega + D^{\perp}AE^{\perp} = 0. \tag{4.16}$$

Formulae (4.15) and (4.16) offer the candidates ωs at which the desired minimum attained. They are readily implemented in Matlab.

Remark 4.3.5. *Perturbing A and B at a time.*
In all of the above cases, if A and B are perturbed simultaneously with the same perturbation structure the stability radius of the problem will be the minimum of the ones resulting from each case. In contrast, if A and B are perturbed with different perturbation then obviously we have two independent robustness problems problems which can be tackled separately.

4.4 Notes and Concluding Remarks

In this chapter we use the approach of Hinrichsen and Pritchard [47] to study the robustness of joint-dissipativity. To the best of our knowledge, the way we formulate and analyse the problem is new. The formula (4.7) is extremely powerful. It reduces the problem of robustness to a simple computable formula. Proposition 4.2.5 is similar to Theorem 4.3 in Hodgson et al. [48]. However in their problem the target eigenvalue was 1 whereas in our case it is 0.

A careful exploration of the literature confirms that the robustness analysis of the Shorten and Narendra [108] is novel. We derive easy computable formulae to check the robustness of a given pair for second order matrices to persist dissipate simultaneously.

Chapter 5

Joint Dissipation and Pattern Formation

Part of this Chapter was published in the Journal of Mathematical Biosciences: 239 (2012) 131-138.

This chapter includes:

- Proposition 5.5.6 a new necessary conditions for Turing instabilities.
- Proposition 5.6.8 which further extends the necessary conditions to include more complicated movement mechanisms.

This chapter starts with necessary background material, Sections 5.1 to 5.4. The main result follows in Sections 5.5.

5.1 Movement mechanisms

In many physical systems, random movements at the microscopic scale play a vital role in the eventual movement trend [10, 81, 23]. These microscopic

motions can vary in type and influence the overall collective motion of the whole macroscopic cluster. One simple possibility is that particles move in a random way through the space. If this probabilistic motion is manifested as a regular motion for the whole body, we usually call this diffusion (or random motility) [81]. Of course, physical environments are not so neutral, and they are biased and so often intervene in and influence the motion. For instance, particles can be carried thorough a moving fluid. This is usually refereed to as advection [81, 52, 60]. In biological particles such as cells, bacteria, animals, etc, the motion can be far more complicated than just simple diffusion or advection. Interactions between the underlying kinetics can be significant [10, 31]. It turns out that biological systems with certain kinetic characteristics can generate travelling wave solutions, a dominant feature of many biological systems [81, 60]. An ecosystem involving a predator prey kinetic, for instance, is greatly influenced by the nature of its predator-prey relationship where the prey tends to be distinguished from the predator by escaping from the territory of the predator [80, 111]. It is also quite common for biological microorganisms to sense the signals from the surrounding environment and respond to them. Organisms either move toward or away from the stimulus. This is usually describe as: (stimulus)+taxis [10, 23]. Food, for example, can act as chemical stimulus attracting bacteria. This is referred to as chemotaxis and the food is called a chemoattractant [6]. A detailed discussion of such chemotactic motions will be given in Section 5.2.1. It is worth adding here that motions of real organisms can be even more specific, as they might follow some particular probability kernel [74]. Furthermore, there can be movements which do not come under any of these motions [60], and in these cases writing down a governing equation(s) is often a challenge. In this Chapter we will be concerned

with phenomena involving reaction, diffusion and chemotaxis. Broadly speaking there are two main approaches in extracting modelling equations which use informations from the microscopic scale to model the whole macroscopic behaviour. One is based on using random walks and basically starts with seeking the probability density function for the location of each individual. The second, which we will adapt here, uses the conservation (balance) equation and is based on assuming a continuum of particle distribution.

5.2 Modelling Reaction-Motion Systems: A Flux-Based Approach

For illustration, we will consider the motion in the 3-dimensional Euclidean space. Let $u(t,x)$ be the density of particles at a spatial point $x \in \mathbb{R}^3$ and time t. We will assume an arbitrary volume element $\Omega \subseteq \mathbb{R}^3$ where particles are, possibly, created (destroyed) in Ω and move out of (into) it across its boundary $\partial\Omega$. The conservation law says that

$$\begin{pmatrix} \text{The net rate of} \\ \text{change of particles} \\ \text{in } \Omega \end{pmatrix} = \begin{pmatrix} \text{The contribtion} \\ \text{due to motion} \end{pmatrix} + \begin{pmatrix} \text{The particles created} \\ \text{or decayed} \end{pmatrix}$$

The conservation equation can be written mathematically

$$\frac{\partial}{\partial t}\int_\Omega u(t,x)dV = -\int_{\partial\Omega} \mathbf{J}\cdot ds + \int_\Omega f dV.$$

Here f is the rate of creation (degradation) of $u(t,x)$ per unit time and is generally a function of u, x and t. The term $\mathbf{J}$ refers to the flux of particles

through the boundary $\partial\Omega$. Details can be found in [60, 80]. An immediate consequence of the divergence theorem is

$$\int_{\Omega} \left(\frac{\partial u}{\partial t} - f + \nabla \cdot \mathbf{J} \right) = 0.$$

Since Ω is an arbitrary volume element, then the integrand above has to be zero. In other words we have

$$\frac{\partial u}{\partial t} = f - \nabla \cdot \mathbf{J}. \tag{5.1}$$

Now equation (5.1) is the general equation of matter conservation with flux $\mathbf{J}$ and a matter source f. Particles can experience various flux scenarios depending on the type of movement they follow. In the case of diffusion, for instance, the mathematical model for the flux is known as Fick's law and it is given as

$$\mathbf{J} := \mathbf{J}_{\text{diffusion}} = -D\nabla u.$$

The negative proportionality constant D represents the diffusivity of the particles. This law is seen in many physical settings where particles descend to lower concentration levels [81, 38]. In other words the process of diffusion tends to smooth out the concentration of particles over the space. Substituting this into (5.1) leads to

$$\frac{\partial u}{\partial t} = f(u) + \nabla \cdot (D\nabla u) = f(u) + D\nabla^2 u. \tag{5.2}$$

This is referred as a **reaction-diffusion (RD) system**, and was first proposed by Turing [131, 115]. Excellent sources of details for the analysis of

reaction diffusion systems can be found in [88, 90]. In a more general setting where $U(x,t)$ is a vector of possibly different, species with possibly different diffusitivities, equation (5.2) takes the form

$$\frac{\partial U}{\partial t} = F(t,x,U) + \nabla \cdot (D \cdot \nabla U)\,. \tag{5.3}$$

Here F is the vector of source (kinetic) terms. The matrix D is a diagonal matrix which can be density [77] or spatially [7, 70] dependent, but for the purpose of this work we will take the density (spatial) independence of D for granted. Further extensions of the system (5.3) to include more general settings is possible. For instance, the reaction part can be replaced by an integral where, in this situation, life history matters. The diffusion part can be substituted by a more general movement as an integral involving some special kernel specifying the random motion of particles (not necessarily a simple random walk) [85, 80, 61]. Furthermore, diffusion can be even more complicated where diffusivity of one species can negatively (positively) affect the time evolution of the other. This is apparently the case in epidemic interactions where diffusion of infectives affects, negatively, the time course of susceptibles, giving so called cross-diffusion [117]. Specifically in [122], a model has the form

$$\begin{aligned} \frac{\partial S}{\partial t} &= f(S,I) + D_S \nabla^2 S + D \nabla^2 I \\ \frac{\partial I}{\partial t} &= g(S,I) + D_I \nabla^2 I, \end{aligned}$$

where D represents the cross-diffusion term and S and I are the density of susceptibles and infectives respectively. As we shall see later in Chapter 5, our main result will even apply to such models with cross diffusion.

5.2.1 Tactic motions

As we have mentioned in Section 5.1 the effect of an environment on the motion of its constituents can be significant. Temperature, light and toxins are all possible environmental actions. For instance, some organisms favour approaching moderate temperatures and bright light and some, possibly most, avoid toxic chemicals and extreme temperature. In biological systems, one widely spread scenario of tactic motions is chemotaxis [24, 126]. It refers to the response of living organisms to chemical cues they are surrounded by. These cues can be chemicals assessing communications among species. An example of this is the long distance (1400 miles) travelled by the green turtle (*Chelonia mydas*) from Brazil towards Ascension Island where chemotaxis is thought to be one of the driving forces [58]. Leukocytes are capable of sensing the invasion of bacteria via chemical changes in the infected tissue [18, 17]. The role of chemotaxis in developmental biology, an important branch of biological sciences, has been extensively explored in [95]. It is worth adding here that chemotaxis can be either towards or away from the chemical signals. In the former, the chemical is a chemoattractant and in the latter a chemorepellent. Modelling the flux due to chemotaxis is intuitive. For instance, if bacteria species $u(t,x)$ sense an attractive chemical signals $a(t,x)$, then the flux towards this signal is likely to be proportional to the gradient of a and the density of bacteria. Mathematically this can be modelled as

$$\mathbf{J} := \mathbf{J}_{\text{chemotaxis}} = \chi_u(a) u \nabla a, \tag{5.4}$$

where $\chi_u(a)$ is the chemotactic coefficient which, possibly, depends nonlinearly on the density of the chemoattractant [80]. However in this thesis we will

always assume $\chi_u(a)$ is a constant (that is $\chi_u(a) = \chi_u$). The model (5.4) of flux is the one most widely used [10]. One of the early usages of this model was by Keller and Segel [22] in the study of slime mould *Dictyostelium discoideum*. A chemical called cyclic-ANP secreted by amoebae attracts them. In principle modelling the flux of other types of tactic motions, for instance hypotaxis (see Chapter 6), follows the same reasoning.

Diffusion with Chemotaxis:

If bacteria experience diffusion and chemotaxis at a time then the net flux will be

$$\mathbf{J} = \mathbf{J}_{\text{diffusion}} + \mathbf{J}_{\text{chemotaxis}}.$$

If the chemoattractant is diffusing, which is likely, with diffusivity D_a and it is created (degraded) with the rate $g(a, x)$ then the dynamical system governing the whole interaction is given as

$$\begin{aligned} \frac{\partial u}{\partial t} &= f(t, x, u) + D_u \nabla^2 u - \nabla . \left(\chi_u u \nabla a\right), \\ \frac{\partial a}{\partial t} &= g(t, x, a) + D_a \nabla^2 a, \end{aligned}$$

where D_u, D_a are the diffusivity of u and a respectively. The tactic influence can be in two directions. For instance, for a given species u and v we can have

$$\begin{aligned} \tfrac{\partial u}{\partial t} &= f(t, x, u, v) + D_u \nabla^2 u + \nabla . \left(\chi_u u \nabla v\right) \\ \tfrac{\partial v}{\partial t} &= g(t, x, u, v) + D_a \nabla^2 v - \nabla . \left(\chi_v v \nabla u\right). \end{aligned} \tag{5.5}$$

In this particular case v is attracted by u while acting as a repellent to u. For more complicated settings, where there are several attractants, repellents and

organisms, we might write

$$\frac{\partial u_i}{\partial t} = f_i(t, x, u_1, u_2, ..., u_n) + d_i \nabla^2 u_i + \sum_{j=1}^{n} \nabla \left(\chi_{ij} u_i \nabla u_j \right) \tag{5.6}$$

where $i, j \in \{1, ..., n\}$, $d_i \geq 0$ and $\chi_{ij} \in \mathbb{R}$. Equation (5.6) is often called the **reaction-diffusion-chemotaxis** equation. This will be crucial to our main result in this chapter.

Key Assumptions:

Throughout this thesis we will assume the following

- The reaction part f is constant or density dependent i.e. it is not spatially dependent and does not involve random elements.
- All diffusion and tactic coefficients are constant.

5.3 Pattern forming systems

Nature exhibits a diversity of patterns and forms. Seeds, plants and flowers are often characterised by certain arrangements of their structures [98]. Some animals are spotted, e.g. leopard and ladybirds, and others can be striped such as angelfish and zebras. Climate change can drive vegetation of plants to obey some patterns [64]. In chemistry it is quite often that chemists are struck with emergence of, possibly, unexpected patterns. An example of this is the pattern emerging due to the chlorite-iodide-malonic acid-starch reaction (CIMA reaction) [20], see Figure 5.1. Explaining how these patterns, and obviously dozens of others scattered in nature, are formed is generally hard [80]. Combining the awareness of the underlying physical laws governing the molecular events with mathematical modelling was a huge step in obtaining interpretations for many

patterns.

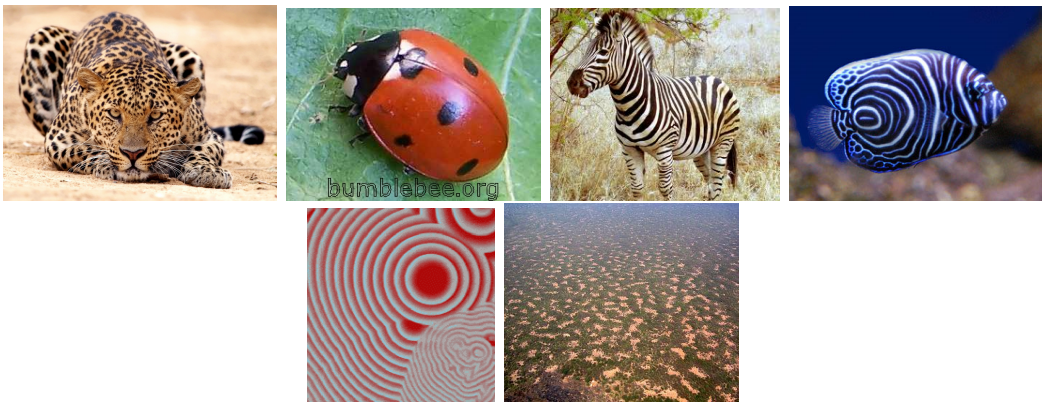

Figure 5.1: Top row from left to right: Leopard, Ladybirds, Zebra and Angelfish. Bottom row from left to right: CIMA pattern and tiger bush in Niger. The photos are taken from: `http://www.google.co.uk/imghp`.

In developmental biology, the evolution of an embryos' shape and form occupies a central position [80, 38, 115]. There have been tremendous amounts of research efforts aiming to understand and explain the detailed mechanism(s) leading to the appearance of organism final shape which, in many cases, is a challenge [52, 80, 69, 68, 27]. A prior knowledge of the genetic structure can serve to predict and pinpoint the gene(s) which are responsible for the appearance of some particular structure or shape. However, it does not explain how, finely, these processes take place towards its final stage [80, 69, 68]. One approach for this is using what is known as chemical pre-pattern models which essentially suggests that development or pattern formation occurs in two distinct stages. In the first, spatial patterns of morphogens is set up, whereas in the second the underlying cells readout the morphogen spatial heterogeneity and respond to it by differentiation or migration [80]. One possible way to form pre-patterns is via the interaction between reaction and diffusion which, as we shall see, is the main proposition of Turing's claim [115] for explaining

development and pattern formation. Since the publication of Turing's seminal paper *"The chemical basis of morphogenesis"* notable advances have been reported for explaining various patterns in biology [80, 68, 59]. Details are given in Subsection 5.4.1. Reaction diffusion (RD) systems have been proposed as candidate mechanisms leading to various patterns [82]. In fact Turing's idea sets up a counter intuitive phenomenon where it essentially states that the coupling of two intrinsically stable mechanisms reaction and diffusion lead to unstable behaviour. In other words, diffusion has the potential to break the symmetry of the spatial chemical concentration, although it is thought to be a homogenizing factor. An alternative approach to the pre-pattern models is what is known as the mechanochemical models [92]. It overcomes the shortcoming of the pre-pattern approach, where pattern formation is assumed to happens in two distinct stages. In the mechanochmical approach the two are assumed to happened simultaneously [10, 27].

5.4 Turing Patterns and Diffusion Driven Instability (DDI)

Turing, Figure 5.2, suggested that adding diffusion to a pair of reacting, spatially uniformed, morphogens can lead to a system exhibiting a spatially nonuniform state. This phenomenon is called *diffusion-driven instability* (DDI) or *Turing instability*.

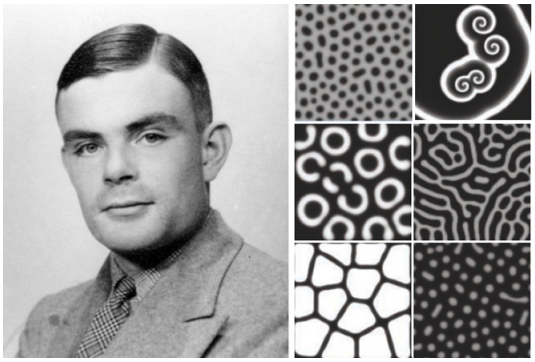

Figure 5.2: Left: Alan Mathison Turing (1912-1954). Right: Turing pattern. Taken from `http://www.google.co.uk/imghp`.

As we have mentioned earlier, this appears to contradict the dogma towards the stabilizing tendency of diffusion. In the context of skin patterning, for instance, reaction and diffusion together, represent a mechanism to blueprint the "prepattern map" which in turn is sensed by the underlying tissue. For the sake of scientific credit Turing recognised the rule of mechanics in morphogenesis. However Turing only considered the chemical one [10]. As we shall see latter diffusion coefficients of both morphogens have to be unequal in order to see Turing's scenario.

5.4.1 Turing patterns in biological and chemical sciences

Turing's analysis of reaction-diffusion systems [115] has had significant impact on several branches of science [68, 59]. RD models have subsequently been widely applied to various biological patterning phenomena [81, 69]. An early application of Turing's theory was to patterning of the body segment in fruit fly *Drosophila* [75, 53]. RD systems have been used to model complex pattern formation of certain animal skins [94, 119]. Reaction diffusion theory has been utilised to examine the spatio-temporal pattern formation on the surface

of tumour spheroids [13]. A Turing model is considered in [3] to understand the origination of *Escherichia coli* biofilm development. Pattern formation via diffusion driven instability plays an important role in chemistry [33, 26] and physics [14]. Ecologists use RD models to understand spatial patterns in populations and communities [124, 23, 105, 127, 71, 121, 73], where for instance, a very fast prey (predator) would intuitively drive the density of the whole population to be spatially dependent.

The Evidence for Turing Patterns in Biological and Chemical systems:

Despite all the promising successes of Turing mechanism to replicate many patterns in nature, as illustrated above, existence of morphogens has not yet been proved for definite. However, there do exist very close candidates for morphogens. Examples for this are

- Calcium as morphogen leading to hair spacing in *Acetabularia.*[36]
- Fibronectin as a morphogen for cartilage formation [21]

Nevertheless, there is no definitive assertion that they are interacting as suggested by Turing. For details see [95]

In chemical systems, Turing structure has been shown by a group in Bordeaux led by De Kepper [54, 12, 51]. The chemical reaction they used was the CIMA reaction.

5.4.2 Classical approaches to determining Turing patterns

A reaction diffusion (RD) system is a system of the form

$$\frac{\partial u}{\partial t} = f(u) + D\nabla^2 u. \tag{5.7}$$

The function f (we assume it is regular) describes the reaction dynamics and D is a diagonal matrix of diffusion coefficients. Here $u(t,x) : [0,\infty) \times \mathbb{R}^n \to [0,\infty)$ is an n-tuple vector of densities at spatial position x and time t on a domain Ω, which typically bounded, with zero flux boundary conditions (i.e. $\nabla.u|_\Omega = 0$). Imposing such boundary conditions is due to their neutral nature as they do not pump the space with any additional material and this makes "self-organization" plausible. Taking other boundary conditions can influence the predictions where this can drive forming different patterns, see [80]. In studying pattern formation in RD systems the key first step is to determine the Turing space for a given model, i.e. the parameter set for the model on which pattern formation can be triggered [131, 79]. This can then be followed by bifurcation analysis of specific pattern formations [52]. Pattern formation is trigged by Turing instability. Turing instability, or diffusion driven instability(DDI), is a concept first proposed by Turing [115]. This concept is defined as follows.

Definition 5.4.3. *We say that a system of the form* (5.7) *exhibits Turing instability, or DDI, if the system without diffusion, i.e.*

$$\frac{\partial u}{\partial t} = f(u). \tag{5.8}$$

has locally stable equilibrium state which becomes unstable in the presence of diffusion.

To analyse DDI mathematically, we use linearised stability analysis. If $\widehat{u}$ is a spatially uniform equilibrium of (5.8), then small disturbances w away from $\widehat{u}$ are governed, qualitatively, by the linear system

$$\frac{dw}{dt} = Aw.$$

Here A, the Jacobian matrix of f evaluated at $\widehat{u}$, is the linearised reaction matrix. If A is stable (all its eigenvalues have negative real parts), which we assume for the remainder of this chapter, then $\widehat{u}$ is an asymptotically stable equilibrium for (5.8). The equilibrium $\widehat{u}$ is also a spatially homogeneous equilibrium of the system with diffusion. Small spatial disturbances v around $\widehat{u}$ are governed by the linearised reaction diffusion equation

$$\frac{\partial v}{\partial t} = Av + D\nabla^2 v. \tag{5.9}$$

Now taking Fourier transform of (5.9) in space, following Neubert et al. [85], and using zero flux boundary conditions we obtain

$$\frac{d\check{v}}{dt} = (A - \boldsymbol{k}^2 D)\check{v} \quad (||\mathbf{k}|| = \boldsymbol{k}),$$

where

$$\check{v} = \int_{-\infty}^{\infty} e^{i\mathbf{k}.x} v(t,x)dx.$$

Here $\mathbf{k}$ is a vector of Fourier frequencies and usually referred to as the wave

vector. Letting

$$J = A - \boldsymbol{k}^2 D, \tag{5.10}$$

equation (5.9) can then be written as

$$\frac{d\check{v}}{dt} = J\check{v}.$$

Keypoint IV

Turing instability (DDI) requires J to be unstable for some $\boldsymbol{k}$, i.e. J has an eigenvalue with positive real part. In other words, for DDI we require

$$\rho(\boldsymbol{k}^2) := \max_{1\leq i\leq n} \textbf{real}(\lambda_i(J)) > 0 \quad \textbf{for some} \quad \boldsymbol{k}. \tag{5.11}$$

Equation (5.11) is often called the *dispersion relation* of the system (5.7). Plotting $\rho(\boldsymbol{k}^2)$ against all possible $\boldsymbol{k}^2$ is a common technique used to determine the range of unstable modes. One approach to determining this parameter set is to compute principle minors [67, 49, 128] of linearised reaction-diffusion matrices. However, this approach leads to tedious calculations in the case of high dimensional systems.

In the particular case where $n = 2$, Murray [80] derives easily verifiable necessary conditions for DDI that are also sufficient for infinite domains. In this case equation (5.7) becomes

$$\begin{aligned} \frac{\partial u}{\partial t} &= f(u,v) + d_u \nabla^2 u \\ \frac{\partial v}{\partial t} &= g(u,v) + d_v \nabla^2 v. \end{aligned}$$

The corresponding A and D in (5.10) are given as

$$A = \begin{pmatrix} f_u & f_v \\ g_u & g_v \end{pmatrix} \quad \text{and} \quad D = \begin{pmatrix} d_u & 0 \\ 0 & d_v \end{pmatrix}.$$

Assuming that A is stable we have

$$f_u + g_v < 0 \quad and \quad f_u g_v - f_v g_u > 0. \tag{5.12}$$

In this case (5.10) becomes

$$J = \begin{pmatrix} f_u & f_v \\ g_u & g_v \end{pmatrix} - \boldsymbol{k}^2 \begin{pmatrix} d_u & 0 \\ 0 & d_v \end{pmatrix} = \begin{pmatrix} f_u - \boldsymbol{k}^2 d_u & f_v \\ g_u & g_v - \boldsymbol{k}^2 d_v \end{pmatrix}. \tag{5.13}$$

To have at least an eigenvalue with positive real part, one of the Hurwitz conditions for $A - \boldsymbol{k}^2 D$ must be violated. Conditions (5.12) assure that

$$\text{trace}(J) = (f_u + g_v) - \boldsymbol{k}^2(d_u + d_v) < 0.$$

So the only way to have an eigenvalue with positive real part is through the determinant. It turns out that the determinant is given by

$$\det(J) = d_u d_v \boldsymbol{k}^4 - (d_v f_u + d_u g_v)\boldsymbol{k}^2 + \det(A) =: h(\boldsymbol{k}^2). \tag{5.14}$$

Essentially equation (5.14) captures the signs of the dispersion relation (5.11) and that is why it is also called the *dispersion relation*. Since $d_u d_v \boldsymbol{k}^4$ and

$\det(A)$ are positive, $\det(J)$ can be negative only if

$$d_v f_u + d_u g_v > 0. \tag{5.15}$$

Conditions (5.12) and (5.15) force the diffusivity coefficients to be unequal. The above condition is necessary but not sufficient for DDI. Negativity of $\det(J)$ can be assured if $h_{min}(\boldsymbol{k}^2)$ is negative. Using standard calculus techniques, we differentiate $h(\boldsymbol{k}^2)$ with respect to $\boldsymbol{k}^2$, and equating the result with zero we eventually get the stationary values

$$\boldsymbol{k}_c^2 = \frac{d_v f_u + d_u g_v}{2 d_u d_v}.$$

Substituting in (5.14) we get

$$h_{min} = \det(A) - \frac{(d_v f_u + d_u g_v)^2}{4 d_u d_v}.$$

Hence $\det(J)$ can be negative if, and only if,

$$(d_v f_u + d_u g_v)^2 - 4 d_u d_v \det(A) > 0.$$

Hence the necessary conditions for DDI (Turing pattern formation) are

$$\begin{aligned} f_u + g_v < 0, \qquad & f_u g_v - f_v g_u > 0, \\ d_v f_u + d_u g_v > 0, \quad & (d_v f_u + d_u g_v)^2 - 4 d_u d_v \det(A) > 0. \end{aligned} \tag{5.16}$$

It is worth mentioning here that the conditions (5.16) are also sufficient if the space is not finite which will be always the case in Chapter 6 where we do not have any restrictions on the domain. If the domain is finite then we require

further investigations to the roots of (5.14).

Example 5.4.9. *Consider the nondimensionalised CIMA reaction [28]*

$$\begin{aligned}\frac{\partial X}{\partial t} &= a - X - \frac{4XY}{1+X^2} + \nabla^2 X \\ \frac{\partial Y}{\partial t} &= \gamma\left[b\left(X - \frac{XY}{1+X^2}\right) + c\nabla^2 Y\right].\end{aligned}$$

This model has been developed by Lengyle and Epstein [26]. Here X and Y refer to the concentrations of Iodine and Chlorine respectively [28]. The parameters a, b, and c are positive constants. Without diffusion the system has the homogeneous steady state

$$X^* = \frac{a}{5}, \quad Y^* = 1 + \frac{a^2}{25}.$$

The Jacobian around (X^*, Y^*) is given as

$$A = \frac{1}{1+\frac{a^2}{25}}\begin{pmatrix} -5+\frac{3a^2}{25} & \frac{-4a}{5} \\ \frac{2\gamma a^2 b}{25} & -\frac{\gamma a b}{5} \end{pmatrix} = \frac{1}{1+\beta^2}\begin{pmatrix} -5+3\beta^2 & -4\beta \\ 2\gamma\beta^2 b & -\gamma\beta b \end{pmatrix},$$

where $\beta = \frac{a}{5}$. Since we always have

$$det(A) = 5\gamma\beta b(\beta^2+1)^{-1} > 0,$$

then the steady state is asymptotically stable if, and only, if trace$(A) < 0$. This requires

$$-5 + 3\beta^2 - \gamma\beta b < 0.$$

Applying (5.16)*, the necessary conditions for Turing instability are*

$$\left.\begin{aligned} &-5+3\beta^2-\gamma\beta b<0,\\ &3\beta^2 c-\gamma\beta b-5c>0,\\ &\tfrac{3\beta^2 c-\gamma\beta b-5c}{(1+\beta^2)^2}+4\gamma c\det(A)>0. \end{aligned}\right\} \tag{5.17}$$

Conditions (5.17) *determine a region in the parameter space* (a, b) *where Turing pattern can be exhibited. Figure 5.3 shows how the stability region (below the black curve) is split into regions, one where DDI is not possible (below the red curve) and another (shaded) where it is.*

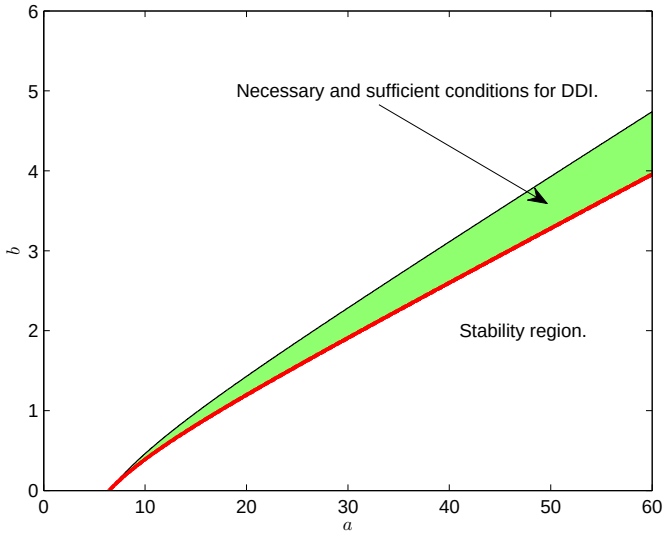

Figure 5.3: The CIMA model with parameter values $\gamma = 9$ and $c = 1.2$. The stability region, below the black curve, accommodates a region (shaded green) where DDI is possible

Figure 5.3 can be achieved by running the *dispersion relation* (5.14) over all the parameters as chosen in the figure. The wave number $\boldsymbol{k}$ plays as an intermediate between a and b in locating the region where DDI is possible. This has been overcome using our result Proposition 5.5.6. As we shall see

it offers a direct relationship between systems reactions and diffusions that determine DDI.

5.4.3 Parameter space determination methods for Turing patterns: The 3 by 3 case

For three reaction diffusion systems a necessary and sufficient conditions for Turing patterns has been obtained in [49]. We summarise this approach. Assume a reaction diffusion system

$$\begin{aligned} \frac{\partial u}{\partial t} &= f(u,v,w) + d_1\nabla^2 u \\ \frac{\partial v}{\partial t} &= g(u,v,w) + d_2\nabla^2 v \\ \frac{\partial w}{\partial t} &= h(u,v,w) + d_3\nabla^2 v. \end{aligned}$$

The corresponding A and D in (5.10) are given as

$$A = \begin{pmatrix} a_{11} & a_{12} & a_{13} \\ a_{21} & a_{22} & a_{23} \\ a_{31} & a_{32} & a_{33} \end{pmatrix}, \quad D = \begin{pmatrix} d_1 & 0 & 0 \\ 0 & d_2 & 0 \\ 0 & 0 & d_3 \end{pmatrix}.$$

Let a_{rr} be the largest diagonal element of A and $Co(A)_{ss}$ be the smallest diagonal cofactor of A. A necessary condition for DDI is

$$a_{rr} > 0; \quad \text{or} \quad \text{Cof}(A)_{ss} < 0 \tag{5.18}$$

A sufficient condition for DDI is

$$(i)\, a_{rr} > 0 \text{ with } \quad d_r \ll 1; \quad \text{or} \quad (ii)\, \text{Cof}(A)_{ss} < 0 \text{ with } \quad d_s \gg 1. \tag{5.19}$$

Remark 5.4.6. *One clear shortcoming of the above result is that it requires very small (large) enough diffusivities. This is obviously not generally the case for natural species. In the Oregonator example, in Section 6.1.2, we shall see that this result is totally inconclusive for large values of diffusivities. Furthermore determining the sign of the diagonal entries (cofactors) can be a difficult task.*

5.5 Reactivity and Turing patterns

In [85] a connection was made between two concepts - diffusion driven instability and reactivity. To describe this connection we again consider the matrix (5.10). Neubert et al.[85] introduced a matrix $H(J)$ given by

$$H(J) = H(A) - \boldsymbol{k}^2 D. \tag{5.20}$$

Here $H(J)$ and $H(A)$ are the Hermitian parts of J and A respectively. More explicitly this can be written as

$$H(J) = \frac{1}{2}(A + A^T) + (-\boldsymbol{k}^2 D).$$

Neubert et al. then used Weyl's theorem, see Appendix B and [50, p.181], applied to $H(J)$ to get

$$\lambda_1(H(J)) = \lambda_1(\frac{1}{2}(A + A^T) + \boldsymbol{k}^2(-D)) \leq \lambda_1(A + A^T) + \boldsymbol{k}^2\lambda_1(-D). \tag{5.21}$$

Hence, one can easily infer that if A is I-dissipative (i.e not I-reactive), then DDI is impossible. In other words, the linearised reaction matrix of a pattern

forming system cannot be I-dissipative. That is, reactivity is necessary for Turing instability.

5.5.1 An observation

The result that reactivity is necessary for DDI is closely related to the existence of a common Lyapunov function for A and $-D$. This can be induced from equation (5.21) where we can write the biconditional statement

$$H(J) \leq 0 \quad \text{for all} \quad \boldsymbol{k} \quad \text{if and only if} \quad A + A^T \leq 0 \quad \text{and} \quad -D \leq 0.$$

Hence, if the identity matrix is a CLF for A and $-D$, then diffusion driven instability is impossible. Restricting the choice of CLF to $P = I$ makes the result [85] limited. DDI can be ruled out by finding any CLF $P > 0$. This can be seen from the following argument. The key matrix which determines diffusion driven instability is $J = A - \boldsymbol{k}^2 D$. If there exists a positive definite matrix P so that

$$(A - \boldsymbol{k}^2 D)^T P + P(A - \boldsymbol{k}^2 D) \leq 0 \quad \text{for all} \quad \boldsymbol{k},$$

then J cannot be unstable and DDI is impossible. Equivalently we require

$$A^T P + PA + \boldsymbol{k}^2(-DP + P(-D)) \leq 0 \quad \text{for all} \quad \boldsymbol{k}.$$

This can be summarised as:

Proposition 5.5.6. *Assume that A is stable.*

1. *If A and $-D$ share a common Lyapunov function P, then diffusion driven*

instability is not possible. Equivalently

2. *Diffusion driven instability for the pair A and D implies A and $-D$ do not share a common Lyapunov function. In particular, $P = I$ cannot be a Lyapunov function for A (the result in [85]).*

3. *The linearised reaction matrix A of a pattern forming reaction-diffusion system cannot be dissipative in any P-norm in which $-D$ is dissipative.*

As we have mentioned in Chapter 2, determining whether a given pair of stable matrices A and B share a CLF is a semi-definite programming problem which can be solved using the Matlab package `cvx`, see Grant et al. [15]. The `cvx` code to check if A and $-D$ have a CLF is given in Appendix B. For details on the `cvx` package we refer to [15]. There is an obvious symmetry in the existence of CLFs for matrices as described in the following proposition.

Proposition 5.5.7. *Two Hurwitz matrices A and B have a CLF, if, and only if, A and B^{-1} have a CLF.*

Proof

Suppose there exists a positive definite matrix $P > 0$ such that

$$A^T P + PA = -Q_1 \qquad B^T P + PB = -Q_2,$$

for some $Q_1 \geq 0$ and $Q_2 \geq 0$. The matrix B is stable and hence invertible. Multiplying the left hand side of the second matrix equation by $(B^T)^{-1}$ and on the right by B^{-1} we obtain

$$(B^{-1})^T P + PB^{-1} = -(B^T)^{-1} Q_2 B^{-1} \leq 0.$$

Hence $P > 0$ is also a Lyapunov function for B^{-1}. □

This symmetry result suggests that the existence of CLFs for A and $-D$, whilst sufficient, is not necessary for ruling out DDI. Consider the linearised reaction and diffusion matrix pair:

$$A = \begin{pmatrix} 1 & 1 \\ -4 & -3 \end{pmatrix} \quad \text{and} \quad D = \begin{pmatrix} 1 & 0 \\ 0 & d \end{pmatrix}.$$

In this case, the necessary and sufficient conditions for DDI are: $d > 9$ for A and D and $d < \frac{1}{9}$ for A and D^{-1}.

We know that A and $-D$ have a CLF with strict inequalities if, and only if, $-AD$ and $-AD^{-1}$ both have no negative real eigenvalues. The latter conditions are equivalent to

$$\left[3d \geq 1 \text{ or } (-1+3d)^2 - 4d < 0)\right] \,\&\, \left[3/d \geq 1 \text{ or } (-1+3/d)^2 - 4/d < 0\right]$$

This reduces to

$$1/9 < d < 9.$$

Using the `cvx` code we can show directly that A and $-D$ have a CLF when $d = 1/9$ or $d = 9$. Hence, in this example, the region where A and $-D$ have a CLF (i.e. $1/9 \leq d \leq 9$) is the same as the region where DDI is not possible for A and $-D$ and A and $(-D)^{-1}$ simultaneously.

5.6 Tactic models

There is reasonable evidence to suggest that cell movement has a crucial role in development of patterns [10, p.229]. Fine investigations of patterns formed by

colonies of aggregating micro-organisms show that purposeful cell movement is essential. Henceforth, reaction diffusion taxis models, closely related to RD models, have been used extensively to generate patterns that are very similar to natural ones, e.g. cellular slime moulds [22] and [8]. In [4], chemotaxis is shown to be leading mechanism to spatial patterns. In [17] reaction-diffusion-chemotaxtic models have been introduced to examine the potential for bacteria and leukocytes to exhibit a non-uniform spatial state. Obviously this state has pathological implications which can be adverse. In the cancer invasion model developed in [116], a great deal of investigations have been given for the formation of nonuniform spatial patterns of the cancer cells due to different types of tactic motions. Obviously, the purpose for looking at this steady state is not "pattern formation" per se, but the probable consequences on the developing of cancer due to being spatially arranged through Turing mechanisms.

5.6.1 Chemotaxis-diffusion driven instability (CDDI)

The analysis of reaction diffusion chemotaxis systems is (almost) the same as that for RD systems. However, the resulting linearisation does not necessary involve a diagonal matrix. The matrix D can have any sparsity structure which depends on the number and nature of the chemical cues involved in the interaction under consideration. To derive the counterpart of the conditions (5.16), we will, for the sake of illustration, choose the scenario (5.5) with reactions f and g depending only on the density of u and v. The system becomes

$$\begin{aligned} \frac{\partial u}{\partial t} &= f(u,v) + D_u \nabla^2 u + \nabla.\left(\chi_u u \nabla v\right), \\ \frac{\partial v}{\partial t} &= g(u,v) + D_v \nabla^2 v - \nabla.\left(\chi_v v \nabla u\right). \end{aligned}$$

Assume that the system has a stable homogeneous steady state (u^*, v^*). Perturbing this state as $u = u^* + u_1$, $v = v^* + v_1$ and substituting in the system we get

$$\begin{aligned}\frac{\partial u_1}{\partial t} &= f(u_1 + u^*, v_1 + v^*) + D_u\nabla^2(u_1 + u^*) + \nabla.\left(\chi_u(u_1 + u^*)\nabla(v_1 + v^*)\right),\\ \frac{\partial v_1}{\partial t} &= g(u_1 + u^*, v_1 + v^*)u_1 + D_v\nabla^2(v_1 + v^*) - \nabla.\left(\chi_v(v_1 + v^*)\nabla(u_1 + u^*)\right).\end{aligned}$$

For convenience we replace u_1 and v_1 by u and v. After a sequence of algebraic manipulations, including using Taylor series and truncation of nonlinear terms, we eventually get a linearised system

$$\frac{\partial}{\partial t}\begin{pmatrix} u \\ v \end{pmatrix} = \begin{pmatrix} f_u(u^*, v^*) & f_v(u^*, v^*) \\ g_u(u^*, v^*) & g_v(u^*, v^*) \end{pmatrix}\begin{pmatrix} u \\ v \end{pmatrix} + \begin{pmatrix} D_u & \chi_u u^* \\ -\chi_v v^* & D_v \end{pmatrix}\nabla^2\begin{pmatrix} u \\ v \end{pmatrix}.$$

We seek a solution of the form

$$\begin{pmatrix} u \\ v \end{pmatrix} = \begin{pmatrix} c_1 \\ c_2 \end{pmatrix} e^{\lambda t + i\mathbf{k}.x}$$

where c_1, c_2 are constants and $\mathbf{k}$ is the wave vector. This leads to a linear system with a governing matrix

$$\begin{pmatrix} f_u + D_u\boldsymbol{k}^2 & f_v - \chi_u u^*\boldsymbol{k}^2 \\ g_u + \chi_v v^*\boldsymbol{k}^2 & g_v + D_v\boldsymbol{k}^2 \end{pmatrix}$$

and this is the counter part of the matrix (5.13). After a similar analysis to

that leading to (5.16), the necessary conditions for CDDI are

$$\left.\begin{array}{l} f_u + g_v < 0, f_u g_v - f_v g_u > 0, \\ D_v f_u + D_u g_v + \chi_u u^* g_u - \chi_v v^* f_u > 0, \\ (D_v f_u + D_u g_v + \chi_u u^* g_u - \chi_v v^* f_u)^2 - 4 D_u D_v \det(A) > 0. \end{array}\right\} \tag{5.22}$$

Remark 5.6.7. *In the case of multispecies incorporating various motions the analysis is very similar to the one performed in Section 5.4.2. The only difference is that the resulting matrix, the counter part of J in* (5.23)*, incorporates a matrix with arbitrary sparsity which is determined by the underlying motion mechanisms* (5.10)

$$A - \boldsymbol{k}^2 \boldsymbol{D}, \tag{5.23}$$

where $\boldsymbol{D}$ *is a matrix incorporating the motion involved in the system.*

Proposition 5.6.8. *If A and* $-\boldsymbol{D}$ *share a CLF then DDI (CDDI) is not possible.*

5.7 Concluding remarks

The problem of detecting Diffusion Driven Instability (DDI) is key to predicting the onset of pattern formation in spatially distributed biological and ecological systems. However, detecting DDI by standard techniques based on eigenvalues is often difficult, especially for large systems. One of the advantages of the necessary condition in Neubert et al. [85] is that it enables detection of DDI even for high dimensional systems with large numbers of parameters. Using a notion of common Lyapunov function (CLF) we show that this necessary condition is a special case of a more powerful, tighter neces-

sary condition. By rewriting the Neubert et al. necessary condition as a CLF problem we infer that it is essentially a question of whether or not the identity matrix I is a CLF for the linearised reaction matrix A and the diffusion matrix $-D$. We generalise the problem to one of whether or not the matrices A and $-D$ share a Lyapunov function P (not necessarily I). A very powerful Matlab package, namely `cvx`, can then be used to verify the existence of CLF. One of the main uses of our necessary condition would be, to quickly rule out areas of parameter space for which DDI is possible. Then refined analyses can devote more computational effort to focusing on the remaining areas of parameter space. In this chapter we essentially showed that Turing dynamics is one of the settings where norm choice is crucial. More precisely, some particular norms can be successful in revealing Turing pattern formation whereas others are inconclusive.

Chapter 6

Applications

Part of this Chapter was published in the Journal of Mathematical Biosciences: 239 (2012) 131-138.

In this chapter we apply the results of Chapter 5 to a diverse range of biological, chemical and ecological systems. In Section 6.1 we consider three important examples. The first is an inhibitor-activator model proposed by Gierer-Meinhardt [33] for modelling regenerative processes in Hydra. The second is the Oregonator [76, 29, 99], a much studied special case of the Belousov-Zhabotinsky reaction and the third a host-hyperparasite-parasite system with diffusion [124]. In Section 6.2, we apply our results to examples of reaction-diffusion-chemotaxis models. We start the section with the Schnakenberg model [131]. In the second example, we extend the model derived in [16], to incorporate bacterial chemoatxis. Our approach shows that there is a negative relation between bacterial taxis and the possibility of the system developing CDDI. The last two examples are high dimensional systems. We consider a multi-species host-parasitoid community and a model of Cancer invasion. For models of dimension higher than 2 we relay on `cvx` to determine CLF. For

the second order models `cvx` and Proposition 2.3.1 are utilized for determining CLF. A comparison with the traditional approaches, such as (5.16), (5.18) and (5.19), is made whenever it is possible.

6.1 Diffusion driven instability (DDI) and Turing patterns

.

6.1.1 The Gierer-Meinhardt Model [33]

In [33], Gierer and Meinhardt proposed an inhibitor-activator model to explain the regenerative properties of *Hydra*. Let a and h stand for the concentration of the activator and the inhibitor at time t and position x, respectively. The spatio-temporal dynamics of the model are given by the reaction-diffusion system:

$$\begin{aligned}\frac{\partial a}{\partial t} &= \rho\rho_0 + c_1\rho\frac{a^2}{h} - \mu a + d_1\nabla_x^2 a \\ \frac{\partial h}{\partial t} &= c_2\rho^{'}a^2 - \nu h + d_2\nabla_x^2 h.\end{aligned}$$

Here d_1 and d_2 are the diffusivities of the activator and the inhibitor; ρ_0 is the basic production of the activator and ρ and ρ' are the source concentrations for the activator and the inhibitor respectively; μ and ν are the degradation rates of the activator and the inhibitor. The parameters c_1 and c_2 are connected with the activator and inhibitor production.

The positive homogeneous steady state of the system is given by:

$$(a^*, h^*) = \left(\frac{c_2\rho'\rho\rho_0 + c_1\rho\nu}{c_2\rho'\mu}, \frac{c_2\rho'(a^*)^2}{\nu} \right).$$

The Jacobian of the system around the homogeneous steady state is given by

$$A = \begin{pmatrix} a_{11} & a_{12} \\ a_{21} & a_{22} \end{pmatrix}$$

where

$$a_{11} = \frac{2c_1\mu\nu}{c_1\nu + c_2\rho^{'}\rho_0} - \mu \qquad a_{12} = \frac{-c_1}{\rho}\left(\frac{\mu\nu}{c_1\nu + c_2\rho^{'}\rho_0}\right)^2$$
$$a_{21} = \frac{2\rho(c_1\nu + c_2\rho^{'}\rho_0)}{\mu} \qquad a_{22} = -\nu.$$

We use our approach to investigate the possibility of DDI in the parameter space of activator and inhibitor degradations μ and ν. Since DDI needs A to be stable, we are only interested in parameters so that

$$\det(A) = \mu\nu > 0 \quad \text{and} \quad \text{trace}(A) = \frac{2c_1\nu}{c_1\nu + c_2\rho^{'}\rho_0} - \mu - \nu < 0.$$

The parameters (μ, ν) for which $P = I$ is a Lyapunov function for A, so that DDI is not possible, is where $A + A^T \leq 0$. Now $A + A^T \leq 0$ if, and only if,

$$a_{11} \leq 0 \quad \text{and} \quad 4a_{11}a_{22} - (a_{12} + a_{21})^2 \geq 0.$$

We consider two sets of parameters. The first set of parameters is used to illustrate the differences between when I is a CLF, when there is a CLF (not necessarily I) and when there is DDI. For this purpose we choose $c_1 = 0.005$, $c_2 = 0.035$, $d_1 = 0.03$, $d_2 = 0.45$, $\rho^{'} = 0.075$ and $\rho = \rho_0 = 3.2$. Then the

space (μ, ν) splits into three distinct regions: where I is a CLF; where there is a CLF; and where there is DDI - see Figure 6.1. Notice that there is a significant part of the stable region in which the I-reactive test is inconclusive. On the other hand, the test based on the existence of a CLF captures all of the no DDI region (at least for $\mu > 10^{-5}$ and $\nu > 10^{-9}$, any smaller values yield unreliable numerical calculations). These findings can be confirmed by applying the test for DDI in the 2 dimensional case [81].

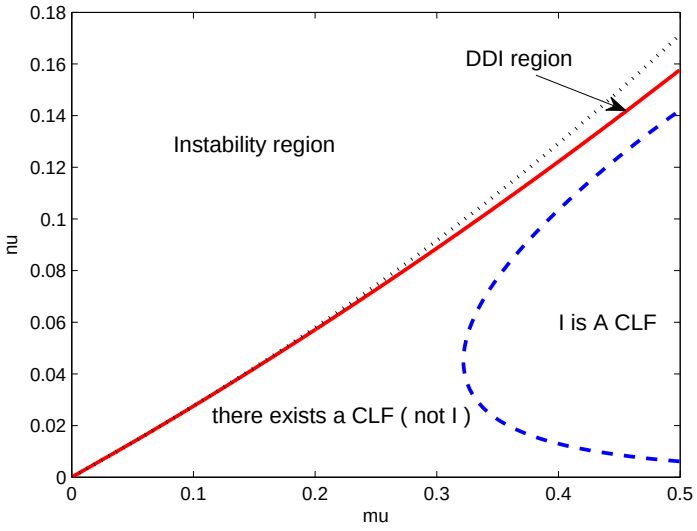

Figure 6.1: Geier-Meinhardt system with parameters $c_1 = 0.005, c_2 = 0.035, d_1 = 0.03, d_2 = .45, \rho_0 = 0.075$ and $\rho = \rho^{'} = 3.2$. The stability region is divided into three regions: A region where there is DDI (top right) enclosed by the solid red and dotted black curves; a region between the dashed blue curve and the solid red curve where there is a CLF (not the identity); a region to the right of the dashed blue curve where the identity I is a CLF

The second set of parameters is taken directly from the original paper [33]. For this we have $c_1 = 0.05$, $c_1 = 0.025$, $d_1 = 0.03$, $d_2 = 0.45$, $\rho^{'} = 0.00075$ and $\rho = \rho_0 = 3.2$. From Figure 6.2 we see that the region where A is stable is precisely where A and $-D$ share a CLF. In this case, there is no DDI, at least for $\mu > 10^{-5}$ and $\nu > 10^{-9}$.

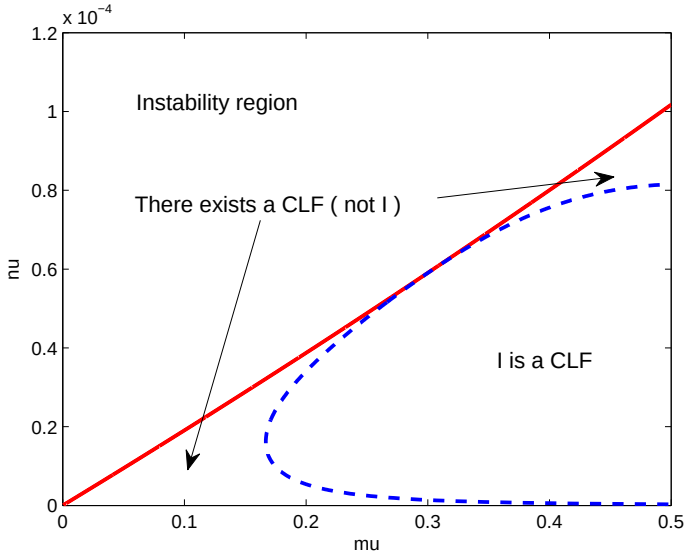

Figure 6.2: Geier-Meinhardt system with parameters $c_1 = .05, c_2 = 0.025, d_1 = 0.03, d_2 = .45, \rho_0 = 0.00075$ and $\rho = \rho^{'} = 3.2$. The stability region is divided in to a region to the right of the dashed blue curve where I is a CLF and a region between the solid red curve and the dashed blue curve where there is a CLF (not I). In this example the stability region and the region where there is a CLF coincide.

Our result uses the `cvx` package to test parameters for whether or not there exists a CLF. Tables 6.1 and 6.2 illustrate this in more detail by focusing on particular values of μ and ν. In Table 6.1, with parameter values $c_1 = 0.005$, $c_2 = 0.035$, $d_1 = 0.03$, $d_2 = 0.45$, $\rho^{'} = 0.075$ and $\rho = \rho_0 = 3.2$, we show the full range of possibilities: I is a CLF, there is a CLF, there is DDI. In Table 6.2, with parameter values $c_1 = 0.05$, $c_1 = 0.025$, $d_1 = 0.03$, $d_2 = .45$, $\rho^{'} = 0.00075$ and $\rho = \rho_0 = 3.2$, we only have: I is a CLF, there is a CLF $P \neq I$. In both cases there is no DDI.

(μ, ν)	A	P	Conclusion
$(0.4, 0.02)$	$\begin{pmatrix} -0.3247 & -0.0014 \\ 0.1360 & -0.02 \end{pmatrix}$	I	NO DDI
$(0.4, 0.12)$	$\begin{pmatrix} 0.0267 & -0.0444 \\ 0.1440 & -0.12 \end{pmatrix}$	$\begin{pmatrix} 3.6612 & -0.8824 \\ -0.8824 & 1.2204 \end{pmatrix}$	NO DDI
$(0.45, 0.1470)$	$\begin{pmatrix} 0.0649 & -0.0819 \\ 0.1299 & -0.1470 \end{pmatrix}$	NO CLF	DDI

Table 6.1: Geier-Meinhardt system with various choices for the degredation rate and the possibility of DDI in the case: $c_1 = 0.005, c_2 = 0.035, d_1 = 0.03, d_2 = 0.45, \rho_0 = 0.075,$ and$\rho = \rho^{'} = 3.2$.

(μ, ν)	A	P	Conclusion
$(0.4, 0.00005)$	$\begin{pmatrix} -0.1440 & -0.0016 \\ 0.0010 & -0.0001 \end{pmatrix}$	I	NO DDI
$(0.45, 0.000085)$	$\begin{pmatrix} -0.0267 & -0.0055 \\ 0.0009 & -0.0001 \end{pmatrix}$	$\begin{pmatrix} 2.7962 & 0.5225 \\ 0.5225 & 2.9157 \end{pmatrix}$	NO DDI

Table 6.2: Geier-Meinhardt system with various choices for the degredation rate and the possibility of DDI in the case: $c_1 = 0.05, c_2 = 0.025, d_1 = 0.03, d_2 = 0.45, \rho_0 = 0.00075$ and $\rho = \rho^{'} = 3.2$.

6.1.2 The Oregonator [76]

The Oregonator is a reduced version of the oscillatory Belousov-Zhabotinsky (BZ) chemical reaction [76]. According to Feild and Noyes [29, 30] the species

of the reaction behave as

$$\begin{aligned} A + Y &\longrightarrow X + P \\ X + Y &\longrightarrow P + P \\ A + X &\longrightarrow 2X + 2Z \\ X + X &\longrightarrow A + P \\ Z &\longrightarrow fY \end{aligned}$$

where $A = BrO_3^-$, $X = HBrO_2$, $Y = Br^-$, $Z = Ce(IV)$ and $P = HOBr$. The nonlinear reaction dynamics of the Oregonator are given by the system of ODEs

$$\left.\begin{aligned} \varepsilon\frac{dx}{dt} &= -qy + xy + x(1-x) \\ \delta\frac{dy}{dt} &= -qy - xy + 2fz \\ \frac{dz}{dt} &= x - z. \end{aligned}\right\} \tag{6.1}$$

Here q, f, ε and δ are positive constants. The non-negative equilibria of the system are the origin and (x_e, y_e, z_e) where

$$\begin{aligned} x_e &= 1/2(1 - 2f - q + \sqrt{(1-2f-q)^2 + 4q(1+2f)}) \\ y_e &= \frac{2fx_e}{q + x_e} \\ z_e &= x_e. \end{aligned}$$

Near the positive equilibrium the system behaves like

$$\dot{x} = Ax,$$

where

$$A = \begin{pmatrix} a_{11} & a_{12} & a_{13} \\ a_{21} & a_{22} & a_{23} \\ a_{31} & a_{32} & a_{33} \end{pmatrix},$$

and

$$\begin{array}{lll} a_{11} = \dfrac{1-2x_e-y_e}{\varepsilon} & a_{12} = \dfrac{q-x_e}{\varepsilon} & a_{13} = 0 \\ a_{21} = \dfrac{-y_e}{\delta} & a_{22} = -\dfrac{x_e+q}{\delta} & a_{23} = \dfrac{2f}{\delta} \\ a_{31} = 1 & a_{32} = 0 & a_{33} = -1. \end{array}$$

The characteristic polynomial of A is

$$\lambda^3+(1-a_{11}-a_{22})\lambda^2+(a_{11}a_{22}-a_{11}-a_{22}-a_{12}a_{21})\lambda+(a_{11}a_{22}-a_{12}a_{21}-a_{12}a_{23}) = 0.$$

For this system (see [81], p. 262) we always have

$$1 - a_{22} - a_{11} > 0 \qquad \text{and} \qquad a_{11}a_{22} - a_{12}a_{21} - a_{12}a_{23} > 0.$$

Hence according to the Routh-Hurwitz criterion [81], the necessary and sufficient condition for A to be stable is

$$2a_{11}a_{22}-a_{22}-a_{11}+a_{12}a_{23}-a_{11}a_{22}^2-a_{11}^2a_{22}+a_{11}^2+a_{22}^2+a_{11}a_{12}a_{21}+a_{12}a_{21}a_{22} > 0.$$

The chemical components of the Oregonator diffuse in space as well. Hence it is natural to consider the system (6.1) with diffusion. Here we will consider the diffusion matrix

$$D = \begin{pmatrix} 0.9 & 0 & 0 \\ 0 & 0.5 & 0 \\ 0 & 0 & 0.1 \end{pmatrix}.$$

The region in the parameter space (f, q) where I is a CLF for A and $-D$ is determined by the inequalities

$$4a_{11}a_{22} - (a_{12} + a_{21})^2 \geq 0 \qquad \text{and} \qquad \det(-(A + A^T)) \geq 0.$$

In the computations we assume the realistic parameter values $\varepsilon = 0.00073$, $\delta = 0.0004$ [81]. The stability region is split into two parts: a narrow strip parallel to the q-axis where $P = I$ is a CLF for A and $-D$, so that DDI is not possible, and its complement where DDI is not ruled out by the I-reactivity test. We can then use `cvx` to determine those parameters for which there is a CLF $P \neq I$ which in turn means that DDI is not possible, see Figure 6.3. For these specific choices of ε, δ and D we find that the stability region is the same as the region for which there exists a CLF for A and $-D$ and so in this case DDI is not possible for all choices of parameters f and q.

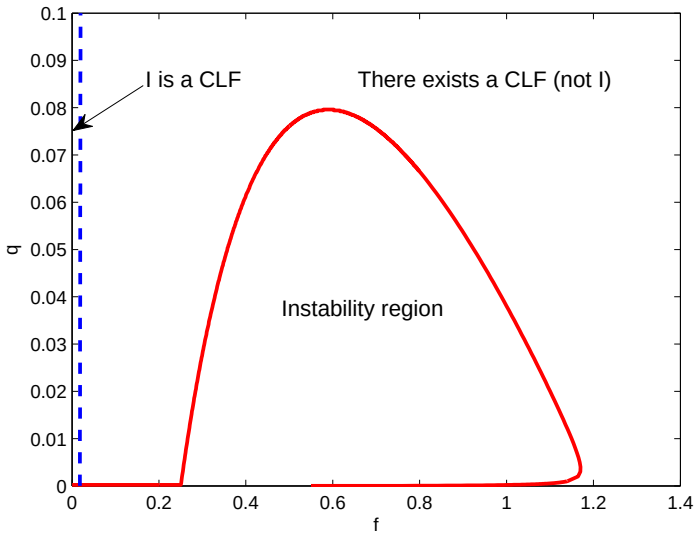

Figure 6.3: The Oregonator system with parameters $\varepsilon = 0.00073$, $\delta = 0.0004$ and $D = \text{diag}[0.9,\ 0.5,\ 0.1]$. I is a CLF in the region between the dashed blue curve and the q-axis. Between the dashed blue curve and solid red curve A and $-D$ have a CLF $P \neq I$. In this example the stability region and the region where there is a CLF coincide.

To illustrate the distinction between $P = I$ being a CLF and $P \neq I$ being a CLF in this example, choose $f = 2.58$ and $q = 0.0099$. Then the reaction matrix A is

$$A = \begin{pmatrix} -2879 & -6 & 0 \\ -7682 & -61 & 12900 \\ 1 & 0 & -1 \end{pmatrix}$$

Here I is not a CLF for A and $-D$ since $\lambda_1(A + A^T) \approx 14381 > 0$ so that A is I-reactive. Using `cvx`, the matrix

$$P = \begin{pmatrix} 0.0926 & -0.0007 & 0.1063 \\ -0.0007 & 0.0004 & 0.0415 \\ 0.1063 & 0.0415 & 651.4660 \end{pmatrix},$$

is a CLF for A and $-D$ and hence, by our result, DDI is not possible.

According to [49, 25] the sufficient condition for Turing instability is

$$A \quad \text{is stable} \quad \text{and} \quad 2qy_e - (q + x_e)(1 - 2x_e) < 0 \quad \text{with very small diffusitivities.} \tag{6.2}$$

Figure 6.4 shows the region determined by (6.2). This region is based on the choice : $d_1 = d_2 \approx 0$ and $d_3 = 0.1$.

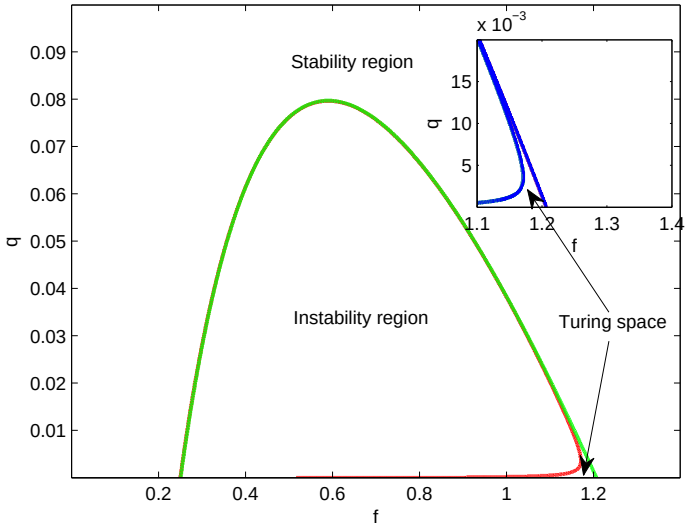

Figure 6.4: The Oregonator system with parameters $\varepsilon = 0.00073$, $\delta = 0.0004$ and $D \approx \text{diag}[0,\ 0,\ 0.1]$. The region for Turing instability, determined by (6.2), is the region shown in the zoomed-in subplot.

The analysis in [49] requires d_1 and d_2 to be very small. The analysis becomes inconclusive as we increase the diffusitivities d_1 and d_2. Here we study this using our approach. We increase the diffusitivities gradually as

follows:

$$d_1 = d_2 \approx 0,\ d_3 = 0.1;\ d_1 = 0.00009,\ d_2 = 0.00005,\ d_3 = 0.1;$$

$$d_1 = 0.009,\ d_2 = 0.005,\ d_3 = 0.1;\ d_1 = 0.9,\ d_2 = 0.5,\ d_3 = 0.1.$$

Using `cvx`, Figure 6.5, shows how the region where Turing patterns is not possible (shaded green) increases as the pair (d_1, d_2) increases until the region where we do not have DDI dominates all the stability region for large enough values of d_1 and d_2.

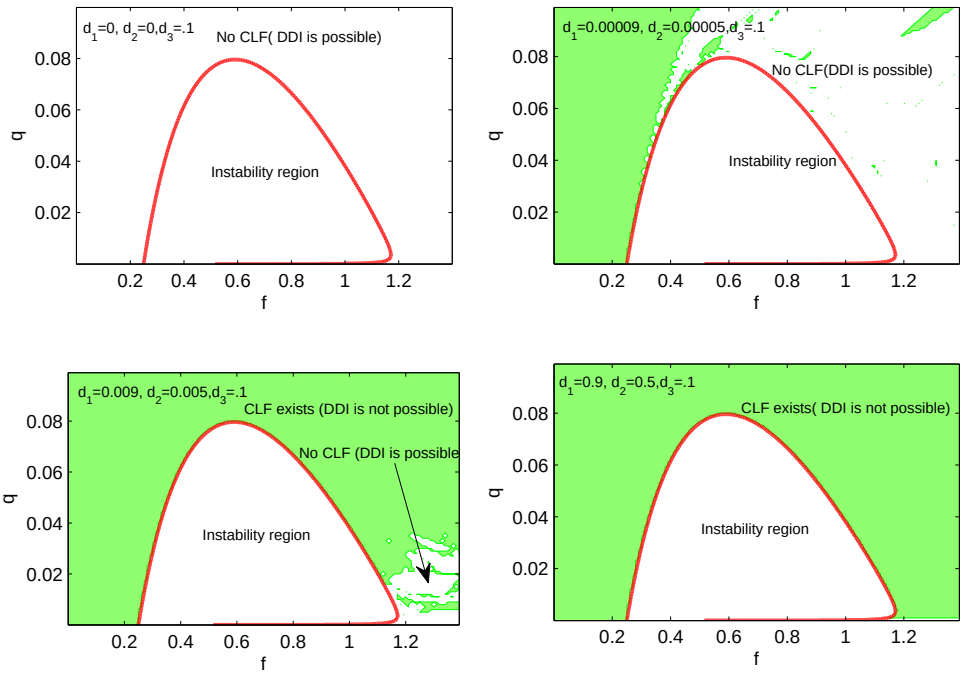

Figure 6.5: The Oregonator model with parameters $\varepsilon = 0.00073$, $\delta = 0.0004$ and different values of d_1 and d_2. The region where CLF exists, (shaded green), gradually dominates the stability region as the diffusitivities d_1 and d_2 increase.

6.1.3 Host-parasite-hyperparasite interaction [124]

Here we consider a model for host-parasite-hyperparasite interactions with host satisfying a logistic growth [124]. The non-dimensionalised, spatio-temporal dynamics of the system are given by the three equations

$$\begin{aligned}
\frac{\partial u}{\partial t} &= \tau[u(1-\frac{u}{K}) - uv)] + d_1\nabla^2 u \\
\frac{\partial v}{\partial t} &= \tau\mu[\frac{uv}{1+g} - \frac{vw}{1+gv}] + d_2\nabla^2 v \\
\frac{\partial w}{\partial t} &= \tau d[v-w] + d_3\nabla^2 w.
\end{aligned}$$

Here u and v represent the host and parasite densities, respectively, whereas w stands for the hyperparasite density. The constants τ, K, μ, g and d are all positive. A detailed description of the model is found in [124]. We will apply our result on the parameter space g, d. The parameter g relates to the degree of density dependence in the hyperparasite-induced parasite mortality, whereas d is the ratio of host growth to hyperparasite death rate. The reaction part has the unique positive steady state

$$\begin{aligned}
u^* &= \frac{(1+g)v^*}{1+gv^*} \\
v^* &= \frac{-J + \sqrt{J^2 + 4K^2 g}}{2Kg} \\
w^* &= v^*,
\end{aligned}$$

where

$$J = 1 + \gamma + K(1-g).$$

The Jacobian of the reaction part around the positive steady state is given by $A = (a_{ij})$ where

$$\begin{aligned} a_{11} &= \tau(1 - \frac{2u^*}{K}) & a_{12} &= \frac{-\tau(1+g)v^*}{1+\gamma v^*} & a_{13} &= 0 \\ a_{21} &= \frac{\tau\mu v^*}{1+g} & a_{22} &= \frac{\tau\mu g {v^*}^2}{(1+gv^*)^2} & a_{23} &= \frac{-\tau\mu v^*}{1+gv^*} \\ a_{31} &= 0 & a_{32} &= \tau d & a_{33} &= -\tau d. \end{aligned}$$

We assume that (u^*, v^*, w^*) is stable. The region in the parameter space (μ, ν), where I is a CLF is determined by the inequalities

$$a_{11} \leq 0, \quad 4a_{11}a_{22} - (a_{12} + a_{21})^2 \geq 0 \qquad \text{and} \qquad \det(-(A + A^T)) \geq 0.$$

We assume diffusion constants $d_1 = 0.02$, $d_2 = 0.2$, $d_3 = 1$ and the specific parameter values $\mu = 15$, $K = 10$ and $\tau = 1$. Figure 3.1 shows the corresponding parameter space partitioned in to two regions. A region to the right of the solid red line where A and $-D$ share a CLF and a region in two parts - one part to the right of one dotted black curve, the other part enclosed by the other dotted black curve - where A is stable. It is worth noting that I is not a CLF for any choices of parameters.

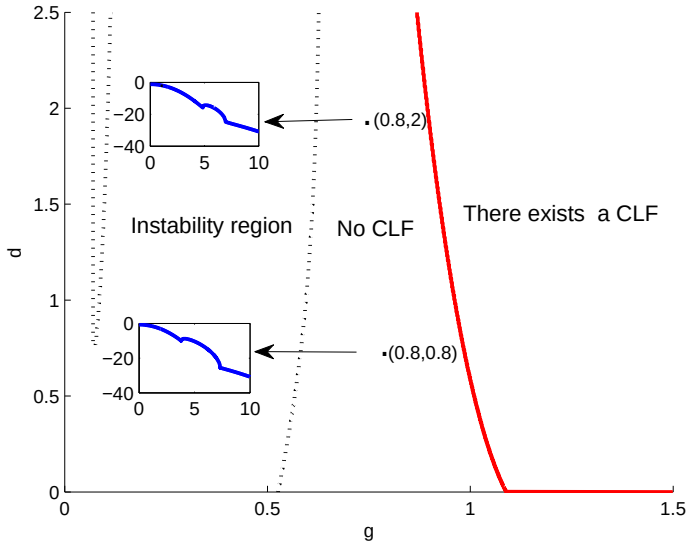

Figure 6.6: A host-parasite-hyperparasite system with parameters $d_1 = 0.02$, $d_2 = 0.2$, $d_3 = 1$, $\mu = 15$, $K = 10$ and $\tau = 1$. A is stable to the right of one dotted black curve and in the region above a second dotted black curve. A and $-D$ share a CLF to the right of the solid red curve. The subplots show the maximum real part of the eigenvalues of $A - k^2 D$ for parameters $(0.8, 0, 8)$ and $(0.8, 2.0)$ showing that there is no DDI in these two particular cases.

In this example, we see that whilst our result does rule out a wide range of parameter values which where not ruled out by I being a CLF, there remains a significant portion of the parameter space in which even our test for DDI is inconclusive. It is on these parameter ranges that more refined calculations should focus their efforts, for example by computing directly the eigenvalues of $A - k^2 D$ for a range of k. To illustrate this idea we add to the plots of parameter space, plots of the maximum real part of the eigenvalues of $A - k^2 D$ for wave numbers k in two cases $g = 0.8, d = 0.8$ and $g = 0.8$ and $d = 2$ where the CLF test is inconclusive. There is no DDI in either case.

6.2 Reaction Diffusion Chemotaxis Models

6.2.1 The Schnakenberg diffusion-chemotaxis model [131]

This system was originally introduced as a model for simple chemical systems with limit cycle behaviour [103]. The non-dimensional dynamics of the system are given by

$$\begin{aligned} \frac{\partial u}{\partial t} &= \gamma(a - u + u^2 v) + \nabla^2 u - \alpha\nabla.(u\nabla v), \\ \frac{\partial v}{\partial t} &= \gamma(b - u^2 v) + d\nabla^2 v\,. \end{aligned}$$

Here the parameters a and b are species' growth rates. The parameter γ results from non-dimensionalising the system and is essentially related to nature of the space. Here α is assumed to be positive which means that species u is attracted to species v. For details of this model, see [131, 104].

Linearisation around the equilibrium $(a+b, \frac{b}{(a+b)^2})$ leads to the reaction-diffusion-chemotaxis matrix:

$$A - \boldsymbol{k}^2 D_\alpha,$$

where

$$A = \gamma \begin{pmatrix} \frac{b-a}{a+b} & (a+b)^2 \\ \frac{-2b}{a+b} & -(a+b)^2 \end{pmatrix}, \quad D_\alpha = \begin{pmatrix} 1 & -\alpha(a+b) \\ 0 & d \end{pmatrix}.$$

The region of stability of A is determined by the inequality $b-a-(a+b)^3 < 0$. In this model the identity matrix I is a CLF when

$$A + A^T \leq 0 \quad \text{and} \quad D_\alpha + D_\alpha^T \geq 0.$$

So I is a CLF in a region in the (a, b) plane determined by the inequalities:

$$b \leq a, \quad 4(a+b)^3(b-a) + \left(2b - (a+b)^3\right)^2 \leq 0 \quad (\text{for } A),$$

$$4d \geq \alpha^2(a+b)^2 > 0 \quad (\text{for } D_\alpha).$$

We apply our results for the particular choice of parameters $d = 100$ and $\alpha = 20$. Figure 6.7 shows the region (to the right of red curve) where A and $-D_\alpha$ do share a CLF and so where it is impossible to have patterns due to chemotaxis and diffusion cooperatively.

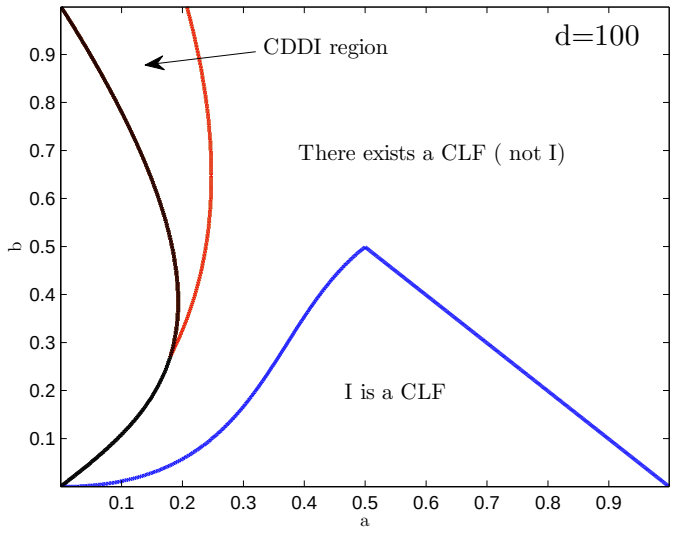

Figure 6.7: The Schnakenberg system with parameters $d = 100$, and $\alpha = 20$. The stability region (right of the black curve) is divided into three regions: A region where I is a CLF (under the blue curve); a region where there is a CLF (not I) (between the blue and red curves); a region where CDDI is possible (guaranteed by the set (5.22).

In the region between the black and red curves there is no CLF and so CDDI may be possible. It is in this region where detailed numerical calcu-

lations should focus there efforts. In [131] a set of inequalities is derived to determine where CDDI is possible. Note, that the solution set of these inequalities coincide with the region where A and D_α do not share a CLF. The parameters $a = 0.15$ and $b = 0.7$ lie in the region of no CLF (where CDDI might be expected). In this case we have

$$A = \begin{pmatrix} 0.6471 & 72.25 \\ -1.6471 & -0.7225 \end{pmatrix}, \quad D_\alpha = \begin{pmatrix} 1 & -17 \\ 0 & 100 \end{pmatrix}.$$

For the wave number $\boldsymbol{k} = \sqrt{0.3}$, the matrix pencil $A - \boldsymbol{k}^2 D_\alpha$ has the positive eigenvalues 25.529, .6948 and hence for these parameters there is indeed pattern formation. For $\gamma = 1$ and chemotactic coefficient $\alpha = 20$ and for various values of diffusivities, namely $d = 10$, $d = 25$, $d = 100$ and $d = 1000$, Figure 6.8 shows how the possibility of getting patterns due to diffusion chemotaxis (CDDI) depends on the intensity of diffusion. Our approach agrees with the analysis in [131], where it has been shown that the possibility for diffusion-chemotaxis driven instability correlates negatively with the diffusion value.

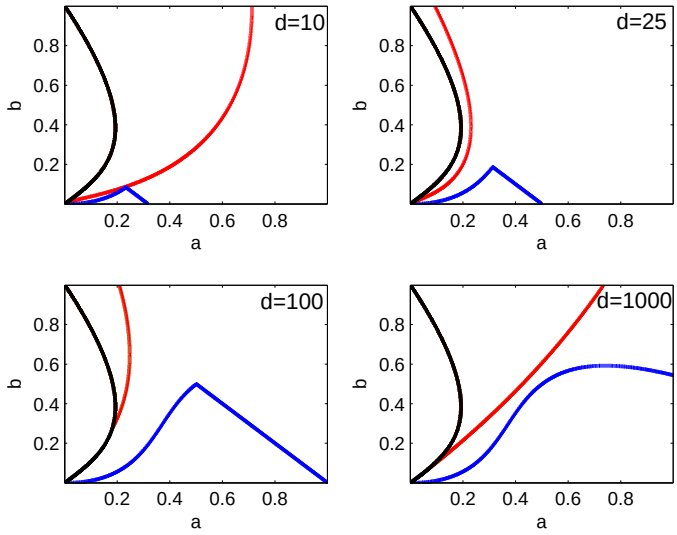

Figure 6.8: The possibility of getting patterns (right of the red curve) the intensity of diffusion. The values of diffusion which are used are: $d = 10$, 25, 100 and 1000.

6.3 Bacterial infection model

The cellular response to antigen invasion is termed an inflammation [110]. The antigen can be any microorganism. Examples include bacteria, viruses or even a macroorganism such as fungi [96]. The reaction against an invading antigen is a sophisticated process which can involve various scenarios either chemical or physical [16]. Typically, phagocytes (a type of white blood cells) surges to the location of infection as a response to the antigen entrance into the body [110, 125]. Leukocytes aim to halt the establishment of the antigens by phagocytosis or by secreting cytotoxic enzymes [102, 63]. The antigen, in some sense, acts as a chemoattractant to the phagocytes. This increase in the emigration rate of leukocytes towards the infected area will return back to normal (intrinsic rate) as the antigen is eradicated from the

tissue. The whole infection process is vast and complicated. Recently there have been extensive efforts to develop mathematical models for these sorts of regimes [131, 81, 23, 94, 113, 112]. Since the process of infection is essentially based on movement, reaction-diffusion-chemoataxis models are suitable candidates for this purpose. Motivated by their work in [16] which describes a lumped model for tissue inflammation dynamics, the authors extend the model to include the random motility of phagocytes and bacteria as well as phagocytes chemotaxis [17]. One of the advantages of this extension is that it serves to check the possibility of forming non-uniform steady states which is, pathologically, of a particular importance where the spatial heterogeneity of bacteria can lead to adverse effects. Specifically, it has been shown that when ρ (the scaled bacteria random motility) is higher than 1, the system can never exhibit such non-uniform spatial patterns. In this chapter, we extend the model constructed in [17] by incorporating bacterial taxis. We assume that bacteria develop this behaviour as a response to phagocytosis. Our assumption, whilst not observed in any laboratory based systems, can not be ruled out [62, 2]. We examine the effect of this hypothetical bacterial taxis on the possibility of forming a Turing pattern in some specific parameter spaces.

In Subsection 6.3.1, we introduce our extended model with its necessary assumptions. An analysis of steady states and their stability properties is given in Subsection 6.3.2. In Subsection 6.3.3 the possibility of developing a non-uniform steady state, due to chemotaxis and diffusion, is discussed. In Subsection 6.3.4, we use numerical simulations to check the effect of bacterial chemotaxis on the system's ability to exhibit a Turing regime.

6.3.1 Model equations

Encouraged by the model introduced in [17, 16] we propose a reaction-diffusion-chemotaxis model which has the same reaction part but we incorporate bacteria chemotaxis. Assuming that $b(t,x)$ and $c(t,x)$ stand for the bacteria and the phagocyte densities at time t and position x respectively then the model considered has the structure

$$\begin{aligned}\frac{\partial b}{\partial t} &= \frac{k_g b}{1+\frac{b}{K_i}} - \frac{k_d bc}{K_b+b} + \mu_b \nabla_x^2 b + \chi_1 \frac{\partial}{\partial x}(b\frac{\partial c}{\partial x}) \\ \frac{\partial c}{\partial t} &= h_0(\frac{A}{V})c_b[1+\frac{h_1}{h_0}b] - gc + \mu_c \nabla_x^2 c - \chi_2 \frac{\partial}{\partial x}(c\frac{\partial b}{\partial x}).\end{aligned}$$

The main assumption here is that bacteria are assumed to move chemotactically away from the leukocytes as a developing defence mechanism and we denote its tactic coefficient by χ_1. The chemotactic movement of the leukocytes (denoted by χ_2) is assumed to be towards the bacterial high gradients (i.e. the bacteria is a chemoattractant). As in [17], phagocytes and bacteria have the random motilities μ_b, μ_c respectively. The parameters K_i, K_b are the bacterial density growth and phagocytosis inhibition constants, respectively. The parameter k_g stands for the bacteria growth rate whereas k_d is the phagocytes killing rate. The parameters h_0, h_1 are the normal and the enhanced emigration rates of the Leukocytes. The fraction $\frac{A}{V}$ is the ratio of the surface area of the venule to the volume of the tissue. The phagocyte death rate is represented by g and its density in the venules is given by c_b. All the movements are assumed to be in 1-dimension ($-\infty < x < \infty$). The boundary conditions are $\frac{\partial b}{\partial x} = \frac{\partial c}{\partial x} = 0 \quad \text{as} \quad x \to \pm\infty$ Letting $c_0 = \frac{h_0(\frac{A}{V})c_b}{g}$ and using the

scaling

$$
\begin{aligned}
&v = \frac{b}{K_i}, \qquad u = \frac{c}{c_0}, \qquad \tau = \left(\frac{k_d c_0}{K_i}\right) t, \quad \zeta = \left(\tfrac{g}{\mu_c \alpha}\right)^{\frac{1}{2}} x, \\
&\gamma = \tfrac{k_g K_i}{k_d c_0}, \quad k = \tfrac{K_b}{K_i}, \quad \sigma = \tfrac{h_1 K_i}{h_0}, \quad \alpha = \tfrac{g K_i}{k_d c_0}, \\
&\rho = \tfrac{\mu_b}{\mu_c}, \quad \delta_1 = \tfrac{\chi_1 c_0}{\mu_c}, \quad \delta_2 = \tfrac{\chi_2 K_i}{\mu_c},
\end{aligned}
$$

$$
\left.
\begin{aligned}
\frac{\partial v}{\partial t} &= \frac{\gamma v}{1+v} - \frac{uv}{k+v} + \rho \nabla_x^2 v + \delta_1 \frac{\partial}{\partial x}\left(v \frac{\partial u}{\partial x}\right) \\
\frac{\partial u}{\partial t} &= \alpha(1 + \sigma v - u) + \nabla_x^2 u - \delta_2 \frac{\partial}{\partial x}\left(u \frac{\partial v}{\partial x}\right)
\end{aligned}
\right\} \tag{6.3}
$$

where, for convenience, we denote τ by t and ζ by x.

Here δ_1, δ_2 are the scaled bacterial and leukocytes chemotactic coefficients whereas ρ is the ratio of the bacterial diffusivity to phagocytes diffusivity. The parameter σ is the ratio of leukocyte emigration rates (enhanced/normal) whilst γ is the ratio of the bacterial maximum growth rate to maximum killing due to phagocyte. The parameter k refers to the ratio of the inhibition effect on bacteria growth due to the increase in its density to inhibition effect on its ability to kill bacteria. The ratio of phagocyte killing and death rate is given by the parameter α. For a detailed derivation see Appendix C.

6.3.2 The system without diffusion and chemotaxis

The system always has the steady state $(v, u) = (0, 1)$. This is termed as the elimination steady state which corresponds to the case where bacteria is absent (or eradicated) from the infected tissue. The system can have two other possible coexistence steady states, $(v_\pm > 0, u = 1 + \sigma v_\pm)$. These are termed compromise steady states and for these steady states bacteria exists at certain levels. In terms of the system parameters, the bacteria steady state density $v_\pm$

is given as

$$v_{\pm} = \frac{1}{2\sigma}\left[(\gamma - 1 - \sigma) \pm \sqrt{(1+\sigma-\gamma)^2 + 4\sigma(\gamma k - 1)}\right].$$

The compromise steady state does not always exist. The existence of a physically acceptable (real and positive) compromise steady state(s) is linked to the relation between the quantities k and $(1+\sigma)^{-1}$. To see this we follow the following argument. At equilibrium we always have

$$\gamma(v) := \frac{(1+v)(1+\sigma v)}{k+v}.$$

This relation, $\gamma(v)$, has the following properties

- $\gamma'(v) = \dfrac{\sigma v^2 + 2\sigma k v + k(1+\sigma) - 1}{(k+v)^2}$,
- $\gamma(0) = \dfrac{1}{k}$,
- $\gamma'(0) = \dfrac{k(1+\sigma) - 1}{k^2}$.

If $k(1+\sigma) - 1 > 0$ then $\gamma'(v) > 0$ for all v, and hence $\gamma(v)$ increases without bound.

If $k(1+\sigma) - 1 < 0$ then $\gamma(v)$ initially decreases till some $v := \widetilde{v} > 0$ where $\gamma'(\widetilde{v}) = 0$ and then starts increasing again. It turns out that

$$\widetilde{v} = -k + \sqrt{k^2 - \frac{k(1+\sigma) - 1}{\sigma}}.$$

This can be summarised as follows.

- If $k > (1+\sigma)^{-1}$: The system has no compromise states when $\gamma < 1/k$ and has only the upper state (v_+) for $\gamma > 1/k$.

- If $k < (1+\sigma)^{-1}$: The system has no compromise steady states when $\gamma < \widetilde{\gamma}$ whereas it has two when $\widetilde{\gamma} < \gamma < 1/k$. The system has only one compromise steady state if $\gamma > 1/k$. Here $\widetilde{\gamma} = \gamma(\widetilde{v})$.

Figure 6.9 depicts the existence of the bacterial model equilibria.

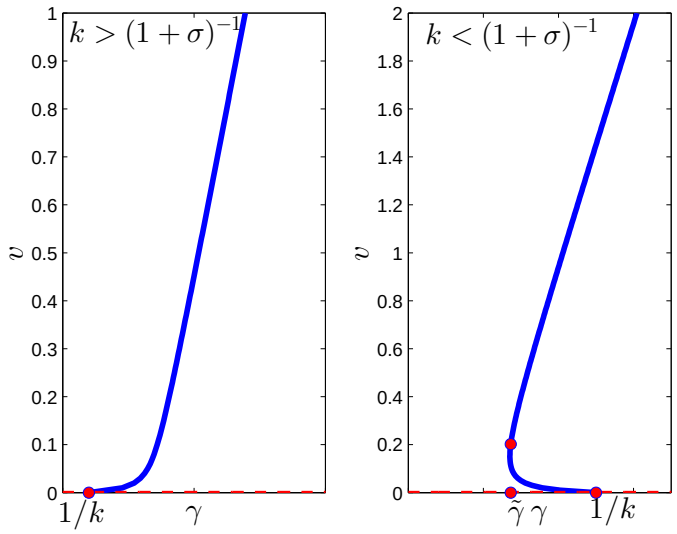

Figure 6.9: The equilibria of the bacterial model in terms of the parameter γ. The elimination steady state (red dashed) always exists. The blue curve indicates the compromise steady state. If $k > \frac{1}{1+\sigma}$ there exists only one compromise steady state, the upper one, whereas if $k < \frac{1}{1+\sigma}$ there exits two compromise steady states, the upper and the lower.

The Jacobian is given by

$$A = \begin{pmatrix} \frac{\gamma}{(1+v)^2} - \frac{ku}{(k+v)^2} & -\frac{v}{k+v} \\ \alpha\sigma & -\alpha \end{pmatrix}. \tag{6.4}$$

Evaluating the Jacobian at the elimination steady $(v, u) = (0, 1)$ state yields

$$A = \begin{pmatrix} \gamma - \frac{1}{k} & 0 \\ \alpha\sigma & -\alpha \end{pmatrix}.$$

Since $\alpha > 0$, the elimination steady state is stable if

$$\gamma < \frac{1}{k}.$$

For the compromise steady state (6.4) becomes

$$A = \begin{pmatrix} \frac{v(1+\sigma v)(1-k)}{(1+v)(k+v)^2} & -\frac{v}{k+v} \\ \alpha\sigma & -\alpha \end{pmatrix}.$$

So the compromise steady state is stable when

$$\det(A) = \frac{\alpha v}{1+v}\gamma'(v) > 0 \quad \text{and} \quad \text{trace}(A) = (\frac{v(1+\sigma v)(1-k)}{(1+v)(k+v)^2} - \alpha) < 0.$$

At all possible lower compromise steady states $\gamma' < 0$ and therefore $\det(A)$ is always negative. Consequently, the lower compromise steady state v_- is always unstable and hence it can never show a Turing pattern.

6.3.3 Possibility of developing a non-uniform steady state

All the above equilibria are also spatially uniform equilibria of the reaction-diffusion-chemotaxis system (6.3). Linearisation around these equilibria gives

$$A = \begin{pmatrix} \frac{\gamma}{(1+v)^2} - \frac{ku}{(k+v)^2} & -\frac{v}{k+v} \\ \alpha\sigma & -\alpha \end{pmatrix}, \quad D = \begin{pmatrix} \rho & \delta_1 v \\ -\delta_2 u & 1 \end{pmatrix}. \qquad (6.5)$$

Here we will discuss the possibility of developing spatial patterns for all possible steady states. We will discuss the possibility of a non-uniform steady state emerging from the elimination and compromise steady states due to chemotaxis and diffusion. We will focus on the parameter spaces (δ_2, ρ) and (σ, γ).

- **The elimination steady state**

  For the elimination steady state the matrices A and D in (6.5) become

$$A = \begin{pmatrix} \gamma - \frac{1}{k} & 0 \\ \alpha\sigma & -\alpha \end{pmatrix}, \quad D = \begin{pmatrix} \rho & 0 \\ -\delta_2 & 1 \end{pmatrix}.$$

  Since $\alpha > 0$, the elimination steady state without diffusion and chemotaxis (i.e $\rho = 0, \delta_1 = 0$ and $\delta_2 = 0$) is stable if

$$\gamma < \frac{1}{k}.$$

  The reaction matrix A and the chemotaxis diffusion matrix $-D$ always share a CLF. We can see this as follows. Assuming that A is stable, form the products

$$X_1 = A(-D) = \begin{pmatrix} -\rho(\gamma - \frac{1}{k}) & 0 \\ -\alpha\rho\sigma - \alpha\delta & \alpha \end{pmatrix},$$
$$X_2 = A(-D^{-1}) = \begin{pmatrix} -\frac{1}{\rho}(\gamma - \frac{1}{k}) & 0 \\ -\frac{1}{\rho}\alpha\sigma - \alpha\delta & \alpha \end{pmatrix}.$$

  Both X_1 and X_2 can not have real negative eigenvalues, which in turn by

Theorem 2.3.1 means that they always share a CLF. By our necessary conditions we conclude that it is impossible for the elimination steady state to give rise to patterns. This agrees with the conclusion made in [17]. Note that the identity matrix I is not a CLF in this case since we always have

$$\det(-(A + A^T)) = 4\alpha(\gamma - \frac{1}{k}) - \alpha\sigma^2 < 0.$$

- **The compromise steady state**

  In terms of the bacterial density at the compromise steady state the matrices A and $-D$ can be written as

$$A = \begin{pmatrix} \frac{v(1+\sigma v)(1-k)}{(1+v)(k+v)^2} & -\frac{v}{k+v} \\ \alpha\sigma & -\alpha \end{pmatrix}, \quad D = \begin{pmatrix} \rho & \delta_1 v \\ -\delta_2 u & 1 \end{pmatrix}.$$

  The matrix A is stable if, and only if,

$$\det(A) = \frac{\alpha v}{1+v}\gamma' > 0 \quad \text{and} \quad \text{trace(A)} < 0.$$

  At the lower compromise steady states we have $\gamma' < 0$ and therefore $\det(A)$ is always negative. Consequently, the lower compromise steady state is always unstable. The matrices A and $-D$ can not be simultaneously I-dissipative since A is always I-reactive. This is clear from the following argument.

$$-(A + A^T) = \begin{pmatrix} -2\frac{v(1+\sigma v)(1-k)}{(1+v)(k+v)^2} & -(\alpha\sigma - \frac{v}{k+v}) \\ -(\alpha\sigma - \frac{v}{k+v}) & 2\alpha \end{pmatrix}.$$

It is clear that if $k < 1$ then the (1,1)-entry is negative and hence $A + A^T$ can not be negative definite. Otherwise (i.e. $k \geq 1$) the determinant

$$\frac{4\alpha(1+\sigma v)(1-k)}{(1+v)(k+v)^2} - (\alpha\sigma - \frac{v}{k+v})^2,$$

is always negative. So restricting to the identity as a CLF is inconclusive here. Again this shows the limitations of the converse of the Neubert et al necessary condition.

6.3.4 Simulations

Here we will study the effect of bacterial chemotaxis on the possibility of forming non-uniform steady states. Our focus will be on the spaces (δ_2, ρ) and (α, γ). In both cases we will consider the situations $\delta_1 = 0$ (no bacterial chemotaxis) and $\delta_1 \neq 0$ (bacteria move away from phagocytes).

6.3.5 Bacterial diffusion vs. leukocytes random motility

Without bacterial chemotaxis ($\delta_1 = 0$) and with the parameter values $\gamma = 400$, $\alpha = 320$, $\sigma = 350$ and $k = .01$, the system has only one compromise steady state (the upper one). In Figure 6.10 our approach shows a region in the parameter space (δ_2, ρ) where CDDI is possible, left of the red curve, where A and $-D$ do not share a CLF. The boundary curve establishes a set of critical phagocytic chemotaxis values where at a certain level of bacterial random motility ρ the phagocytic movement has to be faster than a value given by the intersection of the horizontal line initiated at that level with the curve. For instance, with bacterial diffusion $\rho = .01$ the phagocytes needs to move faster than $\delta_2 \approx 2.75$ in order to halt the forming of steady spatial heterogeneity.

Our results agree with those made in [16].

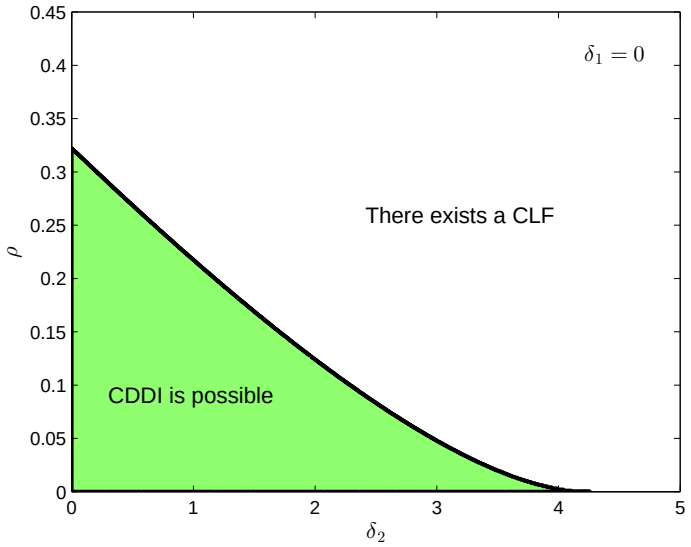

Figure 6.10: The bacteria-leukocyte model with parameters $k = 0.01, \gamma = 400, \alpha = 320, \sigma = 350, \delta_2 = 3.75$ and $\delta_1 = 0$. The stability region (all the parameter space) is divided to two parts. One where CDDI is possible (shaded green) and the other where it is not.

Figure 6.11 shows how the region of no Turing pattern responds to the change in bacterial taxis. Apparently, there is a negative relation between the intensity of bacteria tactic behaviour and the possibility for the system to establish a non-uniform steady state. The values of δ_1 used are 0, 0.0015, 0.005 and 0.0071.

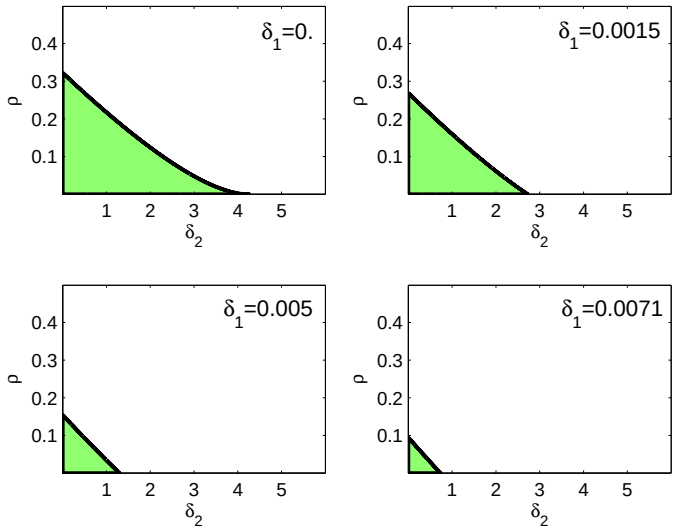

Figure 6.11: The bacteria-leukocyte model with bacteria chemotaxis (δ_1) values : 0, 0.0015,0.005 and 0.0071. The rest of the parameter are taken as in Figure 6.10. The possibility of forming patterns decreases as bacteria chemotaxis increases.

6.3.6 The ratio of maximum bacterial growth to maximum phagocyte killing vs. ratio of phagocyte death rate to maximum phagocytic killing

Here we will use the parameter values $\sigma = 350$, $\rho = 0.01$, $\delta_2 = 3.75$, $k = 0.01$ and $\delta_1 = 0$. The stability region (right of the black curve) in the parameter space (α, γ) is split into three distinct parts: where there is a CLF; where there is no CLF and no CDDI; and where there is no CLF and CDDI is possible, see Figure 6.12.

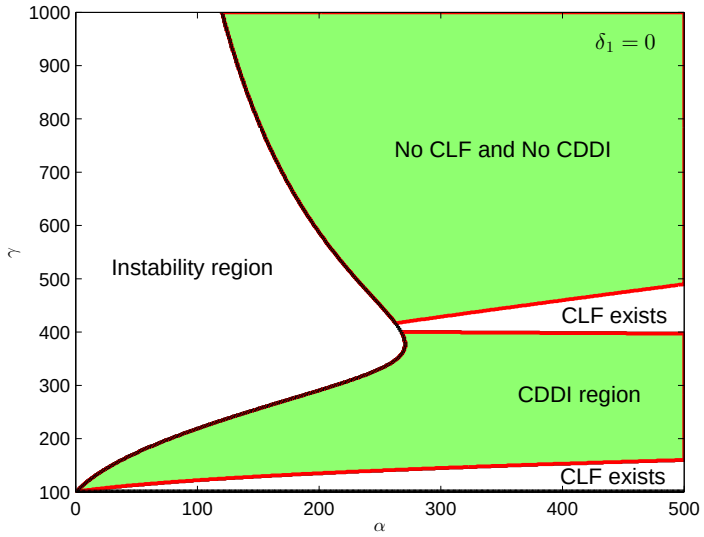

Figure 6.12: The bacteria-leukocyte model without bacteria chemotaxis (i.e. $\delta_1 = 0$). The other parameter values are: $\rho = 0.01$, $\sigma = 350$, $k = 0.01$ and $\delta_2 = 3.75$. Stability region is right to the black curve. The region where CDDI is possible is shaded green.

For a sequence of increasing values of δ_1, namely, 0, .01, 0.09, 0.2, and Figure 6.13 shows how the region where forming a non-uniform steady state is possible shrinks as a response to the increase in bacterial chemotaxis.

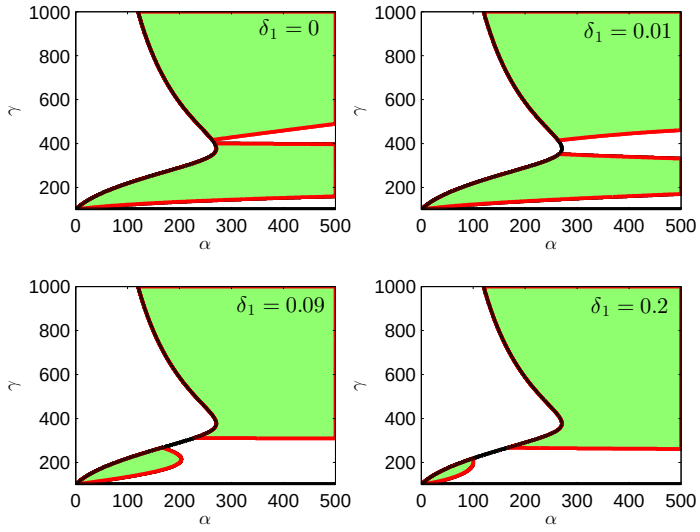

Figure 6.13: The paremeter space (α, γ) for various values of bacteria chemotaxis (in an increasing order), namely, 0, 0.01, 0.09 and 0.2. The other parameters are taken as in Figure 6.12. The possibility of developing non-uniform steady state decreases as the bacteria taxis increases.

6.4 Chemotaxis in a multi-species host-parasitoid community

Here we use our results to investigate the effect of chemotaxis on pattern formation in a multi-species host-parasitoid community. The model is taken from [97]. It addresses the heterogeneity of parasitoides as a response to the chemical cues secreted by plants during host feeding. The hosts are assumed to grow logistically and are consumed by the parasitoids according to Ivlev functional response. The paper [97] specifically studied the interaction among *Cotesia glomerata* and *Cotesia rbecula* as parasitiods and *Pieris brassicae* and *Pieris rapae* as hosts. For a detailed explanation of the model see [97]. The non-dimensionalised reaction diffusion chemotaxis model takes the form of five coupled PDEs :

$$\begin{aligned}
\frac{\partial n}{\partial t} &= d_n\nabla^2 n + n(1-n) - s_1 p(1-e^{-\rho_1 n}),\\
\frac{\partial m}{\partial t} &= d_m\nabla^2 m + \gamma_1 m(1-m) - s_2 p(1-e^{-\rho_2 m}) - s_3 q(1-e^{-\rho_3 m}),\\
\frac{\partial p}{\partial t} &= d_p\nabla^2 p - \chi_p\nabla.(p\nabla k) + c_1 p(1-e^{-\rho_1 n}) + c_2 p(1-e^{-\rho_2 m}) - \eta_1 p,\\
\frac{\partial q}{\partial t} &= d_q\nabla^2 q - \chi_q\nabla.(q\nabla k) + c_3 q(1-e^{-\rho_3 m}) - \eta_2 q,\\
\frac{\partial k}{\partial t} &= d_k\nabla^2 k + \gamma_2(n+\gamma_3 m) - \eta_3 k.
\end{aligned}$$

In the above equations, n and m are the density of the hosts *P. brassicae* and *P. rapae*, respectively, p and q are the density of the parasitoids *C. glomerata* and *C. rubecula*, respectively, k is the density of the chemo-attractant released during feeding by the hosts. The parameters $r_1, r_2, s_1, s_2, s_3, c_1, c_2, c_3, \rho_1, \rho_2, \rho_3, \eta_1, \eta_2$ and η_3 are all positive and have the values [97]:

$$\begin{array}{lllllll}
d_n = 0.0000008, & \rho_1 = 2.5, & \gamma_1 = 0.8, & c_1 = 0.3, & \eta_1 = 0.2, & s_1 = 0.8,\\
d_m = 0.0000008, & \rho_2 = 0.25, & \gamma_2 = 0.01, & c_2 = 0.004, & \eta_2 = 0.1, & s_2 = 0.2,\\
d_p = 0.0000075, & \rho_3 = 2.5, & \gamma_3 = 1, & c_3 = 0.2, & \eta_3 = 0.01, & s_3 = 0.8,\\
d_q = 0.0000075, & & & & & \\
d_k = 0.0000125, & & & & &
\end{array}$$

Without random motility (diffusion) and taxis and according to the given values of parameters the system has the positive steady state

$$(n, m, p, q, k) = (0.3379, 0.3389, 0.5043, 0.3716, 0.6768).$$

Linearisation around this steady state yields a linearised reaction matrix

$$A = \begin{pmatrix} -0.1092 & 0 & -0.4563 & 0 & 0 \\ 0 & -0.0839 & -0.0162 & -0.4571 & 0 \\ 0.1625 & 0.0005 & -0.0286 & 0 & 0 \\ 0 & 0.0796 & 0 & 0.0143 & 0 \\ 0.01 & 0.01 & 0 & 0 & -0.01 \end{pmatrix}.$$

In this case, A is stable since the eigenvalue with largest real part is -0.01. The diffusion-chemotaxis part has the form

$$D = \begin{pmatrix} d_n & 0 & 0 & 0 & 0 \\ 0 & d_m & 0 & 0 & 0 \\ 0 & 0 & d_p & 0 & -\chi_p p^* \\ 0 & 0 & 0 & d_q & -\chi_q q^* \\ 0 & 0 & 0 & 0 & d_k \end{pmatrix}.$$

As with the case of diffusion-only models, pattern formation requires instability of the matrix $A - k^2 D$ for some wave number k. The only difference here is that D is not diagonal. However, as with pure diffusion, pattern formation is not possible when A and (the non-diagonal) $-D$ have a CLF.

In [97], the dispersion relation is computed for four specific choices of the parameters χ_p and χ_q in D:

$$(\chi_p, \chi_q) = (0,0), (0.000535, 0.000535), (0.000545, 0.000545), (0.0015, 0.0015).$$

For the first two, pattern formation is not possible but for the second two pattern formation is possible. For the choice of parameters given by (6.4)

the identity matrix I is not a CLF since $A + A^T$ has the positive eigenvalue 0.321. Figure 6.14 shows the region in parameter space χ_p, χ_q where there is a CLF for A and $-D$. We see that formation of heterogeneous patterns is not possible when the chemotaxis parameters χ_p and χ_q are small. This result was not obtained in [97] and could not be detected by dispersion relation calculations unless applied exhaustively. Outside of the CLF region, formation of heterogeneous patterns is possible.

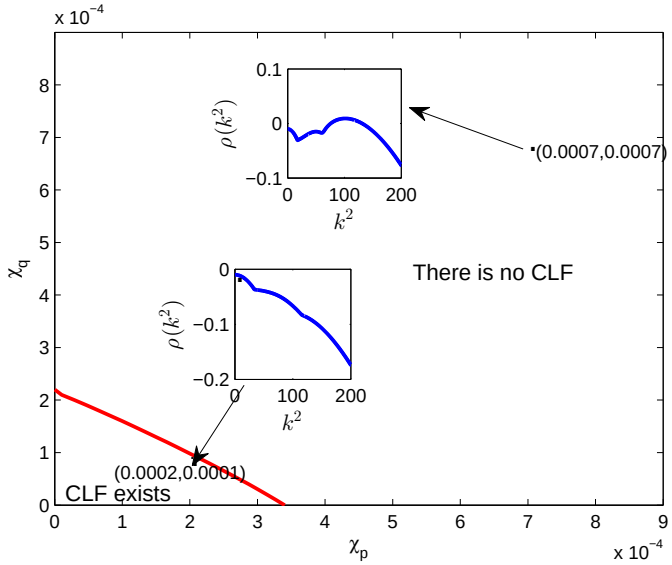

Figure 6.14: Multi-species host-parasitoid system with specific parameter values given by (6.4) and χ_p and χ_q as free parameters. The identity is not a CLF for any choices of χ_p and χ_q, whilst A and $-D$ have a CLF in the region to the left and below the red solid curve. Additionally we show plots of the dominant eigenvalue of $A - k^2 D$ for the specific parameter values $(0.0002, 0.0001)$ inside the CLF region and $(0, 0007, 0.0007)$ outside this region.

6.5 Carcinogenic tumour patterns model

Reaction-diffusion-taxis models are extensively used to model the invasion and metastasis of carcinogenic tumours [1]. Although the development of cancer

involves complicated, sometimes unexplainable, events, it can broadly speaking, be placed in two distinct phases. The avascular (less harmful stage) where cancer cells are confined locally due to the lack of enough nutrients and oxygen supply. In the other so called vascular phase, cancer starts invading the surrounding tissues. Escaping of cancer cell to the neighbouring healthy cells "metastasis" signifies a deadly characteristic. The extracellular matrix which surrounds the cancer cells acts as a barrier to prevent those deadly cells from migration. To overcome this, cancer cells secrets large enough amounts of the following proteolytic enzymes

- urokinase-type plasminogen activator (uPA)
- matrix metalloproteinases (MMPs).

These enzymes break down the (ECM) proteins so paving the way for cancer cells to migrate. In [116], a model of cancer invasion is analysed focusing on the role of urokinase plasminogen activation (uPA) system. Following [116] the uPA system consists of the following components

- uPA: the urokinase plaminogen activator,
- uPAR: the urokinase plaminogen acivator receptor, plasmin, the matrix degrading enzyme.
- VN: the ECM protein vitronectin, and
- PAI-1: the plasminogen activator inhibitor type-1.

To shed some light on the dynamics of the model we first fix some symbols. For the urokinase systems: the spatial density of uPA, UPAR, VN, and PAI-1 are u, p, v and m, respectively. The cancer cell's spatial density is given by

$n(t,x)$. In the model, cancer cells are assumed to move randomly with diffusion coefficient D_n, as well as exhibiting four kinds of tactic motions as follows

- chemotaxis due to uPA with tactic coefficient χ_u,
- chemotaxis due to PAI-1 with tactic coefficient χ_p,
- haptotaxis due to VN with tactic coefficient χ_v,
- haptotaxis due to other ECM components with tactic coefficient.

Also cancer cell proliferation is assumed to be logistic with intrinsic growth rate μ_1. All the urikinase systems are assumed to be randomly motile apart from the ECM. Their motility coefficients are D_u, D_p, D_m, respectively. The non-dimensionalised dynamics of the system reads

$$\begin{aligned}
\frac{\partial n}{\partial t} &= \mu_1 n(1-n) + D_n\nabla^2 n - \nabla.[\chi_u n\nabla u + \chi_p n\nabla p + \chi_v n\nabla v],\\
\frac{\partial v}{\partial t} &= -\delta vm + \phi_{21}up - \phi_{22}vp + \mu_2 v(1-v),\\
\frac{\partial u}{\partial t} &= -\phi_{31}pu - \phi_{33}nu + \alpha_{31}n + D_u\nabla^2 u,\\
\frac{\partial p}{\partial t} &= -\phi_{41}pu - \phi_{42}pv + \alpha_{41}m + D_p\nabla^2 p,\\
\frac{\partial m}{\partial t} &= \phi_{52}pv + \phi_{53}un - \phi_{54}m + D_m\nabla^2 m.
\end{aligned}$$

The parameter δ refers to the rate of degradation of ECM due to plasmin whereas μ_2 stands for the intrinsic remodelling rate. All the other parameters are positive real numbers. We will explain the meaning of parameters when

needed. We assume (as in [116]):

$$\left.\begin{array}{llll} D_n = 0.00035, & \chi_u = 0.0305, \phi_{21} = 0.75, \phi_{31} = 0.75, \phi_{41} = 0.75, \phi_{52} = 0.11, \\ D_u = 0.0025, & \chi_p = 0.0375, \phi_{22} = 0.55, \phi_{33} = 0.3, & \phi_{42} = 0.55, \phi_{53} = 0.75, \\ D_p = 0.0035, & \chi_v = 0.0285, & \\ D_m = 0.00491. & & \end{array}\right\} \tag{6.6}$$

Without random motility and taxis and according to the parameter values (6.6) the system has the positive steady state

$$(n^*, v^*, u^*, p^*, m^*) = (1, 0.047, 0.222, 0.889, 0.343) \tag{6.7}$$

Here A and D corresponding to (5.10) are

$$A = \begin{pmatrix} \mu_1(1-2n) & 0 & 0 & 0 & 0 \\ 0 & -\delta m - \phi_{22}p + \mu_2(1-2v) & \phi 21 & \phi_{22}v & \delta v \\ -\phi_{33}u + \alpha_{31} & 0 & -\phi_{31}p - \phi_{33}n & -\phi_{31}u & 0 \\ 0 & -\phi_{42}p & -\phi_{41}p & -\phi_{41}u - \phi_{42}v & \alpha_{41} \\ \phi_{53}u & \phi_{52}p & \phi_{53}n & \phi_{52}v & -\phi_{54} \end{pmatrix},$$

and

$$D = \begin{pmatrix} d_n & -\chi_v n^* & -\chi_u n^* & -\chi_p n^* & 0 \\ 0 & 0 & 0 & 0 & 0 \\ 0 & 0 & d_u & 0 & 0 \\ 0 & 0 & 0 & d_p & 0 \\ 0 & 0 & 0 & 0 & d_m \end{pmatrix}.$$

Without motion and near (6.7), the reaction part is stable with $\mathrm{Re}(\lambda_1(A)) = -0.24$. Furthermore, it is easy to see that I cannot be a Lyapunov function

for A since $\lambda_1(A + A^T) = 0.4937$. Obviously this makes the Neubert et al. test inconclusive.

6.5.1 Cancer cells heterogeneity and Turing instability

As suggested in [116] the rich heterogeneity in system dynamics which have been observed might result from reaction-diffusion-chemotaxis-hapotaxis driven instability. Although extensive simulations have been done, this implication is left as an open question. Three key parameters of the model have been varied to check the effects of variation on developing a spatially growing mode or in other words heterogeneity of cancer cells. These are, the parameters are D_n, ϕ_{35} and μ_1. The parameter ϕ_{53} is linked to the amount of (ECM) degradation enzyme secreted by cancer cells. In the simulations to follow we consider the parameters spaces (D_n, ϕ_{53}), (D_n, μ_2) and (ϕ_{53}, μ_1).

6.5.2 Cancer random motility (D_n) vs. ECM degradation rate (ϕ_{53})

Cancer cell motility increases as cells become more lethal. Moreover, cancer malignancy leads to an excessive secretion of the ECM degrading enzyme. Hence investigating the effects of changing D_n and ϕ_{53} on forming a nonuniform steady state is important. Based on the parameters (6.6) the authors in [116] exhaustively used the dispersion relation to study these effects. Figure 6.15 is a regeneration of what they obtained.

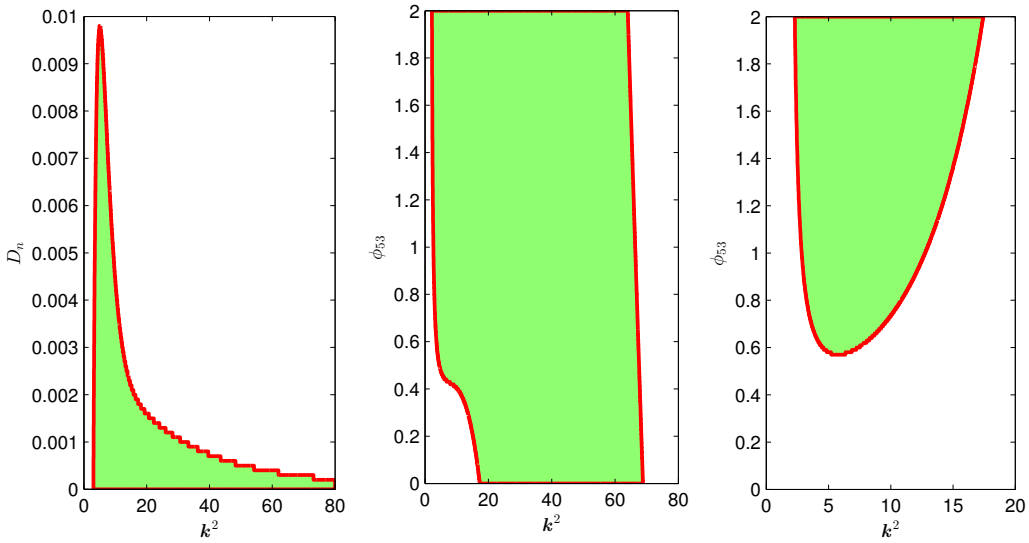

Figure 6.15: The dashed green areas refer to the value of the corresponding parameters indicated in the vertical axes, where spatial density of cancer is heterogenetised in Turing way. All the subplots are based on the set of parameters (6.6) apart from the first subplot from the right where cancer motility is chosen to be $D_n = 0.00425$.

With the same parameter values, but using our approach, we captured, all the above information at once. Figure 6.16 shows how the stability region is divided into distinct regions, one where cancer heterogeneity is absolutely impossible (shaded) and the other where it is.

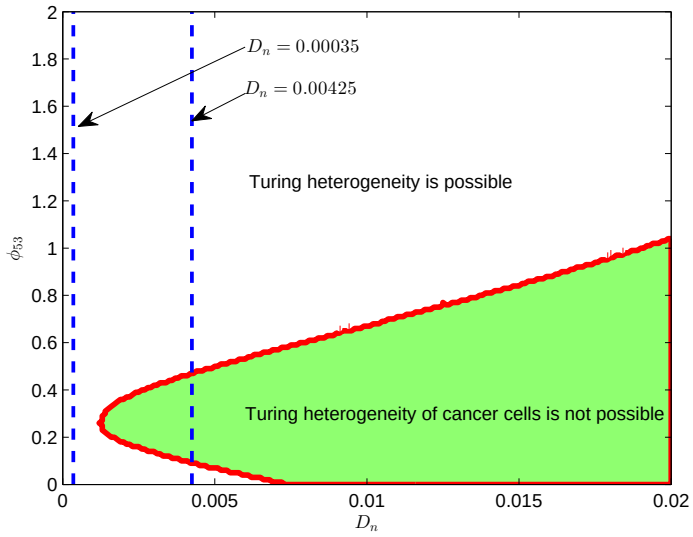

Figure 6.16: The stability region (all the parameter space) is divided into two distinct regions. Formation of Turing patterns is not possible in the shaded region where A and $-D$ are jointly dissipative. The vertical lines correspond to $D_n = 0.00035$ and $D_n = 0.00425$ as indicated. All the parameters are taken from (6.6).

As in Figure 6.15, it can be clearly pointed out that large enough cancer motility suppresses the formation of a nonuniform spatial steady state. On the other hand the effect of changing ϕ_{53} is case dependent. With large enough cancer motility (e.g. $D_n = 0.00425$) there are some values of ϕ_{53} where Turing patterns can not happen. Namely the intersection of the vertical line and the shaded region. For small values ($D_n = 0.00035$) our approach says nothing about Turing patterns.

6.5.3 Varying D_n and μ_1

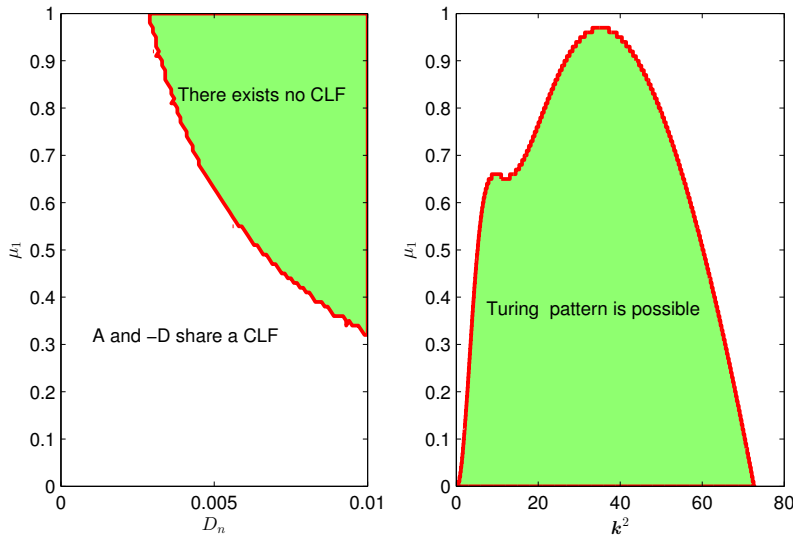

Figure 6.17: The left subplot is based on our approach where it depicts the region of no DDI in the parameter space (μ_1, D_n). The parameter values used her are the same as in (6.6). The right suplot is a regeneration to the one in [116].

At least in the motility-proliferation levels chosen in Figure 6.17, it can be pointed out that simultaneous increase in cancer motility and proliferation will eventually suppress Turing heterogeneity of cancer cells. This is easily seen in the left subplot of Figure 6.17 which based on our approach.

6.5.4 Varying μ_1 and ϕ_{53}

Another phenotypic aspect of cancer malignancy is the increase in cancer cell proliferation. Figure 6.18 shows a region in the parameter space (μ_1, ϕ_{53}) where Turing pattern is not possible.

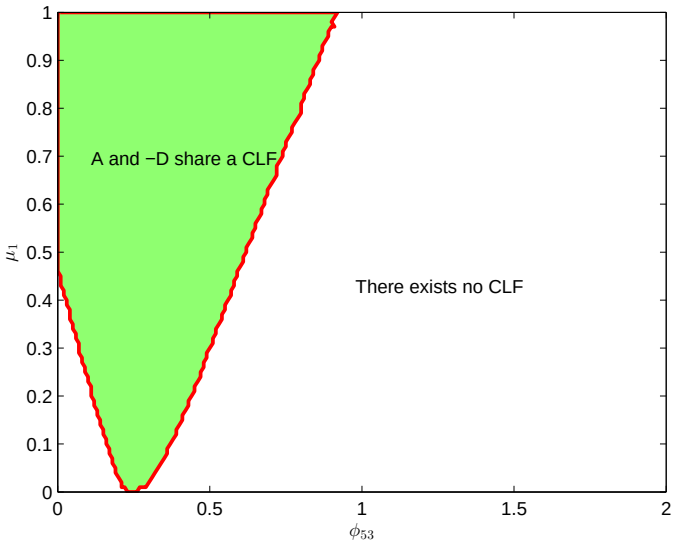

Figure 6.18: The shaded region is where A and $-D$ are jointly dissipative, i.e. where Turing patterns is ruled out. The parameters values are the same as in the parameter set (6.6), the only difference is that $D_n = 0.00425$.

6.6 Conclusion

In this chapter we applied Propositions 5.5.6 and 5.6.8 on a range of important examples found in the literature. We considered systems with diffusions in Section 6.1 and with diffusion and chemotaxis in Section 6.2. In each case, we compared the region we obtained with the region obtained using the already existed techniques mentioned in Chapter 5. The bacterial infection model in [17] has been extended. Specifically we assume that bacteria develops a defence mechanism in response to an increased concentration of leukocytes. This might be ascribed to the bacterial memory recognising the chemical cues produced by phagocytes. Using our approach on the extended model showed that there is a negative relationship between bacterial chemotaxis and the space of Turing patter. Simulations has been focused on two parameter spacer namely,

(δ_2, ρ) and (α, γ). Being higher dimensional systems, the 5×5 examples signifies an advantages of our approach. Our results 5.5.6 and 5.6.8 show an advantage on the classical approaches for detecting Turing patterns. It can be used for any systems with arbitrary dimension. The other advantages is that its a direct parameter link between the reaction part and the movement part this obviously not the case when using the dispersion relation.

Chapter 7

Conclusion

Since each chapter of the thesis has been equipped with its own conclusion we will give a short summary of what has been done in the whole thesis. In summary this thesis has explored a variety of topics. An extensive literature, focusing on measures of transient dynamics, has been presented. Also, a new measure of transient dynamics, so called P-reactivity has been introduced. This measure is essentially a generalisation of reactivity in the sense of Neubert and Caswell [84]. A formula that determines system reactivity with respect to a norm induced by a positive definite matrix P has been obtained. An extension of the result by Shorten and Narendra [108] regarding joint dissipativity in second order systems has been proved. The notion of P-reactivity encourages us to a pose an optimization problem aiming to find the norm with respect to which a given system has maximum P-reactivity. We tackled the problem of joint dissipativity robustness. When the underlying matrices of a jointly dissipative systems are subject to certain specific perturbations, the stability radius has been defined and characterised. The robustness of the Shorten and Narendra necessary and sufficient conditions for joint dissipativity have been

explored. A new, wave number independent necessary conditions has been obtained. This new condition has been extended to include various movement mechanisms such as chemotaxis. The conditions provides a parameter space searching approach for determining Turing instability. The thesis is ended by applications of the new condition to various models found in literature. We also extended the bacterial infection model introduced in [17, 16], to include bacterial chemotaxis.

7.1 Future Work

This work poses various questions. The following highlights some of them.

- Explore the notion of P-reactivity even further and find more examples for its relevance in the context of biosystems. This includes addressing the problem of maximum P-reactivity more closely.

- The question of joint dissiaptivity of systems of orders higher than 3 is still, as far as we know, an open and a challenging question. One possible approach, as suggested by some algebraists at Exeter University, is to use the so called differential Galois theory. As its known that Galois theory has elegantly answered the question of the existence of a general solution of a polynomial of degree $n \geq 5$. The problem of Turing patterns detection of higher order systems would become extremely tractable as the need to numerical solvers would become less important.

- Speed of pattern formation is also an important aspect of Turing theory. There has been some efforts to determine Turing patterns speed. However, that was restricted to second order systems [78]. We speculate that

maximum P-reactivity is related to speed of patterns propagation. This needs a more thorough investigation.

- Conduct a more thorough analysis of the robustness of Turing pattern appearance using the stability radius approach as discussed in Chapter 4.

Appendix A

A.1 Proof of theorem 2.3.1

This proof is a detailed version of the one in the original paper [108]. First we fix some notations and state some definitions. For the matrices A_1 and A_2 the linear combination

$$\sigma_\alpha[A_1, A_2] := \alpha A_1 + (1-\alpha)A_2, \quad \alpha \in [0,1],$$

is referred to as the pencil of A_1 and A_2. This matrix pencil is said to be Hurwitz if the spectrum of $\sigma_\alpha[A_1, A_2]$ is a subset of the left half of the complex plane for all $\alpha \in [0,1]$. To proceed in the proof of the theorem we take the following results for granted.

Lemma A.1.1. *If both pencils $\sigma_\alpha[A_1, A_2]$, $\sigma_\alpha[A_1, A_2^{-1}]$ are Hurwitz then at least one of them has real eigenvalues for some $\alpha \in [0,1]$.*

Lemma A.1.2. *If $\sigma_\alpha[A_1, A_2]$ is Hurwitz for all $\alpha \in [0,1]$ and have real eigenvalues for some $\alpha \in [0,1]$ then there exists positive constants d_1 and d_2 such that the pencil $\sigma_\alpha[B_1, B_2]$ where , $B_1 = A_1 + d_1 I$ and $B_2 = A_2 + d_2 I$ is*

1. *singular for exactly one value α_0 , and*

2. Hurwitz or has purely imaginary eigenvalues for all $\alpha \neq \alpha_0$.

A.1.1 Parts of the proof

We will divide the proof in two steps as follows:

Part I A_1 and A_2 share a CLF $\iff$ $\alpha A_1 + (1-\alpha)A_2$ and $\alpha A_1 + (1-\alpha)A_2^{-1}$ are Hurwitze.

Part II $\alpha A_1 + (1-\alpha)A_2$ and $\alpha A_1 + (1-\alpha)A_2^{-1}$ are Hurwitze $\iff$ $A_1 A_2$ and $A_1 A_2^{-1}$ have no negative real eigenvalues.

From Part I and Part II it is easy to conclude that
A_1 and A_2 share a CLF if, and only if, $A_1 A_2$ and $A_1 A_2^{-1}$ have no (distinct) negative real eigenvalues.

A.1.2 Proof

Part I

Necessity:

In [108] it has been shown that if a matrix X has a Lyapunov function then its inverse X^{-1} enjoys the same Lyapunov function.
Now for our case we assume that A_1 and A_2 share a CLF. Using the above result, P is also a Lyapunov function for A_1 and A_2^{-1}. It can be easily shown that for $\alpha \in [0, 1]$ the matrix P is also a Lyapunov function for

$$\alpha A_1 + (1-\alpha)A_2 \quad \text{and} \quad \alpha A_1 + (1-\alpha)A_2^{-1},$$

hence they are both Hurwitz.

Sufficiency:

Assume that $\sigma_\alpha[A_1, A_2]$ and $\sigma_\alpha[A_1, A_2^{-1}]$ are both Hurwitz. From lemma A.1.1 at least one of them has real eigenvalues for some $\alpha \in [0, 1]$. Without loss generality we can assume that one is $\sigma_\alpha[A_1, A_2]$. According to Lemma A.1.2 there will be two positive constants d_1 and d_2 such that

$$\sigma_\alpha[B_1, B_2]$$

is singular for exactly one value $\alpha_0 \in [0, 1]$ and Hurwitz, or has purely imaginary eigenvalues, for all $\alpha \in [0, 1], \alpha \neq \alpha_0$. We will consider the separate cases

Case I: $\alpha_0 \in (0, 1)$

Since $\sigma_\alpha[B_1, B_2]$ is singular for α_0 then there exists a non zero vector x_0 such that

$$B_1 x_0 = -\gamma_0 B_2 x_0 \quad (\gamma_0 = \frac{1 - \alpha_0}{\alpha_0}). \tag{A.1}$$

If $q \in \mathbb{R}^{2\times 1}$ is orthogonal to x_0, we can deduce that

- x_0 can not be an eigenvector of B_1 or of B_2.

  Proof if x_0 is an eigenvector for B_1 then we have

  $$B_2 x_0 = -\frac{\lambda}{\gamma_0} x_0 \quad \text{for some} \quad \lambda \neq 0$$

  Now if $\lambda > 0$, then this says that B_1 has a positive eigenvalue, other wise B_2 does.

- q can not be an eigenvector of B_1^T (B_2^T).

  Proof:

  If q is an eigenvector of B_1^T then we have $x_0 B_1^T q = q^T B_1 x_0 = 0$. This implies that $B_1 x_0$ is a scalar multiple of x_0 and hence it is an eigenvalue of B_1, which contradicts the previous argument. The case of B_2^T is similar

From the above we conclude that q and $B_1^T q$ are linearly independent, i.e. the matrix $[q, B_1^T q]$ is full rank. Now because B_1 is either Hurwitz or has purely imaginary eigenvalues, using [83, p.66] we have that there is a positive definite matrix P so that

$$B_1^T P + P B_1 = -k_1 q q^T, \quad k_1 \geq 0. \tag{A.2}$$

In terms of A_1, equation (A.2) becomes

$$A_1^T P + P A_1 = -2d_1 P - k_1 q q^T. \tag{A.3}$$

Hence $V(x) = x^T P x$ is a **Lyapunov function for** A_1.

Now multiplying both sides of equation (A.2) by x_0 we get

$$x_0^T (B_1^T P + P B_1) x_0 = (B_1 x_0)^T P x_0 + x_0^T P (B_1 x_0) = 0 \tag{A.4}$$

Substituting from (A.1) into (A.4) we get

$$\gamma_0 x_0^T (B_2^T P + P B_2) x_0 = 0$$

This says that $(B_2^T P + P B_2) x_0$ is either zero or orthogonal to x_0. We will consider each case at a time.

Case 1: $(B_2^T P + P B_2) x_0 = 0$

This implies that the matrix $(B_2^T P + P B_2)$, which is symmetric, has a zero eigenvalue corresponding to x_0. In other words it is a rank one matrix and can

be written as

$$B_2^T P + P B_2 = -k_2 q q^T, \quad k_2 \in \mathbb{R}.$$

If $k_2 < 0$ then B_2 is unstable and this contradicts the fact that both B_1 and B_2 are Hurwitz or have imaginary eigenvalues. Therefore we have

$$B_2^T P + P B_2 = -k_2 q q^T, \quad k_2 \geq 0.$$

and this means that $V(x) = x^T P x$ is also a Lyapunov function for A_2. Hence $V(x) = x^T P x$ is a **CLF** for A_1 and A_2.

Case 2 : $(B_2^T P + P B_2)x_0 \perp x_0$

Now $\gamma_0(B_2^T P + P B_2)x_0$ is orthogonal to x_0. Also with the aid of equation (A.2) it can be easily shown that $B_1^T P x_0$ and $P B_1 x_0$ are also orthogonal to x_0. To see this we multiply both sides of equation (A.2) by x_0 we get

$$x_0^T (B_1^T P + P B_1) x_0 = x_0^T B_1^T P x_0 + x_0^T P B_1 x_0 = -k_1 x_0^T q q^T x_0 = 0.$$

Hence we have

$$x_0^T B_1^T P x_0 + x_0^T P B_1 x_0 = 2 x_0^T B_1^T P x_0 = 0 \Longrightarrow x_0^T B_1^T P x_0 = x_0^T (B_1^T P x_0) = 0,$$

and this implies that $B_1^T P x_0$ and $P B_1 x_0$ are orthogonal to x_0. Therefore there exists a real number $k \neq 0$ such that

$$\gamma_0 (B_2^T P + P B_2) x_0 = k B_1^T P x_0$$

from equation (A.1) we have

$$(\gamma_0 B_2^T P - P B_1)x_0 = k B_1^T P x_0$$

from equation (A.2) we get

$$(\gamma_0 B_2^T + (1-k)B_1^T)Px_0 = 0 \tag{A.5}$$

Lets rewrite equation (A.5) as

$$(\gamma B_2^T + B_1^T)Px_0 = 0 \quad \text{where} \quad \gamma = \frac{\gamma_0}{1-k} \tag{A.6}$$

Lets assume that equation (A.6) is satisfied for some $k = \overline{k}$ (i.e $\gamma = \overline{\gamma} = \frac{\gamma_0}{1-\overline{k}}$). In other words

$$(\overline{\gamma} B_2^T + B_1^T)Px_0 = 0.$$

Since P is non-singular we conclude that the matrix $(\overline{\gamma} B_2^T + B_1^T)$ is singular. Also since B_1 and B_2 are Hurwitz or have imaginary eigenvalues we have

$$\det(\gamma B_2^T + B_1^T) = 0 \quad \text{for at most two values of} \quad \gamma$$

Also since $\det(B_1) > 0$ and $\det(B_2) > 0$, both values of γ are positive or both are negative. But we already know that $\det(\gamma B_2 + B_1)$ is zero at $\gamma_0 > 0$. This implies that $\overline{\gamma} = \gamma_0$ and hence $k = \overline{k} = 0$. With this the problem returned the same as case 1.

Case II: $\alpha_0 = 0$ or $\alpha_0 = 1$

According to [108], this case delivers the following possibilities:

(a) A_1 and A_2 are both upper triangular matrices.

(b) $A_1 = -kI$, $k > 0$ and A_2 is a general Hurwitz matrix.

(c) A_1 is diagonal and the diagonal entries of A_2 are negative.

The case (b) is obvious since any Lyapunov function for A_2 is a Lyapunov function of A_1. The case (a) has been proved in [107] whereas case (c) has been proved in [106].

Part II:

We will show $\sigma_\alpha[A_1, A_2]$ is Hurwitze, if and only, if $A_1 A_2^{-1}$ has no negative real eigenvalues. The proof of the other part is similar.

For all α we have

$$\text{trace}(\sigma_\alpha[A_1, A_2]) = \alpha \text{trace}(A_1) + (1-\alpha)\text{trace}(A_2) < 0.$$

We can also write

$$\det(\sigma_\alpha[A_1, A_2]) = \det(\alpha A_1 + (1-\alpha)A_2) = \alpha^2 \det(\lambda I + A_1 A_2^{-1})\det(A_2), \quad \text{(A.7)}$$

where $\lambda = \frac{1-\alpha}{\alpha} \in (0, \infty)$.

Now if $A_1 A_2^{-1}$ has no negative real eigenvalues, then $\det(\sigma_\alpha[A_1, A_2]) > 0$ for all α. In other words $\sigma_\alpha[A_1, A_2]$ is Hurwitz for all α

The other direction is obvious since assuming that $\sigma_\alpha[A_1, A_2]$ is Hurwitz for all α leads, from (A.7), to

$$\det(\lambda I + A_1 A_2^{-1}) > 0 \quad \text{for all} \quad \alpha,$$

and this implies that $A_1 A_2^{-1}$ has no negative real eigenvalues. The conclusion will remain the same if we allow negative, but equal, real eigenvalues. This is

actually our extension. The other case (i.e. $\sigma_\alpha[A_1, A_2^{-1}]$) is similar.

A.2 The equilibria of Gray and Scott model

We have

$$-uv^2 + F(1-u) = 0, \tag{A.8}$$

$$uv^2 - F(F+k)v = 0. \tag{A.9}$$

From A.9 we get either $v = 0$ (we will ignore this) or

$$v = \frac{F+k}{u}. \tag{A.10}$$

Substituting from A.10 in A.9 yields

$$(-u)(\frac{(F+k)^2}{u^2}) + F(1-u) = 0.$$

Simplification of this leads to

$$u^2 - u + \frac{(F+k)^2}{F} = 0.$$

Hence we get

$$u_{1,2} = \frac{1 \pm \sqrt{1 - 4\frac{(F+k)^2}{F}}}{2} = \frac{1 \pm \sqrt{d}}{2}$$

where $d = 1 - \frac{4(F+k)^2}{F}$. Substituting in A.10 we get

$$\begin{aligned} v_{1,2} &= \frac{2(F+k)}{1 \pm \sqrt{d}} = \frac{2(F+k)(1 \mp \sqrt{d})}{(1 \pm \sqrt{d})(1 \mp \sqrt{d}} \\ &= \frac{2(F+k)(1 \mp \sqrt{d})}{1-d} = \frac{2(F+k)(1 \mp \sqrt{d})}{1-(1-\frac{4(F+k)^2}{F})} = \frac{F}{2(F+k)}(1 \mp \sqrt{d}) \end{aligned}$$

Hence we have the two equilibria

$$u_1 = \frac{1+\sqrt{d}}{2}, \quad v_1 = \frac{\alpha(1-\sqrt{d})}{2},$$

or

$$u_2 = \frac{1-\sqrt{d}}{2}, \quad v_2 = \frac{\alpha(1+\sqrt{d})}{2}.$$

A.3 Proof of (4.5)

We will proof the equivalent statement

λ is not an eigenvalue of $A+UV \iff 1$ is not eigenvalue of $V(\lambda I - A)^{-1}U$.

Substitution of $(\lambda I - A)$ for A in the *Sherman-Morrison-Woodbury formula* gives

$$(\lambda I - A + UV)^{-1} = (\lambda I - A)^{-1} - ((\lambda I - A)^{-1}U(I + V(\lambda I - A)^{-1}U)^{-1}V(\lambda I - A)^{-1}).$$

Now if 1 is not an eigenvalue of $V(\lambda I - A)^{-1}U$, then the right hand side exists and hence the left hand side exists too. This implies that λ is not an eigenvalue of $A+UV$. The other direction (i.e. λ is not an eigenvalue of $A+UV$) follows the same argument.

A.4 Details of Proposition 4.2.5

The matrix M_Δ can be expanded as

$$\begin{aligned} M_\Delta =& M + \delta_1 E_1^T D_1^T P + \delta_2 E_2^T D_2^T P + \ldots + \delta_k E_k^T D_k^T P + \delta_1 P D_1 E_1 + \delta_2 P D_2 E_2 \\ & + \ldots + \delta_k P D_k E_k E_k. \end{aligned}$$

This can be written as

$$M_\Delta = M + \delta_1(P D_1 E_1 + E_1^T D_1^T P) + \delta_2(P D_2 E_2 + E_2^T D_2^T P) + \ldots + \delta_k(P D_k E_k + E_k^T D_k^T P).$$

The above equation can be written as

$$M_\Delta = \begin{pmatrix} PD_1 & E_1^T & PD_2 & E_2^T & \ldots & PD_k & E_k^T \end{pmatrix} \begin{pmatrix} \delta_1 & 0 & 0 & \ldots & \ldots & \ldots & 0 \\ 0 & \delta_1 & 0 & \ldots & \ldots & \ldots & 0 \\ 0 & 0 & \delta_2 & 0 & \ldots & \ldots & 0 \\ \vdots & \vdots & 0 & \delta_2 & 0 & \ldots & 0 \\ \vdots & \vdots & \vdots & 0 & \ddots & \ldots & 0 \\ 0 & 0 & \ldots & 0 & \ldots & \delta_k & 0 \\ 0 & 0 & \ldots & 0 & \ldots & 0 & \delta_k \end{pmatrix} \begin{pmatrix} E_1 \\ D_1^T P \\ E_2 \\ D_2^T P \\ \vdots \\ E_k \\ D_k^T P \end{pmatrix}$$

Now applying 4.5, 0 will be an eigenvalue of M_Δ if, and only if, 1 is an eigenvalue of

$$\begin{pmatrix} \delta_1 & 0 & 0 & \dots & \dots & 0 \\ 0 & \delta_1 & 0 & \dots & \dots & 0 \\ 0 & 0 & \delta_2 & 0 & \dots & 0 \\ \vdots & \vdots & 0 & \delta_2 & 0 & \dots 0 \\ \vdots & \vdots & \vdots & 0 & \ddots & \dots 0 \\ 0 & 0 & \dots & 0 & \dots & \delta_k \quad 0 \\ 0 & 0 & \dots & 0 & \dots & 0 \quad \delta_k \end{pmatrix} \begin{pmatrix} E_1 \\ D_1^T P \\ E_2 \\ D_2^T P \\ \vdots \\ E_k \\ D_k^T P \end{pmatrix} N \begin{pmatrix} PD_1 & E_1^T & PD_2 & E_2^T & \dots & PD_k & E_k^T \end{pmatrix}$$

where $N = (0I - M)^{-1} = -M^{-1}$. That is, 0 is an eigenvalue of M_Δ if, and only if, 1 is an eigenvalue of

$$\begin{pmatrix} \delta_1 & 0 & 0 & \dots & \dots & 0 \\ 0 & \delta_1 & 0 & \dots & \dots & 0 \\ 0 & 0 & \delta_2 & 0 & \dots & 0 \\ \vdots & \vdots & 0 & \delta_2 & 0 & \dots 0 \\ \vdots & \vdots & \vdots & 0 & \ddots & \dots 0 \\ 0 & 0 & \dots & 0 & \dots & \delta_k \quad 0 \\ 0 & 0 & \dots & 0 & \dots & 0 \quad \delta_k \end{pmatrix} \begin{pmatrix} E_1NPD_1 & E_1NE_1^T & \dots & E_1NPD_k & E_1NE_k^T \\ D_1^TPNPD_1 & D_1^TPNE_1^T & \dots & D_1^TPNPD_k & D_1^TPNE_k^T \\ \vdots & \vdots & \vdots & \vdots & \vdots \\ E_kNPD_1 & E_kNE_1^T & \dots & E_kNPD_k & E_kNE_k^T \\ D_k^TPNPD_1 & D_k^TPNE_1^T & \dots & D_k^TPNPD_k & D_k^TPNE_k^T \end{pmatrix},$$

The above matrix product can be written as

$$\begin{bmatrix} \mathbf{D_{11}} & \dots & 0 \\ \vdots & \ddots & \vdots \\ 0 & \cdots & \mathbf{D_{kk}} \end{bmatrix} \begin{bmatrix} G_{11} & \dots & G_{2k} \\ \vdots & \ddots & \vdots \\ G_{2k1} & \cdots & G_{2k2k} \end{bmatrix}.$$

where G_{ij} are defined as in (4.11). The block matrices $\mathbf{D_{ii}}$ are defined as

$$\mathbf{D_{ii}} = \begin{pmatrix} \delta_i & 0 \\ 0 & \delta_i \end{pmatrix}_{\mathbf{2\times 2}} .$$

Appendix B

B.1 Weyl's theorem

Assume that A and B are two Hermitian matrices. Assume that their eigenvalues are ordered in a increasing order as follows.

$$\lambda_{min} = \lambda_n(A) \leq \lambda_{n-1}(A) \leq \lambda_{n-2}(A) \ldots \leq \lambda_2(A) \leq \lambda_1(A) = \lambda_{max},$$

$$\lambda_{min} = \lambda_n(B) \leq \lambda_{n-1}(B) \leq \lambda_{n-2}(B) \ldots \leq \lambda_2(B) \leq \lambda_1(B) = \lambda_{max},$$

$$\lambda_{min} = \lambda_n(A+B) \leq \lambda_{n-1}(A+B) \leq \lambda_{n-2}(A+B) \ldots \leq \lambda_2(A+B) \leq \lambda_1(A+B) = \lambda_{max},$$

then for each $k = 1, 2, \ldots n$ we have

$$\lambda_k(A) + \lambda_n(B) \leq \lambda_k(A+B) \leq \lambda_k(A) + \lambda_1(B).$$

B.2 A `cvx` code

The following Matlab code uses the `cvx` package to find, where possible, a CLF for stable A and $-D$:

```
cvx_begin sdp
variable P(n,n) symmetric
A'*P+P*A<=zeros(n);
-D'*P+P*(-D)<=zeros(n);
P>=eye(n);
cvx_end
```

Appendix C

C.1 Detailed derivation of the reduction of parameters in 6.3.1

We have the

$$\frac{\partial b}{\partial t} = \frac{\partial b}{\partial v}\frac{\partial v}{\partial \tau}\frac{\partial \tau}{\partial t} = k_d c_0 \frac{\partial v}{\partial \tau}$$
$$\frac{\partial c}{\partial t} = \frac{\partial c}{\partial u}\frac{\partial u}{\partial \tau}\frac{\partial \tau}{\partial t} = \frac{k_d c_0^2}{K_i}\frac{\partial u}{\partial \tau},$$

$$\begin{aligned}\nabla_x^2 b &= \frac{\partial}{\partial x}\left(\frac{\partial b}{\partial x}\right) = \frac{\partial}{\partial x}\left(\frac{\partial b}{\partial v}\frac{\partial v}{\partial \xi}\frac{\partial \xi}{\partial x}\right) = \left(K_i\sqrt{\frac{g}{\mu_c\alpha}}\right)\frac{\partial}{\partial x}\left(\frac{\partial v}{\partial \xi}\right)\\ &= \left(K_i\sqrt{\frac{g}{\mu_c\alpha}}\right)\nabla_\xi^2 v\frac{\partial \xi}{\partial x} = \left(\frac{K_i g}{\mu_c\alpha}\right)\nabla_\xi^2 v,\end{aligned}$$

$$\begin{aligned}\nabla_x^2 c &= \frac{\partial}{\partial x}\left(\frac{\partial c}{\partial x}\right) = \frac{\partial}{\partial x}\left(\frac{\partial c}{\partial u}\frac{\partial u}{\partial \xi}\frac{\partial \xi}{\partial x}\right) = \left(c_0\sqrt{\frac{g}{\mu_c\alpha}}\right)\frac{\partial}{\partial x}\left(\frac{\partial u}{\partial \xi}\right)\\ &= \left(c_0\sqrt{\frac{g}{\mu_c\alpha}}\right)\nabla_\xi^2 u\frac{\partial \xi}{\partial x} = \left(\frac{c_0 g}{\mu_c\alpha}\right)\nabla_\xi^2 u\end{aligned}$$

$$\frac{\partial}{\partial x}\left(b\frac{\partial c}{\partial x}\right) = K_i\frac{\partial}{\partial x}\left(v\frac{\partial c}{\partial x}\right) = K_i\frac{\partial}{\partial x}\left(v\frac{\partial c}{\partial u}\frac{\partial u}{\partial \xi}\frac{\partial \xi}{\partial x}\right) = \left(c_0K_i\sqrt{\frac{g}{\mu_c\alpha}}\right)\frac{\partial}{\partial x}\left(v\frac{\partial u}{\partial \xi}\right)$$
$$= \left(c_0K_i\sqrt{\frac{g}{\mu_c\alpha}}\right)\left(v\nabla_\xi^2 u\frac{\partial \xi}{\partial x} + \frac{\partial v}{\partial \xi}\frac{\partial \xi}{\partial x}\frac{\partial u}{\partial \xi}\right) = \left(\frac{c_0K_ig}{\mu_c\alpha}\right)\left(v\nabla_\xi^2 u + \frac{\partial v}{\partial \xi}\frac{\partial u}{\partial \xi}\right)$$
$$= \left(\frac{c_0K_ig}{\mu_c\alpha}\right)\frac{\partial}{\partial \xi}\left(v\frac{\partial u}{\partial \xi}\right)$$

$$\frac{\partial}{\partial x}\left(c\frac{\partial b}{\partial x}\right) = c_0\frac{\partial}{\partial x}\left(u\frac{\partial b}{\partial x}\right) = c_0\frac{\partial}{\partial x}\left(u\frac{\partial b}{\partial v}\frac{\partial v}{\partial \xi}\frac{\partial \xi}{\partial x}\right) = \left(c_0K_i\sqrt{\frac{g}{\mu_c\alpha}}\right)\frac{\partial}{\partial x}\left(u\frac{\partial v}{\partial \xi}\right)$$
$$= \left(c_0K_i\sqrt{\frac{g}{\mu_c\alpha}}\right)\left(u\nabla_\xi^2 v\frac{\partial \xi}{\partial x} + \frac{\partial u}{\partial \xi}\frac{\partial \xi}{\partial x}\frac{\partial v}{\partial \xi}\right) = \left(\frac{c_0K_ig}{\mu_c\alpha}\right)\left(u\nabla_\xi^2 v + \frac{\partial u}{\partial \xi}\frac{\partial v}{\partial \xi}\right)$$
$$= \left(\frac{c_0K_ig}{\mu_c\alpha}\right)\frac{\partial}{\partial \xi}\left(u\frac{\partial v}{\partial \xi}\right)$$

C.1.1 Substitution in equations:

- **Equation One**

  substitution on both sides we get

$$k_dc_0\frac{\partial v}{\partial \tau} = \frac{k_gK_iv}{1+v} - \frac{k_dK_ic_0uv}{kK_i + K_iv} + \mu_b\left(\frac{K_ig}{\mu_c\alpha}\right)\nabla_\xi^2 v + \chi_1\left(\frac{c_0K_ig}{\mu_c\alpha}\right)\frac{\partial}{\partial \xi}\left(v\frac{\partial u}{\partial \xi}\right)$$
$$\frac{\partial v}{\partial \tau} = \frac{\left(\frac{k_gK_i}{k_dc_0}\right)v}{1+v} - \frac{uv}{k+v} + \left(\frac{1}{k_dc_0}\right)\mu_b\left(\frac{K_ig}{\mu_c\alpha}\right)\nabla_\xi^2 v$$
$$+ \left(\frac{1}{k_dc_0}\right)\chi_1\left(\frac{c_0K_ig}{\mu_c\alpha}\right)\frac{\partial}{\partial \xi}\left(v\frac{\partial u}{\partial \xi}\right)$$
$$\frac{\partial v}{\partial \tau} = \frac{\gamma v}{1+v} - \frac{uv}{k+v} + \left(\frac{1}{k_dc_0}\right)\mu_b\left(\frac{K_i}{\mu_c\alpha}\right)\left(\frac{\alpha k_dc_0}{K_i}\right)\nabla_\xi^2 v$$
$$+ \left(\frac{1}{k_dc_0}\right)\chi_1\left(\frac{c_0K_i}{\mu_c\alpha}\right)\left(\frac{\alpha k_dc_0}{K_i}\right)\frac{\partial}{\partial \xi}\left(v\frac{\partial u}{\partial \xi}\right)$$
$$= \frac{\gamma v}{1+v} - \frac{uv}{k+v} + \left(\frac{\mu_b}{\mu_c}\right)\nabla_\xi^2 v + \left(\frac{\chi_1c_0}{\mu_c}\right)\frac{\partial}{\partial \xi}\left(v\frac{\partial u}{\partial \xi}\right).$$

Denoting τ by t and ξ by x we get

$$\frac{\partial v}{\partial t} = \frac{\gamma v}{1+v} - \frac{uv}{k+v} + \rho\nabla_x^2 v + \delta_1 \frac{\partial}{\partial x}\left(v\frac{\partial u}{\partial x}\right).$$

- **Equation Two**

$$\begin{aligned}
\frac{k_d c_0^2}{K_i}\frac{\partial u}{\partial \tau} &= h_0\left(\frac{A}{V}\right)c_b\left(1+\frac{h_1 K_i}{h_0}v\right) - gc_0 u + \mu_c\left(\frac{c_0 g}{\mu_c\alpha}\right)\nabla_\xi^2 u \\
&\quad - \chi_2\left(\frac{c_0 K_i g}{\mu_c\alpha}\right)\frac{\partial}{\partial\xi}\left(u\frac{\partial v}{\partial\xi}\right) \\
&= g\left(\left(\frac{h_0\left(\frac{A}{V}\right)c_b}{g}\right)(1+\sigma v) - c_0 u\right) + \mu_c\left(\frac{c_0}{\mu_c\alpha}\right)g\nabla_\xi^2 u \\
&\quad - \chi_2\left(\frac{c_0 K_i}{\mu_c\alpha}\right)g\frac{\partial}{\partial\xi}\left(u\frac{\partial v}{\partial\xi}\right) \\
&= gc_0\left(1+\sigma v - u\right) + \mu_c\left(\frac{c_0}{\mu_c\alpha}\right)g\nabla_\xi^2 u - \chi_2\left(\frac{c_0 K_i}{\mu_c\alpha}\right)g\frac{\partial}{\partial\xi}\left(u\frac{\partial v}{\partial\xi}\right) \\
&= \left(\frac{K_i}{k_d c_0^2}\right)(gc_0)\left(1+\sigma v - u\right) + \left(\frac{K_i}{k_d c_0^2}\right)\mu_c\left(\frac{c_0}{\mu_c\alpha}\right)\left(\frac{\alpha k_d c_0}{K_i}\right)\nabla_\xi^2 u \\
&\quad - \left(\frac{K_i}{k_d c_0^2}\right)\chi_2\left(\frac{c_0 K_i}{\mu_c\alpha}\right)\left(\frac{\alpha k_d c_0}{K_i}\right)\frac{\partial}{\partial\xi}\left(u\frac{\partial v}{\partial\xi}\right) \\
\frac{\partial u}{\partial\tau} &= \left(\frac{gK_i}{k_d c_0}\right)\left(1+\sigma v - u\right) + \nabla_\xi^2 u - \left(\frac{\chi_2 K_i}{\mu_c}\right)\frac{\partial}{\partial\xi}\left(u\frac{\partial v}{\partial\xi}\right).
\end{aligned}$$

Denoting τ by t and ξ by x we get

$$\frac{\partial u}{\partial t} = \alpha\left(1+\sigma v - u\right) + \nabla_x^2 u - \delta_2\frac{\partial}{\partial x}\left(u\frac{\partial v}{\partial x}\right).$$

Bibliography

[1] J. A. Adam and N. Bellomo. *A survey of models for tumour-immune system dynamics*. Birkhauser, Boston, 1996.

[2] J. Adler and W. Tso. Decision-making in bacteria: Chemotaxis response of escherichia coli conflicting stimuli. *Science*, 184:1292–1294, 1974.

[3] A. Agladze, D. Jackson, and T. Romeo. Periodicity of cell attachment during escherichia coli biofilm development. *J. Bacteriology*, 185:5632–5638, 2003.

[4] A. Aotani, M. Mimura, and T. Mollee. A model aided understanding of spot pattern formation in chemotactic *E. coli* colonies. *Japan J. Indust. Appl. Math*, 27:5–22, 2010.

[5] C. Belta, P. Finin, L. C. G. J. M. Habets, A. M. Halasz, M. Imielinski, R. V. Kumar, and H. Rubin. Understanding the bacterial stringent response using reachability analysis of hybrid systems. In *Proc. 7th Int. workshop on hybrid systems: computation and control (HSCC)*, volume 2993, pages 111–126, 2004.

[6] H. Berg. Chemotaxis in bacteria. *Annual review of bioengineering*, 4:119–136, 1975.

[7] M. Bertsch and D. Hilhorst. A density dependent diffusion equation in population dynamics: Stabilization to equilibrium. *Hiroshima Math. J*, 17:863–883, 1986.

[8] E. Bonabeau1, G. Theraulaz, J. L. Deneubourg, O. Rafelsberger, N. R. Franks, J. L. Joly, and S. phane. A model for the emergence of pillars, walls and royal chambers in termite nests. *Philosophical Transactions of the Royal Society B: Biological Sciences*, 353:1561–1576, 1998.

[9] S. Boyd and L.Vandenberghe. *Convex Optimization*. Cambridge University Press, 2004.

[10] N. F. Britton. *Essential Mathematical Biology*. Springer-Verlag, London, 2003.

[11] G. C. Calafior. A probabilistic analytic center cutting plane method for feasibility of uncertain lmi. *Automatica*, 43:2022–2023, 2007.

[12] V. Castets, E. Dulos, J. Biossonade, and P. D. Kepper. Experimental evidence of a sustained standing turing-type nonequilibrium chemical pattern. *Phys. Rev. Lett*, 64:2953–2956, 1990.

[13] M. Chaplain, M.Ganesh, and I. Graham. Spatio-temporal pattern formation on spherical surfaces: Numerical simulation and application to solid tumour growth. *Bull. Math.Biol.*, 42:387–423, 2001.

[14] M. Cross and P. Hohenberg. Pattern formation outside of equilibrium. *Rev. Mod. Phys*, 65:851–1112, 1993.

[15] I. CVX Research. CVX: Matlab software for disciplined convex programming, version 2.0 beta, Sep 2012.

[16] C. R. K. D. Lauffenburger. Analysis of a lumped model for tissue inflammation dynamics. *Mathematical Biosciences*, 53:189–221, 1981.

[17] C. R. K. D. Lauffenburger. Localised bacterial infection in a distributed model for tissue inflamation. *Mathematical biology*, 16:141–163, 1983.

[18] K. H. K. D. Lauffenburger. Effects of leukocyte random motility and chemotaxis in tissue inflammatory response. *Journal of theoretical biology*, 81:475–503, 1979.

[19] G. Dahlquist. Stability of error bounds in numerical integration of ordinary differential equations. *Transactions Royal Inst. of Technology*, 130, 1959.

[20] P. Dekepper, V. Castesls, E. Dolos, and J. Boissonade. Turing-type chemical patterns in the chlorite-iodide-malonic acid reaction. *Physics D*, 49:161–169, 1991.

[21] W. Dessaul, H. V. D. Mark, K. V. D. Mark, and S. Fischer. Changes in the patterns of collagens and fibronectin during limb-bud chondrogenesis. *J Embryol Exp Morphol*, 57:51–60, 1980.

[22] L. A. S. E. F. Keller. Initiation of slime mold aggregation viewed as an instability. *Journal of theoretical biology*, 26:399–425, 1970.

[23] A. Edelstein-Keshet. *Mathematical Models in Biology.* McGraw-Hill Companies, 1988.

[24] M. Eisenbach, J. W. Lengel, M. Varon, a. R. A. F. D. Gutnick, and R. Meili, J. E. Segall, G. M. Omann, and a. F. M. A. Tamada. *Chemotaxis.* Imperial College Press, 2004.

[25] A. S. Elragig and S. Townley. Turing pattern in the oregonator revisited. *Submited to Applied Mathematics Letters*.

[26] I. Epstein and K. Showalter. Nonlinear chemical dynamics: oscillations, patterns and chaos. *J. Phys. Chem*, 100:13132–13147, 1996.

[27] G. f. Oster and J. Murray. Pattern formation models and developmental constraints. *The Journal of experimental zoology*, 251:186–202, 1989.

[28] Y. Fengqi, W. Junjie, and S. Junping. Diffusion-driven instability and bifurcation in lengyel-epstein system. *Nonlinear Analysis: Real World Applications*, 9:1038–1051, 2008.

[29] R. Field and R. Noyes. Oscillations in chemical systems. iv. limit cycle behaviour in a model of a real chemical reaction. *J.Chem.Phys.*, 60:1877–1884, 1974.

[30] R. J. Field and F. W. Schneier. Oscillating chemical reactions and nonlinear dynamics. *J. Chem. Educ.*, 66:195, 1989.

[31] R. A. Fisher. The wave of advance of advantageous genes. *Ann. Eugenics*, 7:421–422, 1937.

[32] P. Gahinet, A. Nemirovskii, A. J. Laub, and M. Chilali. The lmi control toolbox. In *Decision and Control, 1994., Proceedings of the 33rd IEEE Conference on*, volume 3, pages 2038–2041. IEEE, 1994.

[33] A. Gierer and H. Meinhardt. A theory of biological pattern formation. *Kybernetik*, 12:30–39, 1972.

[34] R. Goeble, R. Sanfelice, and A. Teel. *Hybrid dynamical systems: modeling stability and robustness*. Princeton University press, 2012.

[35] G. H. Golub and C. F. V. Loan. *Matrix computations*. John Hopkins University press, Boltimore, 3 edition.

[36] B. C. Goodwin and L. E. H. Trainor. Tip and whorl morphogenesis in acetabularia by calcium-regulated strain fields. *Journal of theoretical biology*, 117:79–106, 1985.

[37] P. Gray and S. K. Scott. Autocatalytic reactions in the isothermal, continous stired tank reactor: Oscillations and instabilities in the system $a + 2b \rightarrow 3b$, $b \rightarrow c$. *Chem. Eng. Sci.*, 39:1087–1097, 1984.

[38] P. Grindrod. *Patterns and waves: The theory and applications of reaction-diffusion equations*. Oxford university press, 1991.

[39] A. Hasting. Transients : the key to long-term ecological understanding. *Trends in ecology and evolution*, 19:39–45, 2004.

[40] A. Hasting. Timescales, and ecological understanding. *Ecology*, 9:3471–3480, 2010.

[41] L. V. Hein, Q. P. Ha, and V. N. Phat. Stability and stabilization of switched linear dynamic systems with time delay and uncertainties. *Applied mathematics and computation*, 200:223–231, 2009.

[42] D. Hinrichhsen and A. J. Pritchard. New robustness results for linear systems under real perturbations. In *Decision and Control, 1988., Proceedings of the 27th IEEE Conference on*, pages 1375–1379, 12 1988.

[43] D. Hinrichsen, B. Kelb, and A. Linnemann. An algorithm for the computaion of the structured stability radius. *Automatica*, 25:771–775, 1989.

[44] D. Hinrichsen and A. J. Prichard. A note on some differences between real and comlex stability radii. *Systems & control letters*, 14:401–408, 1990.

[45] D. Hinrichsen and A. J. Pritchard. Stability radii of linear systems. *Systems & control letters*, 7(1):1–10, 1986.

[46] D. Hinrichsen and A. J. Pritchard. Stability radius for structured perturbations and the algebraic riccati equation. *Systems & control letters*, 8(2):105–110, 1986.

[47] D. Hinrichsen and A. J. Pritchard. *Mathematical Systems Theory I: Modelling, State Space Analysis, Stability and Robustness*. Springer, 2005.

[48] D. Hodgson, S. Townley, and D. McCarthy. Robustness: predicting the effects of life history perturbations on stage-structured population dynamics. *Theoretical Population Biology*, 70(2):214–224, 2006.

[49] Q. Hong and J. Murray. A simple method of parameter space determination for diffusion driven instability with three species. *Applied Math. Letters*, 14:405–411, 2001.

[50] R. A. Horn and C. Johnson. *Matrix Analysis*. Cambridge University press, 1990.

[51] J. Horvath, I. Szalai, and P. D. Kepper. An experimental design method leading to chemical turing patterns. *Science*, 324:772–775, 2009.

[52] R. B. Hoyle. *Pattern formation : An Introduction to Methods*. Cambridge University press, 2006.

[53] S. Kauffman, R. Shymko, and K. Trabert. Control of sequential compartment in drosophila. *Science*, 199:259–270, 1978.

[54] P. D. Kepper, V. Castets, E. Dulos, and J. Biossonade. Turing-type chemical patterns in the chlorite-iodide-malonic acid reaction. *Physica D*, 49:161–169, 1991.

[55] W. G. Kermack and A. G. McKendrick. Contributions to the mathematical theory of epidemics. *Proc. R. Soc. Lond. Ser. A*, 115:700–721, 1927.

[56] H. K. Khalil. *Nonlinear systems*. Prentice Hall, 2001.

[57] D. Kidd and P. Amarasekare. The role of transient dynamics in biological control: insights from a host-parasitoid community. *Journal of animal ecology*, 81:47–57, 2012.

[58] A. L. Koch, A. Cair, and D. Ehrenfeld. The problem of open-sea navigation: The migration of the green turtle to ascension island. *Journal of theoretical biology*, 22(1):163–179, 1969.

[59] S. Kondo and T. Miura. Reaction-diffusion model as a framework for understanding biological pattern formation. *Science*, 329:1616–1620, 2010.

[60] M. Kot. *Elements of Mathematical Ecology*. Cambridge University press, 2001.

[61] M. Kot, M. A. Lewis, and P. V. V. den Criessche. Dispersal data and the spread of invading organisms. *Ecology*, 77:2027–2024, 1996.

[62] D. Lauffenburger. Personal communication. 2012.

[63] D. Lauffenburger and K. Keeler. Effects of leukocytes random motility and chemotaxis in tissue inflammatory response. *Journal of theoretical biology*, 81:475–503, 1979.

[64] R. Lefever and O. Legeune. On the origine of tiger bush. *Bulletin of mathematical biology*, 59:263–294, 1997.

[65] D. Liberzon and A. Morse. Basic problems on stability and design of switched systems. *IEEE Control Systems Magazine*, 34:1914–1946, 1999.

[66] H. Lin and P. Antsaklis. Stability and stabilizability of switched linear systems : A survey of recent results. *IEEE Trans. Aut. Control*, 54:308–322, 2009.

[67] L.Wang and M. Y. Michael. Diffusion-driven instability in reaction-diffusion systems. *J. Math. Anal. Appl*, 254:138–153, 2001.

[68] P. Maini. The impact of turing's work on patterns formation in biology. *Mathematics Today*, 4:140–141, 2004.

[69] P. Maini, K. Painter, and H. Chau. Spatial pattern formation in chemical and biological systems. *Faraday Trans.*, 93:3601–3610, 1997.

[70] P. K. Maini, D. L. Benson, and J. A. Shrratt. A density dependent diffusion equation in population dynamics: Stabilization to equilibrium. *Math. Med. Biol*, 9:197–213, 1992.

[71] H. Malchow, S. Petrovskii, and V. Venturino. *Spatio-temporal Patterns in Ecology and Epidemiology: Theory, Models, and Simulation.* Chapman and Hall/CRC, 2007.

[72] O. Mason and R. Shorten. The geometry of convex cones associated with the lyapunov inequality and the common lyapunov function problem. *Electronic journal of linear algebra*, 12:42–63, 2005.

[73] J. McNair. A reconciliation of simple and complex models of age-dependent predation. *Theor. Popul. Biol.*, 32:383–392, 1987.

[74] J. Medlock and M. Kot. Spreading disease: integro-differential equations old and new. *Mathematical Biosciences*, 184:201–222, 2003.

[75] H. Meinhardt. *Models of Biological Pattern Formation.* Academic Press, London, 1982.

[76] J. Merkin. Travelling waves in the oregonator model for the bz reaction. *IMA J. Appl. Math*, 74:622–643, 2009.

[77] M. Mimura. Stationary pattern of some density-dependent diffusion system with competitive dynamics. *Hiroshima Math. J*, 11:621–635, 1981.

[78] T. Miura and P. Maini. Speed of pattern formation in reaction-diffusion models: Implications in the pattern formation of limb bud mesenchymme cells. *Bulletin of Mathematical Biology*, 66(4):627–649, 2004.

[79] J. Murray. Parameter space for turing instability in reaction diffusion mechanisms: a comparison of models. *J. Theo. Biol*, 98:143–163, 1982.

[80] J. Murray. *Mathematical Biology II: Spatial Models and Biomedical Applications.* Springer, Berlin, 2003.

[81] J. Murray. *Mathematical Biology I: An introduction.* Springer, Berlin, 2008.

[82] J. D. Murray. A pre-pattern formation mechanism for animal coat markings. *Journal of Theoretical biology*, 88:161–199, 1981.

[83] K. S. Narendra and A. M. Annaswamy. *Stable Adaptive systems*. Prentice-Hall international editions, 1989.

[84] M. Neubert and H. Caswell. Alternatives to resilience for measuring the responses of ecological systems to perturbations. *Ecology*, 78:653–665, 1997.

[85] M. Neubert, H. Caswell, and J. Murray. Transient dynamics and pattern formation: reactivity is necessary for turing instabilities. *Mathematical Biosciences*, 175:1–11, 2002.

[86] M. Neubert, H. Caswell, and A. R. Solow. Detecting reactivity. *Ecology*, 90:2683–2688, 2009.

[87] M. G. Neubert, T. Klanjscek, and C. H. Reactivity and transient dynamics of predator-prey and food web models. *Ecological modelling*, 179:29–38, 2004.

[88] B. N.F. *Reaction-diffusion Equations and Their Applications to Biology*. Academic Press Inc, 1986.

[89] Y. Nishiura and D. Ueyama. Spatio-temporal chaos for gray-scott model. *Pysica D*, 150:137–162, 2001.

[90] A. Ocubo. *Diffusion and Ecological Problems: Modern Perspectives*. Springer, 2002.

[91] K. Ogata. *Modern control engineering*. Prentice Hall, 2003.

[92] G. F. Oster, J. D. Murray, and A. K. Harris. Mechanical aspects of mesenchymal morphogenesis. *J. Embryol. Exp. Morph.*, 78:83–125, 1983.

[93] E. Ott. *Chaos in dynamical systems*. Cambridge university press, 2002.

[94] K. Painter, P. Maini, and H. Othmer. Development and applications of a model for cellular response to multiple chemotactic cues. *J. Mathematical Biology*, 41:285–314, 2000.

[95] K. J. Painter. *Chemotaxis as a mechanism for morphogensis*. PhD thesis, Brasenose college, University of Oxford, 1997.

[96] P. Parham. *The immune system*. Garland science, 2009.

[97] I. Pearce, M. Chaplain, P. Schofield, A. Anderson, and S. Hibbard. Chemotaxis-induced spatio-temporal hererogeneity in multi-species host-parasitoid systems. *Mathematical biology*, 55:365–388, 2007.

[98] B. Philip. *Shapes: Nature's patterns: a tapestry in three parts*. OUP Oxford; Reprint edition, 2011.

[99] I. Prigogine and R. Lefever. Symmetry-breaking instabilities in dissipative systems ii. *J. Chem. Phys*, 48:1695–1700, 1968.

[100] L. Qiu, B. Bernhardsson, S. A. Rantzer, S. E. J. Davison, P. M. Young, and J. C. Doyle. A formula for computation of the real stability radius. *Automatica*, 31:897–890, 1995.

[101] M. L. Rosenzweing and R. H. MacArthur. Graphical representation and stability conditions of predator-prey interactions. *Am. Nat.*, 79:209–223, 1963.

[102] R. S. S. Mergenhagen. Peridical disease: a model for the study of inflammation. *J. Inf. Dis*, 123:676–677, 1971.

[103] J. Schnakenberg. Simple chemical reaction systems with limit cycle behaviour. *Theoretical biology*, 81:389–400, 1979.

[104] J. Schnakenberg. Simple chemical reaction systems with limit cycle behaviour. *Journal of theoretical biology*, 81:389–400, 1979.

[105] L. Segel and J. Jackson. Dissipative structure: an explanation and an ecological example. *J. Theo. Biol*, 37:545–559, 1972.

[106] R. Shorten and K. Narendra. A sufficient condition for the existence of a common lyapunov function for two second order systems. Technical Report 9701, Center of systems and science, Yale university, April 1997.

[107] R. Shorten and K. Narendra. On the stability and existence of common lyapunov functions for linear stable switching systems. Technical Report 9805, Center of systems and science, Yale university, April 1998.

[108] R. Shorton and K. Narendra. Necessary and sufficient conditions for the existence of a common quadratic lyapunov function for a finite number of stable second order time-invariant systems. *Int. J. of Adaptive Control & Signal Processing*, 16:709–728, 2002.

[109] R. Snyder. What makes ecological systems reactive. *Theoretical population biology*, 77:243–249, 2010.

[110] T. P. Stossel. Phagocytosis : the department of defence. *N.E.J. Med*, 286:776–777, 1972.

[111] C. Tian, Z. Ling, and Z. Lin. Turing pattern formation in a predatorpreymutualist system. *Nonlinear Analysis: Real World Applications*, 12:3224–3237, 2011.

[112] M. J. Tindal, E. A. Gaffney, P. K. Maini, and J. P. Armitage. Theoretical insights into bacterial chemotaxis. *Syst. Biol. Med*, 4:247–259, 2012.

[113] M. Tindall, P. Maini, S. Porter, and J. Armitage. Overview of mathematical approaches used to model bacterial chemotaxisi ii : Bacterial population. *Bulletin of mathematical biology*, 70:1570–1607, 2008.

[114] L. N. Trefethen and M. E. Embree. *Spectra and Pseudospectra: The Behaviour of Non-normal Matrices and Operators*. Princeton University Press, Princeton, NJ, 2005.

[115] A. Turing. The chemical basis of morphogenesis. *Phil. Trans. Roy. Soc. Lond. B*, 237(641):37–72, 1952.

[116] A. G. V. Andersari, G. Lolas, A. P. South, and M. Chaplain. Mathematical modeling of cancer cell invasion of tissue: biological insight from mathematical analysis and computational simulation. *Mathematical biology*, 63:141–171, 2011.

[117] V. K. Vanag and I. R. Epstein. Cross-diffusion and pattern formation in reactiondiffusion systems. *Phys. Chem. Chem. Phys*, 11:897–912, 2009.

[118] L. Vandenberghe and S. Boyd. Semidefinite programming. *SIAM Review*, 38:49–95, 1996.

[119] C. Varea, J. Aragon, and R. Barrio. Confined turing patterns in growing systems. *Phys. Rev.*, 56:1250–1253, 1997.

[120] A. verdy and H. Caswell. Sensitivity analysis of reactive ecological systems. *Bulletin of mathematical biology*, 77:243–249, 2010.

[121] M. Wang. Stability and hopf bifurcation for prey-predator model with prey-stage structure and diffusion. *Mathematical Biosciences*, 212:149–160, 2008.

[122] Y. Wang, J. Wang, and L. Zhang. Cross diffusion-induced pattern in an si model. *Applied Mathematics and Computation*, 217:1665–1970, 2010.

[123] A. Weinmann. *Uncertain models and robust control*. Springer Verlag, New York, 1991.

[124] K. A. J. White and C. A. Gilligan. Spatial heterogeneity in three-species, plant-parasite-hyperparasite, systems. *Phil. Trans. R. Soc. Lond. B*, 353:543–557, 1998.

[125] J. A. Wilkinson. *Chemotaxis and inflamation*. Churchil-Livingston, 1974.

[126] T. C. Williams. *Chemotaxis: Types, Clinical Significance and Mathematical Models*. Nova Science Publishers Inc, 2011.

[127] W. Wilson, S. Harrison, A. Hastings, and K. McCann. Exploring stable pattern formation in models of tussock moth populations. *J. Anim. Ecol*, 68:94–107, 1999.

[128] G. Xiaoqing and A. Murat. A sufficient condition of d-stability and applications to reaction diffusion models. *Sys. & Cont. Letters*, 58:736–741, 2009.

[129] G. Zhai and H. Lin. Controller failure time analysis for symmetric H_∞ control systems. *Inter. J. Contr.*, 77:598–605, 2005.

[130] G. Zhai, X. Xu, and A. N. Michel. Analysis and design of switched normal systems. *IEEE Trans. Automat. Contr.*, 65:2248–2259, 2006.

[131] M. Zhu and J. Murray. Parameter domains for generating spatial pattern: a comparison of reaction-diffusion and cell chemotaxis models. *Int. J. Bifurc. Chaos*, 5:1503–1524, 1995.